Volume 5, December 2025

BORNEO INTERNATIONAL JOURNAL OF BIOTECHNOLOGY

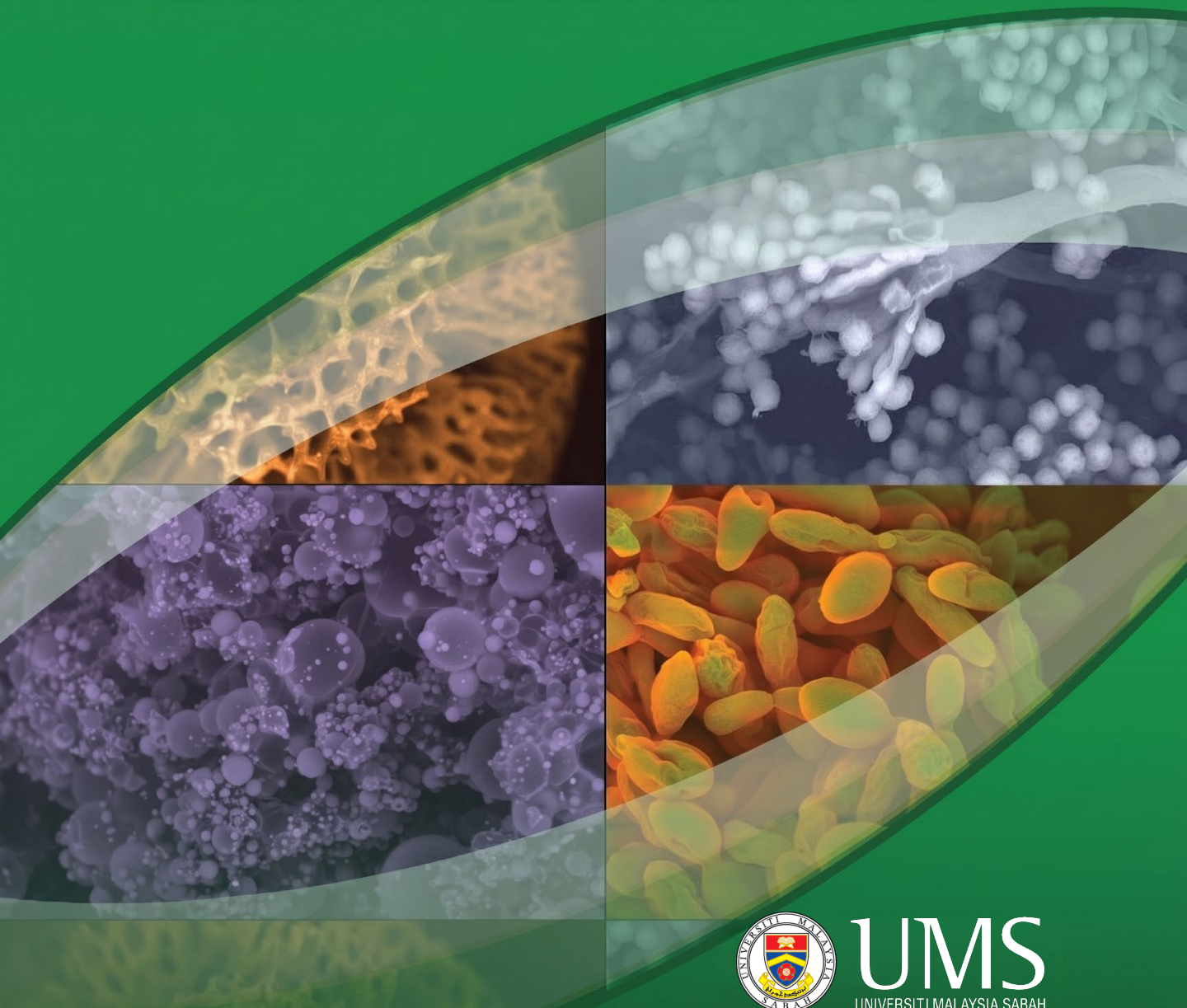

UMS
UNIVERSITI MALAYSIA SABAH

Borneo International Journal of Biotechnology

https://jurcon.ums.edu.my/ojums/index.php/bijb
e-ISSN 2716-697X

Contents

https://jurcon.ums.edu.my/ojums/index.php/bijb
e-ISSN 2716-697X

Borneo International Journal of Biotechnology (BIJB)
Vol. 5 (December 2025), 1-11.

e-ISSN 2716-697X

Evidence of *Klebsiella pneumoniae* and SARS-CoV-2 Infections among patients presenting with Cough and Fever attending chest clinic, Aminu Kano Teaching Hospital, Kano

Jamilu Abubakar Bala[1,2,3]*, Isah Abubakar Aliyu[1], Baba Maiyaki Musa [1], Taiwo Goluwaga Amole [1], Abdulhadi Sale Kumurya[1], Hayatu Saidu[1], Alhassan Sharif Abdullahi[4], Krishnan Nair Balakrishnan[5], Hassan Isah[1], Bilkisu Ahmed[3], Hadiza Shehu Galadanci *[3]

[1]Department of Medical Laboratory Science, Faculty of Allied Health Sciences, Bayero University Kano, Nigeria, P.M.B. 3011, Kano, Nigeria
[2]Centre for Infectious Diseases Research, Bayero University Kano, Nigeria, P.M.B 3011, Kano, Nigeria [3]African Centre of Excellence for Population Health and Policy, Bayero University Kano, P.M.B 3011, Kano, Nigeria [4]Department of Medical Microbiology and Parasitology, Faculty of Clinical Sciences, Bayero University Kano, Nigeria, P.M.B. 3011, Kano, Nigeria
[5]Biotechnology Research Institute, Universiti Malaysia Sabah, Jalan UMS, 88400 Kota Kinabalu, Sabah, Malaysia
*Corresponding author's email: hgaladanci@yahoo.com
Received: 11 November 2024 | Accepted: 22 December 2025 | Published: 31 December 2025

ABSTRACT

Extensive antibiotic use during early COVID-19 management may reduce bacterial co-infection but contributes to increasing antibiotic resistance, particularly in *Klebsiella pneumoniae*. Accurate detection of *K. pneumoniae* is therefore important to support diagnosis and treatment of COVID-19 patients. This study aimed to identify and detect *K. pneumoniae* and SARS-CoV-2, and to assess associated demographic characteristics and comorbidities among patients attending the chest clinic at Aminu Kano Teaching Hospital (AKTH), Kano. Demographic data and risk factors were collected using questionnaires. A total of 300 sputum samples were cultured on MacConkey agar and incubated aerobically at 37°C, followed by phenotypic identification using standard biochemical tests. SARS-CoV-2 was detected using real-time PCR. The prevalence of *K. pneumoniae* and SARS-CoV-2 infections was 17.0% and 3.3%, respectively, with a co-infection

e-ISSN 2716-697X

rate of 1.3%. Males showed a higher prevalence of *K. pneumoniae* infection (64.7%) than females (35.3%). Common symptoms included cough and fever. The findings highlight the association of respiratory tract infections with *K. pneumoniae* and emphasize the need for routine diagnostic testing to detect and manage co-occurring respiratory infections in COVID-19 patients.

Keywords: Bacteria; *Klebsiella pneumoniae;* antibiotics; COVID-19; RT-PCR; co-infections; SARS-CoV-2.

INTRODUCTION

Co-infection of *Klebsiella pneumoniae* and SARS-CoV-2 among patients presenting fever and cough has created major problems for social and healthcare system worldwide. The misused of antibiotic may result in increased antimicrobial resistance. This can involve bacteria becoming resistant to antibiotics (WHO 2020). The effect may be felt among the wider population and have toxic consequences, therefore, there is need to conduct research to evaluate the clinical features and characteristics of patients with SARS-CoV-2 and *Klebsiella pneumoniae* co-infections and the exact current prevalence trends of *K. pneumoniae* and SARS-CoV-2 co-infection with a view to formulating a control regimen for the environment (Guo et al., 2019).

Bacterial co-infections are commonly identified in viral respiratory tract infections. The mechanism underlying the synergy between COVID-19 and *K. pneumoniae* paves the way for the discovery of novel therapeutic agents to prevent the mortality rate in patients co-infected with COVID-19 and bacteria (CDC 2020). In the current situation, appropriate and systematic analysis of COVID-19 suspected patients diagnosed with bacterial co-infection should be implemented to choose proper antibiotics to increase the survival of patients and limit the spread of drug-resistant bacteria (Caly et al., 2020).

Despite the increase number of reports with *K. pneumoniae* infection in many regions, little is known about COVID-19 associated with *K. pneumoniae* in Nigeria especially in the North. The need for bacterial screening for *K. pneumoniae* may arise if this study reveals a significance prevalence among suspected COVID-19 patients so that transmission of this virus can be prevented (Huttner et al., 2020). Result generated from this study will not only add to the body of knowledge but will also be essential in preventing misdiagnosis and provide a helpful reference for diagnosis and clinical treatment in infected patients. Hence, there is an urgent need to carryout research to determine the occurrence of COVID-19 associated with *Klebsiella pneumoniae* infection.

e-ISSN 2716-697X

MATERIALS AND METHODS

Study design and Site

This is a cross-sectional prospective study conducted at Aminu Kano Teaching Hospital, Kano, Nigeria. The hospital has a Tuberculosis-Directly Observed Therapy Unit (TB-DOTS) also known as Chest-clinic, which is situated within Kano Metropolis. Three hundred (300) participants age between 20-79 were enrolled.

Ethical approval

Ethics approval for the study was obtained from the Research Ethics Committee of Aminu Kano Teaching Hospital, Kano Nigeria with registration number (NHREC/28/01/2020/AKTH/EC/3358). A written informed consent was obtained from the study participants after a verbal explanation was made to each participant.

Data and Sample Collection

Demographic data was collected using a design questionnaire. Detail information about the study was given to the clients and consent to participate was obtained before patient sample and data is taken. Early morning sputum was aseptically collected in a clean 20ml sterile screw-capped and wide mouthed universal container, the patient was instructed not to open the container until he/she is ready to use and prior to the sample collection, the patient was instructed to wash mouth, find an open area, the patient was instructed to inhale deeply 2 to 4 times before coughing out from the chest and to ensure it spit inside the container (Guo et al., 2019). All specimens were labeled and taken to the laboratory for culture.

Laboratory Identification of *Klebsiella pneumoniae*

The phenotypic detection of *K. pneumoniae* to the species level was performed based on standard biochemical reactions for microbial identification; these included; morphological characteristics on culture media, reaction on SH2/indole/motility (SIM) medium, triple sugar iron (TSI) agar, urease production on urea agar, growth on Simmons' citrate agar medium (Guo et al., 2019). Before analysis, all isolates were cultured on MacConkey agar medium.

e-ISSN 2716-697X

Reverse transcription real-time polymerase chain reaction (RT-PCR) for the detection of COVID-19

Naso-pharyngeal samples were obtained using a specific swab and then placed in a separate collection tube containing three ml of viral transport medium and immediately sent to the coronavirus reference laboratory of the university. First, the inactivation of the sample was achieved using lysis buffer and ethanol, extraction of the viral RNA was performed using a commercial kit according to the manufacturer's protocol (QIAGEN viral RNA mini kit). Next, RT-PCR was performed using GeneFinder^{TM} COVID-19 Plus Real*Amp* Kit (Ochei and Kolhatkar 2008).

Inclusion and Exclusion Criteria

This study included those who do have respiratory tract infections and presented with fever and cough and excluded if they do not have respiratory tract infection and do not present with fever and cough.

Statistical Analysis

Statistical analysis was conducted with the aid of SPSS (statistical package for social sciences V22). Descriptive statistics of the categorical variables are expressed as frequency and percentage. The continuous variables were expressed interquartile ranges (IQRs). Chi-square test was used to evaluate and compare differences between patients who had other infections and those who did not. A p-value of <0.05 was considered statistically significant.

RESULTS AND DISCUSSION

The study included 300 participants, 177 (59%) males and 123 (41%) females. The mean age average of the participants was 39.06±19 years. Eighty-nine (29.7%) and forty-two (14%) had cough and fever respectively. Among the participants, *Klebsiella pneumoniae* was found to be 51(17.0%) among the bacterial isolates, whereas other non-*K. pneumoniae* bacterial culture was 94(31.3%) and the remaining that yielded negative culture were 155(51.7%).

Male participants were found to have the higher percentage of *K. pneumoniae* infection with 33(64.7%) followed by female participants with 18(35.3%). The study shows prevalence of SARS-CoV-2 among the participants to be 10(3.3%) using real time polymerase chain reaction (RT-PCR) method. There were 4(1.3%) of *K. pneumoniae* co-infection with SARS-CoV-2 in the study. The prevalence of comorbidities was found to be for pneumonia 13.3%, Diabetes mellitus 6%, tuberculosis 5.3% and Asthma 5.0%. Clinical signs recorded among the participants with *K. pneumoniae* and SARS-CoV-2 infection reveals; 5.3% and 2.0% had cough, whereas 2.0% and 1.3% had fever respectively.

e-ISSN 2716-697X

Table 1: Relationship between demography and positivity rates of SARS-CoV-2 and *K. pneumoniae* infections.

Demographic characteristics	SARS-CoV-2 Positive n (%)	Negative n (%)	K. pneumoniae Positive n (%)	Negative n (%)
Gender n (%)				
Male 177 (59.0)	6 (2.0)	171 (98.0)	33 (11.0)	144 (89.0)
Female 123(41.0)	4 (1.3)	119 (98.7)	18 (6.0)	105 (94.0)
Age groups (n)				
20-30 (107)	2 (1.9%)	105 (98.1%)	21 (19.6%)	86 (80.4%)
31-40 (74)	3 (4.1%)	71 (95.9%)	11 (14.9%)	63 (85.1%)
41-50 (58)	3 (5.3%)	55 (94.7%)	9 (15.5)	49 (84.5%)
51-60 (30)	0 (0%)	30 (100%)	4 (13.3%)	26 (86.7%)
61-70 (23)	2 (8.7%)	21 (91.3%)	4 (17.4%)	19 (82.6%)
≥71 (8)	0 (0%)	8 (100%)	2 (25.0%)	6 (75.0%)
Marital status				
Single	4(1.3)	168(56.0)	19(6.3)	154(51.3)
Married	6(2.0)	122(40.7)	32(10.7)	95(31.7)
Educational status				
Primary	0(0)	12(4.0)	0(0)	122(40.7)
Secondary	4(1.3)	98(32.7)	15(5.0)	74(24.7)
Tertiary Others	4(1.3) 2(0.7)	92(30.7) 88(29.3)	29(9.7) 7(2.3)	78(26) 85(28.3)

e-ISSN 2716-697X

Table 2: *Klebsiella pneumoniae* and SARS-CoV-2 co-infection

	K. pneumoniae n (%)	SARS-CoV-2 (%)	n	Co-infection (%)	n	P-value
Positive	51(17)	10(3.3)		4(1.3)		0.054
Negative	249(83)	290(96.7)		296(98.7)		
Total	300	300		300		

p-value ≤0.05 was considered statistically significant.

Table 3: SARS-CoV-2 and *K. pneumoniae* infection in relation to cough and fever

Symptoms	SARS-CoV-2 n (%) Positive Negative	Total	P-value	*K. pneumoniae* Positive Negative	Total (%)	P-value
Cough	6(2.0)	89(29.7)	0.033	16(5.3)	89(29.7)	0.392
Yes	83(27.7)	211(70.3)		73(24.3)	211(70.3)	
	4(1.3)			35(11.7)		
No	207(84.0)			176(58.6)		
Fever	4(1.3)	42(14.0)	0.016	6(2.0)	42(14.0)	0.902
Yes	38(12.7)	258(86)		36(12.0)	258(86.0)	
	6(2.0)			45(15.0)		
No	252(84.0)			213(71.0)		

p-value ≤0.05 was considered statistically significant.

e-ISSN 2716-697X

Table 4: Risk factors associated with SARS-CoV-2 and *K. pneumoniae* infection among the study participants

Risk factors	SARS-CoV-2 Positive Negative	P-value	*K. pneumoniae* Positive Negative	P-value
Asthma	1(0.3)	0.418	4(1.3)	0.680
Yes	14(4.7)		11(3.7)	
	9(3.0)		40(13.3)	
No	276(92.0)		245(81.7)	
Pneumonia	1(0.3)	0.733	9(3.0)	0.355
Yes	39(13.0)		31(10.3)	
	9(3.0)		20(6.7)	
No	251(83.7)		240(80.0)	
Tuberculosis	2(0.7)	0.036	4(1.3)	0.132
Yes	14(4.7)		12(4.0)	
	8(2.7)		39(13.0)	
No	276(92.0)		245(81.7)	
Diabetes	1(0.3)	0.589	2(0.7)	0.939
Yes	17(5.7)		16(5.3)	
	9(3.0)		35(11.7)	
No	273(91.0)		247(82.3)	

The overall prevalence of *Klebsiella pneumoniae* was found to be 17% which varied slightly by participant's gender, ranging from (11%) in males to (6%) in females. These agrees with studies conducted by Corman et al. 2020 in Pennsylvania with a prevalence of 16%, also in agreement with 29.2% reported by Cornelius et al. 2020 in India and in contrast with 7.8% reported by Ravichitra et al. 2014 in Lagos Nigeria, which is lower than this study. The high prevalence of *Klebsiella pneumonia* found in this study could be because the study was conducted during raining season, a period of the year where there is usually a high rate of respiratory tract infection.

The prevalence of SARS-CoV-2 among the study participants was found to be 3.3%, which is in agreement with the study conducted in the United State by Ogunsola et al. 2018, who reported the prevalence of 5.0%. However, the prevalence recorded in this study was lower compared to the prevalence recorded by Blasco et al. 2020, who reported a prevalence of 25.6% in Egypt. This could be attributed to the huge populations, low amount of screening testing, temperature and difference in the demography of the study population (Musaif et al., 2021). With regards to *Klebsiella pneumoniae* coinfection with COVID-19 in patients

presenting cough and fever, the findings in this research shows a prevalence of 1.3%. The results are in consistent with those of previously published studies in China conducted by Gomez et al. 2015 with 1% co-infection. Similar study has also been carried out in the United Kingdom, reported a prevalence of 3.2% (Liu et al., 2020). However, meta-analysis done by Hughes et al. 2020, in Washington reported a coinfection rate of 6.8% in hospitalized COVID-19 cases. This variation could be because most of the participants of this study were outpatients as such there is reduced risk of acquiring hospital-acquired infections. However, male gender demonstrated high prevalence of coinfections.

One plausible reason for the gender differences could be due to hormonal differences as estrogen may play a protective role with other susceptible factors by inhibiting the entry of SARS-CoV-2 virus into the host cells (Lansbury et al., 2020). The prevalence of comorbidities in the study participants were as follows; pneumonia (13.3%), diabetes mellitus (6%), tuberculosis (5.3%) and asthma (5.0%), which are similar to the findings reported by Ye et al. 2020 in China. The co-infected participants compared to the total COVID-19-positive population showed significantly high comorbidity rates for tuberculosis. This can be supported by the fact that tuberculosis itself downregulates the immune system by decreasing the effective T-cell and neutrophil response. It causes decreased phagocytosis, ineffective chemotaxis, and decreased killing of the invading microbes by the neutrophils and macrophages leading to increased susceptibility to secondary bacterial infection (Gomez et al., 2015).

Diabetes mellitus were observed in the co-infected participants. This might be due to the fact that diabetes mellitus is associated with elevated plasma glucose which influence SARS-CoV-2 replication through a mechanism of mitochondrial reactive oxygen species production and activation of hypoxia-inducible factor 1a (Wu et al., 2020). Therefore, the viral proliferation might also have been encouraged by hyperglycemia. On the contrary, this study shows low significant rate of 0.3% for both asthma and pneumonia, which is in line with the study conducted by Montero et al. 2020 with the prevalence of 1.5%. This might be attributed to the fact that SARS-CoV-2 enters lung cells via angiotensin-converting enzyme 2 (ACE2) receptor. Several studies suggest that interleukin-13, an important cytokine involved in T2 inflammation, reduces ACE2 expression and therefore, asthma would not be a significant risk factor for the development of COVID-19 and bacterial co-infections (Rosana et al., 2020).

The study showed that, patients on medication were (29.7%). The result is similar to reports from other countries in the African Region (47% in Kenya, 55% in South Africa and 61% in Uganda). In contrast, a study from Singapore reported a very low prevalence of 5.0% antibiotic use but higher in Spain and USA with 78% and 83% respectively (Budiarti et al., 2022). The clinical symptoms presented by the participants were 88(29.3%) for cough and 42(14.0%) for fever and both gives a significant correlation of p-value 0.033 and 0.016 respectively. This result agrees with the report from Center for Disease Control (CDC) in the United States with 43% and 50% for fever and cough respectively (Tan et al., 2022).

e-ISSN 2716-697X

CONCLUSION

The *Klebsiella pneumoniae* were isolated and identified using the standard culture and biochemical methods. The overall prevalence of the isolate among participants were 17%. Sputum sample was analyzed by real-time polymerase chain reaction (RT-PCR) kits and RNA of SARS-CoV-2 were detected among 10(3.3%) of the participants. Demographic characteristics of the participants were reported. Male gender recorded high prevalence of coinfections with 4:1 ratio. Cough (29.3) and fever (14.0%) are the most presented clinical symptoms among the participants. The possible risk factors associated with coinfection of *Klebsiella pneumoniae* and SARS-CoV-2 was identified whereby pneumonia had (13.3%), diabetes mellitus (6%), tuberculosis (5.3%) and
asthma (5.0%).

ACKNOWLEDGMENTS

We will like to appreciate the Staff of Aminu Kano Teaching Hospital, Murtala Muhammad Teaching Hospital, Kano and Center for infectious diseases research, BUK.

CONFLICT OF INTEREST

The authors declare that they have no known competing financial interests or personal relationships that could have appeared to influence the work reported in this paper.

e-ISSN 2716-697X

REFERENCES

Blasco, M.L., Buesa, J., Colomina, J., Forner, M.J., Galindo, M.J., Navarro, J., Noceda, J., Redón, J., Signes-Costa, J. and Navarro, D. (2020), Co-detection of respiratory pathogens in patients hospitalized with Coronavirus viral disease-2019 pneumonia. *Journal of Medical Virology*. 92, 1799-1801.

Budiarti, C. A., Ghisetti, V., Burdino, E., Trunfio, M., Allice, T., Boglione, L., (2022). Co-infection with other respiratory pathogens in COVID-19 patients. *Clinical Microbiology and Infection*. 27(2), 297-298.

Caly, L., Druce, J. D., Catton, M. G., Jans, D. A., & Wagstaff, K. M. (2020). The FDA-approved drug ivermectin inhibits the replication of SARS-CoV-2 in vitro. *Antiviral research*. 178, 104787.

Center for Disease Control (2020). Antibiotic Resistance Threats in the United States, 2020.

Corman VM, Landt O, Kaiser M, Molenkamp R, Meijer A, Chu DK, Bleicker T, Brünink S, Schneider J, Schmidt ML (2020). Detection of 2019 novel coronavirus (2019-nCoV) by real-time RT-PCR. *Eurosurveillance*. 25(3), 2000045

Cornelius, C. J. and Nguyen M. H. (2020). COVID-19, superinfections and antimicrobial development: What can we expect. *Clinical Infectious Diseases*. 109-143.

Gomez, S., Obiamiwe, U., Henry, G. and Burke, A. C. (2015). Mortality and morbidity of Klebsiella pneumoniae infection. *American Journal of Physicians*. 25 (5), 52 – 100.

Guo, D., Dong, N., Zheng, Z., Lin, D., Huang, M. and Wang, L. (2019). A fatal outbreak of ST1carbapenem-resistant hypervirulent Klebsiella pneumoniae in a Chinese hospital: a molecular epidemiological study. *Lancet Infectious Diseases*. 18, 37–46.

Hughes, B., Vallon, M., Zai, J. and Chaillon, A. (2020). Transmission dynamics and evolutionary history of 2019-nCoV. *Journal of Medical Virology*. 92(5), 501-511

Huttner, B., Catho, G., Pano-Pardo, J. R., Pulcini, C. and Schouten, J. (2020). COVID-19 Antimicrobial stewardship principles. *Clinical Microbiology Infection*. 26, 808e10.

Lansbury, L., Lim, B., Baskaran, V. and Lim, W. S. (2020). Co-infections in people with COVID-19: a systematic review and meta-analysis. *Journal of Infection*. 81(2), 266-275.

Liu, C. C., Shih, T. P., Ko, W. C., Tang, H. J. and Hsueh, P. R. (2020). Severe acute respiratory syndrome coronavirus 2 (SARS-cov-2) and coronavirus disease-2019 (COVID19): The epidemic and the challenges. *International Journal of Antimicrobial Agents*. 55(3), 105924.

Montero, M., D. W., Sun, K., J., Mirzaei, R., Goodarzi, P., Asadi, M. (2020). Bacterial co-infections with SARS-CoV-2. Immune dysfunction and bacterial coinfections following influenza. *IUBMB Life*. 72, 2097–2111.

Musaif, A., M., Alvi, I. and Rehman, S. (2021). Insight into Acinetobacter baumannii: pathogenesis, global resistance, mechanisms of resistance, treatment options, and alternative modalities. *Infectious Drug Resistance*. 21(11), 1249-1260.

Ochei, J. and Kolhatkar, A. (2008). Medical Laboratory Science, Theory and Practices. *McGraw-Hill Education*. 311-347.

Ogunsola, O., Öksüz, S., Acar, A., Ülkür, E., Turhan, V., Uygur, F. and Görenek, L. (2018). Nosocomial infection characteristics of klebsiella pneumoniae in a burn intensive care unit: analysis of an eleven-year active surveillance. *Burns*. 40 (5), 835-841.

Ravichitra, K. N., Prakash, H. P., Subbarayudu, S. and Rao, S. U. (2014). Isolation and antibiotic sensitivity of Klebsiella pneumoniae from pus, sputum and urine samples. *International Journal of Current Microbiology and Applied Sciences*. 3(3), 115-119.

Rosana, N., G., Khani M., Hodadadi J., Fotouhi-Ardakani R., Koohpaei A. (2020). Evaluation of bacterial co-infections of the respiratory tract in Covid-19 patients admitted to ICU. *BMC Infectious Diseases*. 20(1), 646.

Tan, A. N., Khan, M., Saleem, W., Karobari, M. I., Mohamed, R. N., Haboyan, A. and Alestad, J. H. (2022). Evaluation of bi-lateral coinfection and antibiotic resistance rates among COVID-19 patients. *Journal of Antibiotics*. 3(2), 5456.

World Health Organization (WHO), (2020). Laboratory testing for coronavirus disease COVID-19 in suspected human cases. Interim guidance, (No. 08 WHO/COVID-19/laboratory/2020.

Wu, Z., B., Liu, S. and Tan, T. (2020). Treatment with convalescent plasma for critically ill patients with SARS-CoV-2 infection. *Chest Medicine*. 158(1),9–13.

Ye, C., Zhang, S., Zhang, X., Cai, H., Gu, J., Lian, J., ... & Yang, Y. (2020). Impact of comorbidities on patients with COVID-19: A large retrospective study in Zhejiang, China. *Journal of medical virology*. 92(11), 2821-2829.

.

Borneo International Journal of Biotechnology
(BIJB) Vol. 5 (December 2025), 12-31.

e-ISSN 2716-697X

Geographic Isolation of Riparian Ecosystems Determine Population Diversity of *Tor* sp in Sabah, Malaysia.

Helena Biun[1], Ahemad Sade[2], Kenneth Francis Rodrigues[1]

[1]Biotechnology Research Institute, Universiti Malaysia Sabah, 88400, Kota Kinabalu, Sabah, Malaysia
[2]Jabatan Perikanan Sabah, 4th Floor, Wisma Pertanian Sabah, 88624 Kota Kinabalu, Sabah, Malaysia
*Corresponding author's email: kennethr@ums.edu.my
Received: 23 September 2025 | Accepted: 20 December 2025 | Published: 31 December 2025

ABSTRACT

Tor sp is a cyprinid riverine fish known as Pelian in the local dialect in Sabah, that is currently facing challenges due to climate change and habitat degradation. Applying conservation strategies and a sustainable management program for this species requires a primary assessment of the genetic diversity and overall structure of the geographically isolated populations. Eighteen wild Pelian populations from across ten river systems were analyzed based on eleven microsatellite markers. The gene diversity and allelic richness based on microsatellite loci ranged from 0.40-0.68 and 2.63-6.10, respectively. Pairwise FST values for microsatellites were significant ($P<0.05$) between the majority of populations. Microsatellites analyses of molecular variance, AMOVA analyses detected variation within populations that ranged from 60.85% to 50.74% within the entire watershed, with significantly high FST values. Mantel tests supported weak patterns of differentiation based on isolation by distance. The overall population comprised two distinct clusters that exhibited further sub structuring based on the watershed. The topographical features of the landscape in Borneo comprise a combination of isolation by distance, river fragmentation and historical isolation by the Crocker Trusmadi mountain range all support the hypothesis that population substructure was driven by isolation in distinct ecological niches. These results will be used in the application of conservation strategies and management program for Pelian in Sabah.

Keywords: Borneo, microsatellites, Pelian, population genetics, *Tor* sp

e-ISSN 2716-697X

INTRODUCTION

Tor tambra is a species of ray-finned fish of the family Cyprinidae in the genus *Tor*. In Sabah, East Malaysia, all *Tor* species are known by the ethnic group, the Dusuns, as 'Pelian'. *Tor* is referred in the local dialects as 'Empurau' and 'Semah' in Sarawak, and 'Kelah' in Peninsular Malaysia. The geographic range extends across Cambodia, Yunnan, Jawa, Kalimantan, Sumatera, Laos, Malaysia, Thailand, and Vietnam (Pinder et al., 2019). Pelian is endemic to Malaysian Borneo river basins and is presumably the most widespread Tor species recorded in Malaysian Borneo (Esa et al., 2008). Analysis of the mitochondrial DNA (mtDNA) *coxI* gene imply that specimens collected from Malaysian Borneo may represent a new *Tor* species (Walton et al., 2017). Pelian is an important fisheries resource to the local communities associated with riparian settlement that line the Kinabatangan, Kanarom, Labuk Sugut along the East coast of Sabah, and Pagalan Padas, Wariu Kadamaian, Tuaran, Moyogm Kimanis and Bongawan that all flow into the South China sea (Ahmad et al., 2006). Pelian inhabits the shallow, rocky areas of the river with strong currents. Their preferred diet comprises plant matter, insects, flowers and fruit. The breeding behaviour involves multiple spawners, with spawning occurring in streams up to 500 meters above sea level. Upstream migration from lower reaches of rivers by schools of Pelian starts when the breeding season commences, which coincides with the monsoon rains. Sub-adult Pelian can be found in the upper reaches of the water column at both higher and lower reaches of rivers, whereas larger adult Pelian are mostly found at the lower reaches of rivers, occupying the deepest portions of pools. Sarawak has reported the successful breeding of both *T. tambroides* and *T. douronensis* from brood stock reared in captive culture (Ingram et al., 2007). The riparian communities in Sabah are actively engaged in a community-based conservation scheme termed as "Tagal", that consists of villagers who manage and protect Pelian along selected stretches of the rivers. Fishing is prohibited in these areas and harvesting is only permitted at specific days in a year in order to promote sustainable fisheries. Within the island of Borneo, Pelian is genetically distinct as compared to the *Tor sp* endemic to the rivers of Sarawak (Esa et al., 2008). Microsatellite markers have been popular for population genetics studies of marine and freshwater fish species due to their codominance, polymorphism, ability to amplify specific loci, hyper variability, reproducibility across varieties, ease of application in laboratory setting and amenability to statistical analysis and interpretation using generally accepted statistical methods (Abdul-Muneer, 2014). Population characteristics of *T. tambra* such as fragmentation, isolation and unbalanced sex ratios observed in the wild, make the populations susceptible to the phenomenon of genetic drift, bottleneck and inbreeding processes. This study was conducted with the aims of demonstrating the utility of population genetic studies using microsatellite markers in understanding population diversity and structures of Pelian for appropriate conservation and management strategies in Sabah.

e-ISSN 2716-697X

MATERIALS AND METHODS

Sample Collection

The samples of *Tor tambra* were obtained from 18 village communities who were involved in managing Tagal systems in the respective villages as listed in **Table 1**. The location of the sampling sites is indicated in **Figure 1**. The identity of the species was established based on morphological features consistent with *Tor* sp (e.g., median lobe length, coloration). While recent mtDNA studies suggest potential cryptic diversity in Borneo, our initial screening and morphological validation treat the sampled populations as a single coherent genetic unit ('Pelian') for the purpose of population structure analysis. A single caudal fin clip was excised from each of the specimens (Figure 2), stored in a 50 ml tube containing 95% Ethanol and shipped to the laboratory at the Department of Fisheries, Likas, Sabah. Total DNA was extracted as per the manufacturers protocol using a Wizard Genomic DNA Extraction Kit (Promega, Madison WI, USA). The DNA was eluted in 50 microliters of elution buffer and the final concentration was adjusted to 50 nanograms per microliter using elution buffer. DNA was quantified using a Spectrophotometer and stored at -20^{o} C prior to PCR amplification.

Table 1: The river systems and abbreviations for the localities at which the samples were collected.

River system	Locality	Abbreviation
Kanarom	Sorinsim	KSO
	Tangkol	KTA
	Sunsui	KSU
	Marak Parak	KMP
Sugut	Luanti	SLU
	Poring	SPO
Labuk	Kinarasan	SKI
	Paus	SPA
Kinabatangan	Pinipi	SPI
	Kironggu	SKIR
Pagalan	Menserulong	IME
	Rugading	IRU
Kadamaian	Tokulung	WCTO
	Lingkubang	WCLI
Tuaran	Gontung	WCGO
Moyog	Babagon	WCBA
Kimanis	Doingin	WCDO
Bongawan	Telantang	WCTE

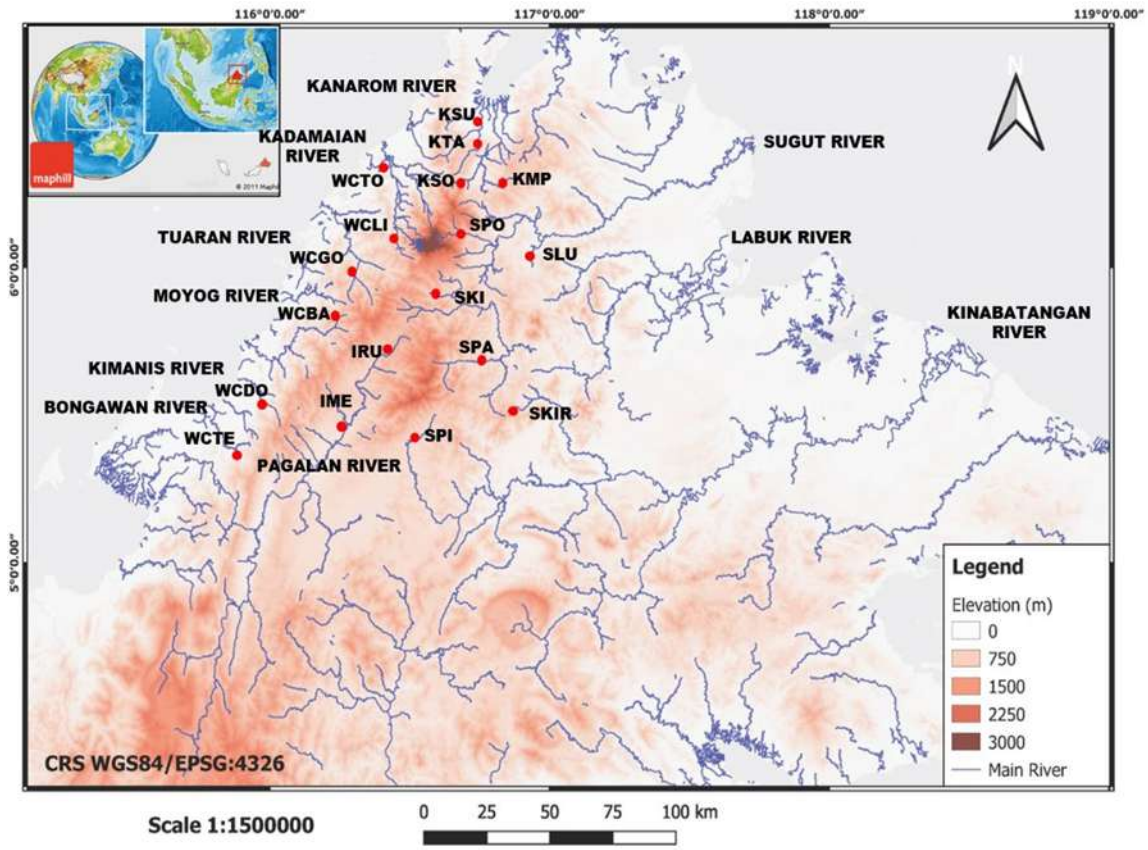

Figure 1: The locations at which sample were collected. The abbreviations are listed in Table 1.

Microsatellite analysis

For microsatellite analysis, polymerase chain reaction amplification was set up in a 50 µL reaction mixture containing 1× TopTaq Master Mix buffer (Qiagen, Germany), 0.2 µM of each forward and reverse primers, and 50 - 100 ng of template DNA. Twelve primer pairs were used to amplify anonymous microsatellite loci: 11 of these (loci Tt1.A06, Tt2.DO1, Tt2.H08, Tt1.C10, Tt2.F04, Tt2.F07, Tt1.E11, Tt2.B02, Tt1.B01, Tt1.F02, and Tt2.B07) were described from *Tor tambroides* (Nguyen et al., 2007) while the locus MFW7 was derived from *Cyprinus carpio* (Crooijmans et al., 1997) **(Table 2)**. The forward primers were labelled with the TAMRA/HEX/FAM/ROX dye at the 5' end. Thermal cycling protocol for all loci was as follows: initial denaturation at 94 °C for 3 min followed by 30 cycles of denaturation at 94 °C for 30 s, annealing at 48 °C for 30 s, and extension at 72 °C for 30 s, with a final extension step at 72 °C for 10 min.

e-ISSN 2716-697X

Table 2: The 12 primers that were used in this study indicating the locus, the repeat motifs, the expected size of the amplicons and the primer sequence.

Locus	Repeat Motif	Size (bp)	Primer Sequence (5'-3')
A06	(ATTT)3(GTTT)4(ATT)8	217-231	F: CCGAAATGCATTCTTGTCTT R: GGACTGACACTGGGGATCAT
DO1	(TG)15	210-248	F: CCATTACGCCTTTGGAGTGT R: TGGGAGATGTTGTTTCTCCA
H08	(TC)14	178-188	F: GGCTGTGAATGTGTTTGTGG R: GCCAGGATGATGAGCATGTA
C10	(TG)13	181-217	F: GCTGAAGCAGGTGAATCTGA R: TGATGCCTGTCAAACCTGTG
F04	(AC)11	120-150	F: ATGCCAGCTACAGGTCCAAT R: CGTGTGTATGATGCCACCTC
F07	(AG)9	141-180	F: GAGACGACTCTAGTCGCTGACA R: GTGTGGCCAGTGTAGCTGAA
E11	(TG)23	146-230	F: GAGTCCCTACAGACGTATTTCCA R: TTCAGCTCAGAGGGGACACT
B02	(TG)15...(TG)3	137-203	F: CTGGGAACGTCAGTTTACGG R: GTCCCCACAAGGATAGCAGA
B01	(AC)8AT(AC)3...(TC)3	245-265	F: GAGGGGCATTTTGTTCTTGA R: GCTTCCCCTCATAAGCCTTC
F02	(TG)2TA(TG)4TC(TG) 2	246-258	F: CATGGACCAAATTACAAGGATTT R: AACCTGTGAGGGATGTCCAG
B07	(TG)3(TC)6TT(TC)3T T(TC)6	225-255	F: TGGAAATTGAGACAAAGCTTCA R: TATGTGGTTTCAGGCAGCAG
MFW	CA	284-384	F: TACTTTGCTCAGGACGGATGC R: ATCACCTGCACATGGCCACTG

e-ISSN 2716-697X

All the DNA amplifications were performed in a Mastercycler® gradient (Eppendorf AG, Germany). Upon successful amplification of microsatellite, PCR products were dispatched for fragment analysis service using Genetic Analyser ABI3730XL system (Applied Biosystems). Aliquots of amplified products with different fluorescent dyes were multiplexed. One microlitre of this mixture was mixed with 9 µL of highly deionised formamide spiked with GeneScan 500 LIZ Size Standard (Applied Biosystems) and denatured at 95 ºC for 5 min. The amplicons were resolved on an ABI 3730XL Genetic Analyser.

For microsatellite analyses, allele scoring, and genotyping of microsatellite traces was performed using Geneious Prime (Biomatters, 2014). Binning of microsatellite allele lengths was done using Tandem (Matschiner & Salzburger, 2009). For each locus in each population sample MICRO-CHECKER 2.2.3 (Van Oosterhout et al., 2004) was used to detect the presence of null alleles, large allele drop out and stuttering. ML-NullFreq (Kalinowski & Taper, 2006), a maximum likelihood estimator of the frequency of null alleles in a sample with or without missing data was used to estimate the frequency of null alleles for each locus in each population. To account for the bias introduced by null alleles, we utilized the ENA (Excluding Null Alleles) correction method implemented in the software FreeNA (Chapuis and Estoup, 2007) to estimate global and pairwise Fst values. These corrected values were compared against uncorrected estimates to ensure the robustness of the population structure inference. GENEPOP 4.2 (Raymond & Rousset, 1995) was employed at each locus for each population to test for statistically significant departures of genotype frequencies from expectations under Hardy–Weinberg equilibrium (HWE) using Fisher's exact test with P-values estimated via Markov Chain with 10 000 dememorizations, 200 batches, 5000 iterations and Bonferroni correction. Linkage between microsatellite loci was investigated using GENEPOP 4.2 The null hypothesis was tested using the Bonferroni correction (Rice et al., 2008). Freedom from selection pressure was verified using Ewens–Watterson test of neutrality (Slatkin, 1994) that involves testing the null hypothesis that observed homozygosity value for each locus lies within the 95% confidence interval (CI) of the expected homozygosity estimates provided by 1,000 simulated samples. Phylogeographical structuring among the populations using the microsatellites marker was inferred using a distance-based method. A matrix of pairwise genetic distance (Takezaki & Nei, 1996) was generated in Microsatellite Analyser (MSA) v4.05 (Dieringer & Schlötterer, 2003) with 10,000 iterations. A majority-rule consensus tree from 10,000 sets of unweighted paired group method (Dieringer & Schlötterer, 2003) with arithmetic mean (UPGMA) dendrogram was constructed using PHYLIP v3.965 (Felsenstein, 1989). To infer the directionality and magnitude of contemporary gene flow between river basins, we performed a Bayesian assignment test using the software [BAYESASS v3.0 / Migrate-n]. This analysis distinguishes between historical connectivity and recent migration rates (m). Additionally, evidence for recent genetic bottlenecks was rigorously tested using BOTTLENECK v1.2.02, applying the Two-Phase Model (TPM) with 95% single-step mutations and 5% multi-step mutations, as this model is most appropriate for microsatellite data.

e-ISSN 2716-697X

Population Structure Inference

Population genetic clustering was further assessed using STRUCTURE v2.3.4 under the admixture model with correlated allele frequencies. Ten independent runs were performed for K = 1–10, each with 100,000 burn-in iterations followed by 500,000 MCMC iterations. The optimal number of clusters (K) was determined using the ΔK method implemented in STRUCTURE HARVESTER.

Isolation by Distance

Isolation by distance was evaluated using a Mantel test implemented in GenAlEx v6.5, correlating pairwise genetic distances (F_{st}) with geographic distances (river-to-river) based on 10,000 permutations to assess significance.

RESULTS AND DISCUSSION

The microsatellite loci selected for this study were successfully employed across all the individuals across populations, with the following exceptions. Locus B02 did not show discernible amplicons in 34 individuals across ten populations (6-SLU, 8-SKI, 4-SKIR, 2-WCTE, 2-WCBA, 2-WCTO, 3-KSO, 7- KSU, 1-IRU, 2-KMP). Locus A06 did not show amplification patterns in 1 individual from SKI. Microchecker detected null alleles for D01 (19-28%), H08 (32-35%), C10 (16-32%), E11 (16-25%) and B02 (23-33%) at certain populations **(Table 3).**

Table 3: The total number of samples, number of alleles, observed heterozygosity, expected heterozygosity, and Hardy Weinberg Equilibrium observed at each of the 12 loci used in this study. Two of the loci (DO1) and (MFW7) were excluded from the statistical analysis due to the ambiguity in their amplification profile.

Locus	N	Na	Ho	He	HWE
A06	174	8	0.661	0.667	0.032
DO1*	175	22	0.726	0.889	0.005
H08*	173	10	0.225	0.499	0.000
C10*	175	23	0.646	0.920	0.001
F04	174	5	0.316	0.368	0.992
F07	174	4	0.155	0.164	0.831
E11*	174	46	0.506	0.945	0.000

B02*	141	22	0.468	0.777	0.000
MFW7*[a]	175	6	0.434	0.592	0.003
B01	175	13	0.566	0.804	0.549
F02[b]	175	2	0.011	0.011	NA
B07*	175	11	0.703	0.836	0.000

*The locus departed significantly from Hardy–Weinberg equilibrium after Bonferroni correction. N: sample size, Na: number of alleles, Ho: observed heterozygosity, He: unbiased expected heterozygosity, HWE (P): Probability at $P<0.05$,

NA: tests were not applicable, HS: Highly significant. [a]Excluded due to possible misgenotyping,

[b]Excluded due to being monomorphic

Higher null alleles frequencies were recorded when stutters were present. The locus E11 was reported to be not reliable and was rejected from the analysis to avoid errors in interpretation of the results. Post sequential Bonferroni correction, with ($P<0.05$), 16 of 216 comparisons were determined to deviate significantly from Hardy–Weinberg equilibrium exact tests. After computing the fraction of significant test on each vector and overall combined of P value using Fisher's method, it was shown that all HWE deviation could be traced to 5 loci (H08, B02, D01, C10, E11) with departures representing heterozygotes deficiencies.

F02 was almost exclusively homozygous (99%) and therefore regarded as monomorphic. Thus, ten loci were retained in subsequent analysis (A06, DO1, H08, C10, F04, F07, B02, MFW7, B01 and B07) after confirming neutrality and absence of linkage. The markers were polymorphic, yielding 124 alleles combined and with an average of 15 alleles per locus. The lowest number of alleles was observed in locus F07 with 4 and the highest in locus C10 with 23. Locus DO1 was the most polymorphic with respect to heterozygosity (Ho = 0.726) while F04 was the least polymorphic (Ho = 0.155) (Table 4).

Table 4: Bottleneck analysis

Subpopulation	Wilcoxon Test P (one tail for Hex)
River Kanarom	
Marak-Parak (KMP)	0.752
Sunsui (KSU)	0.809
Tangkol (KTA)	0.344
Sorinsim (KSO)	0.344
River Sugut	
Luanti (SLU)	0.722
Poring (SPO)	0.455
River Labuk	
Kinarasan (SKI)	0.125
Paus (SPA)	0.410
River Kinabatangan	
Kironggu (SKIR)	0.180
Pinipi (SPI)	0.545
River Pagalan	
Rugading (IRU)	0.320
Menserulong (IME)	0.248
River Kadamaian	
Tokulung (WCTO)	0.156
Lingkubang (WCLI)	0.500
River Tuaran	
Gontung (WCGO)	0.125
River Moyog	
Babagon (WCBA)	0.014
River Kimanis	
Doingin (WCDO)	0.273
River Bongawan	
Telantang (WCTE)	0.064

P, probability, Hex, heterozygosity excess. ($P<0.05$).

e-ISSN 2716-697X

The subpopulation in IME possessed the highest genetic diversity with respect to the expected heterozygosity and allelic richness (n = 9, uHE = 0.549, AR = 2.316). Allelic richness (Ar) is based on the smallest sample size for a site of 2 diploid individuals. Samples from KSU had the lowest genetic diversity (n = 8, uHE = 0.325, AR = 1.677). An insignificant excess and deficient heterozygote were observed in 12 (FIS: –0.018 to –0.875) and 8 localities (FIS: 0.002 to 0.362), respectively. After sequential Bonferroni correction, with ($P<0.05$), two localities departed significantly from HWE; WCGO and WCTE. Results from the BOTTLENECK analysis (Table 4) indicated that across nine populations, there was no evidence of genetic variation. Specifically, the lack of significant heterozygosity excess under the TPM model confirms the absence of recent severe bottlenecks in the majority of populations.

The graphical representation (Figure 3) shows the geographic distance-based substructure of the populations as two different groups that branch into three discrete clades. Rivers that originate in the Crocker Range and drain into the South China Sea are represented by the Western clade. The five rivers that flow into the Sulu Sea are host to populations from the Eastern clade.

e-ISSN 2716-697X

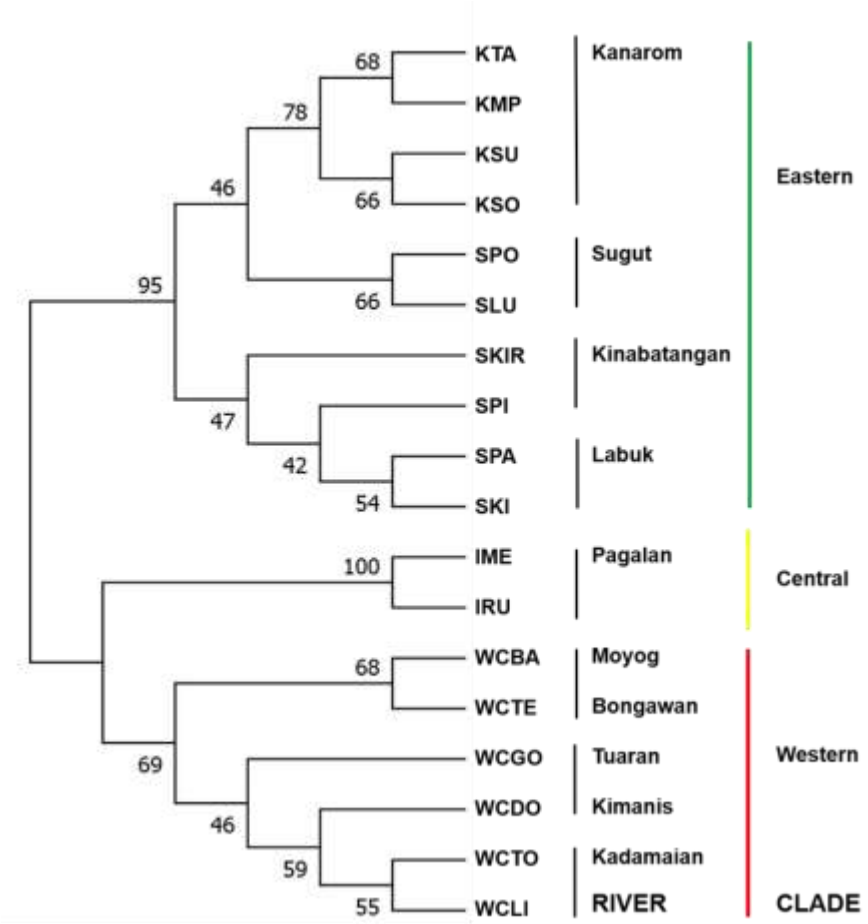

Figure 3: Majority-rule consensus tree of Pelian populations showing geographic structuring with some of the branches with lower statistical support (42–100%) in which two distinct major groups correspond to two independent evolutionary clades: (1) the western clade representing populations from the rivers Kadamaian, Tuaran, Moyog, Kimanis, and Bongawan; (2) the eastern and central clade representing populations from the rivers Kanarom, Sugut, Labuk and Kinabatangan, and Pagalan. The bootstrap values are shown in percent in the nodes

Directional Gene Flow:

Bayesian migration analysis revealed asymmetric gene flow patterns. Migration rates were generally low ($m < 0.05$), consistent with high Fst values. However, significant directional flow was observed from upstream to downstream populations in the Eastern clade, suggesting unidirectional dispersal likely driven by water currents and limited upstream migration due to physical barriers. The amount of variance explained by each model (Models 1, 2, and 3; populations grouped by current river distributions; and Model 4; populations grouped by current river distributions relative to the Crocker Trusmadi Range separation) was estimated using AMOVAs for the microsatellites data set

e-ISSN 2716-697X

In comparison to groups of five (70.27%, F_{st} = 0.230, p = 0.000 0.000), six (70.77%, F_{st} = 0.293, p = 0.000 0.000), and two (66.34%, F_{st} = 0.337, p = 0.000 0.000), rivers grouped as ten accounted for the biggest variability (72.21%, F_{st} = 0.278, p = 0.000 0.000). According to the AMOVA data, nearly all of the variation (70%) occurred within the populations, suggesting extensive gene flow between groups.

There was a significant but weak correlation between genetic and geographical distances (R2 = 0.206), with the exception of populations within a single riparian system, pairwise F_{st} suggested substantial genetic variance across the populations (F_{st} = 0.575-1.000, p 0.05) (Figure 4).

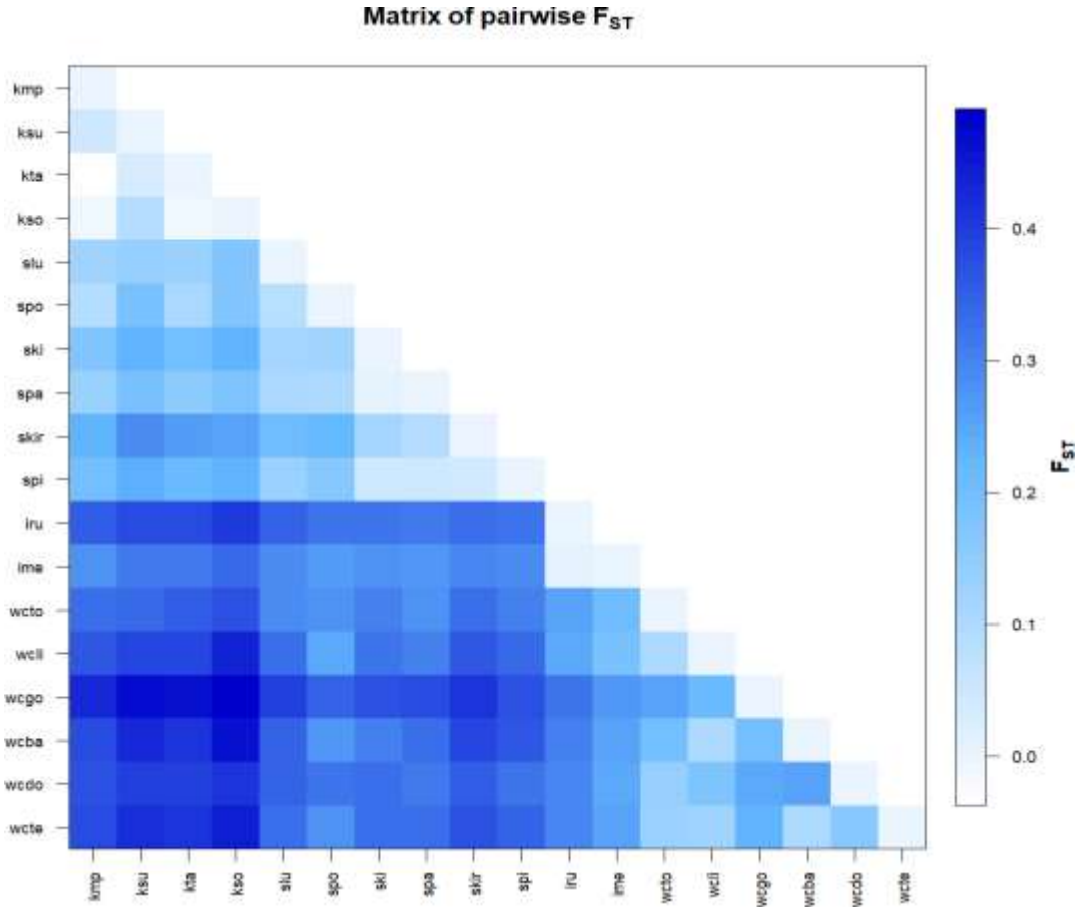

Figure 4. Heat map of pairwise F_{st} estimates for each locality. Pairwise F_{st} estimates for each locality, using microsatellites; dark blue squares represent high F_{st} values, and light blue squares represent low F_{st} values between localities.

Using microsatellite markers, the main genetic clusters, K with respect to ΔK, were at K = 2 (ΔK = 426.51) where grouping of the 175 individuals was consistent with the two major clades outlined using the UPGMA clustering method. The first cluster consisted of individuals from Clade 1 (Q = 97.1 – 99.6%) while the second cluster was made up of clade 2 (Q = 81.9 – 99.6%). Relatively weak differentiation was observed at K = 4 (ΔK = 43.35). The smallest mean value of Ln[P(X|K)] was at K = 1 {Ln[P(X|K)] = –5,570} before plateauing at K = 5 to K = 10 with mean Ln[P(X|K)] between -4138.89 and -3895.94. At K = 4, the proportion of ancestry in cluster one and cluster two was ranging from 40% to 98%, indicating some degree of genetic exchange between clusters whereas cluster three and four consistently above 78% indicating limited genetic exchange between the genetic clusters. The first cluster comprised individuals from KMP, KSU, KTA, KSO, SLU and SPO (Q = 34.0 – 98.1%), the second K comprised SLU, SPO, SKI, SPA, SKIR, and SPI (Q = 40.6 – 97.9%), the third K comprised IRU and IME (Q = 92.6 – 98.0), and the fourth K comprised WCTO, WCLI, WCGO, WCBA, WCDO, and WCTE (Q = 77.8 – 98.7%).

During the initial process of screening the microsatellite loci for deviations from HWE, the robustness of the HWE and Fis results were evaluated by comparing results with and without the inclusion of loci that did not amplify. Fis and HWE analysis were run with the complete 12 loci but removing a different locus at a time for each new analysis using the same parameters to identify the level of information provided by each locus on the level of HWE and Fis determination. When E11 was included in the determination of HWE across 18 populations, 8 populations deviated from HWE. The departures in these populations reflected a consistent deficiency of heterozygotes. Factors that generally result in heterozygote deficiencies include null alleles, the Wahlund effect and inbreeding. All the loci were affected equally thus eliminating the possibility of inbreeding being the cause of heterozygote deficiency. When this locus was discarded, those populations were in HWE except for 2 populations (WCGO and WCTE). E11 is suspected to be the source of HWE deviation to the populations because it is an unreliable locus to genotype which might lead to errors. Nguyen (2006) reported that this locus was unreliable in his study and our findings in this study concurred with his observations, leading to the decision to discard this locus.

The signature of the Wahlund effect was not detected in the multilocus analysis across loci and subsamples. The Wahlund effect registers concordantly across loci instead of just one or a few whereas null alleles are locus specific. Wahlund effect is a phenomenon when two genetically distinct groups are inadvertently grouped into a single sampling unit, either because they co-exist but rarely interbreed, or because the spatial scale chosen for sampling a site is larger than the true scale of a population, there will be more homozygotes than expected under HWE. Often the mutations that lead to the formation of null alleles will only occur in one or a few populations, so a heterozygote deficit might not be apparent across all populations in which this pattern is detected. Global significant deviation from Hardy–Weinberg proportions showed excessive variation across loci of F-statistics which represents a signature of null alleles that also recovered in this study. Thus , the factor that is most likely to produce HWE deviations in WCTE and WCGO population islikely to be presence of null alleles, and this has been reiterated by

the divergent conclusions can be arrived at when comparing biological significance and statistical significance (Waples & Allendorf, 2015).

Inbreeding is quite common in *Tor,* however, in this study, inbreeding was not evident in *T. tambra* populations which was represented by insignificant global Fis value across populations. There is very little evidence to suggest that there was a significant bottleneck event in the past that impacted the composition of the population and genetic diversity in Sabah, despite the decline in abundance observed in prior decades. The latest discovery appears to confirm that *T. tambra* is resistant to challenges presented by human interference in the riparian ecosystems examined in this study.

The population IME exhibited the highest microsatellite diversity (uHe=0.549, Ar=2.316) and KSU the lowest diversity uHE = 0.325, AR = 1.677). Across nine populations, there was no evidence of genetic variation, regardless of sample size. Nuclear loci exhibit biparental inheritance and allow different alleles to be distributed and combined at higher rates (Allendorf, 2017; Freeland et al., 2000). This suggests that colonization began in Sandakan before populations dispersed to eastern clades.

The major clades are in congruence with the results of the study of *Channa striata* (Robert et al., 2019),in which it has been reported that the populations are subdivided into two sub structured populations that are referred to as western and eastern clusters, respectively. The major clade grouping and the separation of Sabah into two parts by the Crocker and Trusmadi Range (CTR) coincide, even though the major river systems and the subclades do not. The historical and current linkages between rivers have a significant impact on the phylogeographical distribution of freshwater fish species, which is used to assess the genetic links between populations that have been detected. The main geological barrier separating Sabah's western and eastern riverine and floodplain environments is represented by the CTR. The Crocker Range (CR), which spans nearly 200 km and has mountains up to 4000 m in height, is the tallest range in Sabah's hilly western region. It has an average elevation of 2000 m and is more than 40 km broad. The second-highest mountain peak in Malaysia is located inside the 80 km Trusmadi Range (TR), which is next to the CR. On Sabah's east, middle, and north coasts, rivers that drain into the South China Sea originate in CTR and its mountains. Lower mountain ranges and plains with intermittent hills separating significant rivers like Kinabatangan River, Labuk River, and Sugut River, which flow into the Sulu Sea, extend into the western beaches, southern plains, and the interior or central part of Sabah. The eastern and central rivers range in length from 100 to 560 km, with the Kinabatangan River being the longest and widest floodplain. In general, the length of the western and northern rivers is less than 100 km. With the elevation of the Borneo Mountain ranges, the division of the eastern, central, northwestern, and southwestern clades took place in the late Miocene and Pliocene (5–1 mya). Through dispersal and subsequent population diversification brought on by geographic isolation, climate variations throughout the Pleistocene may have affected modern species distribution patterns. "The major clade grouping coincides with the Crocker and

Trusmadi Range (CTR). It is crucial to distinguish the temporal signals of different markers: while mitochondrial DNA (e.g., Cytb or D-loop) typically reflects ancient divergence events driven by geological barriers like the CTR, our microsatellite data reveals finer-scale, contemporary population structuring. The discordance between broad historical separation (mtDNA) and the highly fragmented current population structure (microsatellites) highlights that recent river fragmentation acts as a potent barrier to gene flow, superimposed on the historical vicariance templatesAs an alternative, the Pleistocene's low sea level permitted dispersal at river mouths and eventual isolation during sea level increases. Isolation by distance (IBD) (Briñoccoli et al., 2021), isolation by barriers (IBB) (Tsuji et al., 2022), and isolation by resistance (IBR) (De Queiroz et al., 2017) have been reported to influence genetic variation in riverine freshwater fishes.

The historical isolation by CTR and the current physical isolation of the rivers following the SHM, respectively, are demonstrated by the notable high genetic differentiation between clades and river systems, which are the causes of genetic variances in Tor populations. Additionally, the Mantel test revealed that, according to the IBD model, geographic distance had an impact on the genetic makeup of Tor populations. Due to the rugged terrain in Sabah, the majority of the rivers are divided from one another by mountain ridges; as a result, the populations along adjoining rivers are not connected genetically. However, some populations from geographically isolated but contemporaneously separated river basins, such as WCBA (Moyog River) and WCGO (Tuaran River), WCDO (Kimanis River) and WCTE (Bongawan River), SKIR (Kinabatangan River) and SKI, SPA (Labuk River), were found to be highly homogeneous. This finding lends support to the idea that there are gene flows between rivers. Using microsatellites, it was also found that the Moyog and Tuaran populations have a significant degree of affinity. Dispersal via a geomorphological phenomenon, such as river capture, stream piracy, flood occurrences, the historical connection between river systems, and manmade activity, including restocking programs and translocation, could account for the lack of genetic patterning.

If a population or group of populations has been reproductively isolated for long enough to contain unusual evolutionary combinations that are unlikely to revolve around an ecological time scale, then it fits the requirements for an evolutionarily significant unit (ESU) (Hallerman & Hilsdorf, 2014; Hutama et al., 2017). The analysis of data obtained from microsatellite markers implicated that the genetic differentiation between ESU is due to barriers by CTR. This study suggests that three clades be designated as ESU since they are all historically isolated, monophyletic, and have a high degree of genetic differentiation.

The Eastern clade comprises the Rivers Kanarom, Sugut, Kinabatangan, and Labuk. The Central clade encompasses the Pagalan River, the Western clade includes the of Rivers Bongawan, Kimanis, Moyog, Tuaran and Kadamaian. Short-term management depends on the identification of Management Units (MU), which can be used to direct current management initiatives including stocking programmes, quota allocation, alternative harvesting scenario modelling, and monitoring programme design. Populations from different river systems may have become isolated from each other due to habitat fragmentation.

Furthermore, based on our gene flow analysis, translocation strategies should prioritize 'upstream' conservation. Since downstream populations show higher admixture, they may serve as sources for genetic rescue, but care must be taken not to disrupt the unique local adaptations of isolated upstream populations (ESUs). Future barrier mitigation (e.g., fish ladders) should target areas where our Bayesian analysis identified blocked migration pathways. Consequently, gene flow might not be able to reverse genetic depletion if these populations were significantly affected by specific conditions, including overfishing. To maintain the persistence of the local populations that make up a fished stock, fisheries managers should manage local populations independently so that a sufficient proportion of individuals from each local population escape catch and reproduce.

Populations of MU show less evolutionary divergence than reciprocal monophyly and have significantly different allele frequencies at numerous loci (Moritz, 1999); however, allele frequency differentiation cannot be taken as direct proof of demographic independence (Palsbøll et al., 2007) proposed that the amount of genetic divergence at which populations become demographically independent should be used to identify MUs from population genetic data. MU status would then be given when the observed estimate of genetic divergence is significantly higher than a predetermined threshold value (Karjalainen et al., 2022) . Microsatellite results for Tor populations in Sabah appear to be significantly structured into geographically distinct subpopulations across major drainages, supporting data from mtDNA, where inter-stock dispersal and migration patterns were constrained by habitat fragmentation. (Biun et al., 2021). Gene flow is at least somewhat limited between populations, yet it still occurs frequently enough to guarantee genetic structure is generally homogenised to 5 genetic clusters.

The Department of Fisheries could use watersheds to delineate provisional MU. A similar study on Brook Trout, that reported on the delineation of structure based on riparian watersheds revealed that each watershed contained a population that was genetically distinct and demographically independent (Habera & Moore, 2005). Additionally, significant positive correlations between genetic differentiation and geographic distance among Tor populations might generate unique adaptations in each population due to variation of habitat conditions and contemporary environmental conditions. Studies has reported that local adaptation can contribute to the evolution of reproductive barriers and differences in life (Rajkov et al., 2018). *Tor* appear to be river specific in their migrations, indicating that the subpopulations acquired behavioural and or physiological adaptations to each river (Haryani, 2022; Hestirianoto et al., 2021).

Although studies of local adaptations have not been done to support this, minor genetic differences at neutral genomic loci, are indicators of fixation of alleles that can be interpreted as adaptations to a unique ecological niche (Larsen et al., 2007). Isolated populations undergo evolution in situ over time and can acquire distinct traits as well as reproductive barriers that curtail any attempt at artificial breeding with recruits from other populations.. The ten rivers investigated in for study were categorised as separate management unis of Tor all over Sabah drainage. The large spatial distribution and the diversity of ecological niches are representative

e-ISSN 2716-697X

of unique opportunities for evolution and adaptation and the outcome of this study recommend that the populations in each management unit be divided into multiple zones to conserve the locally adapted populations from being stocked with individuals from other populations.

CONCLUSION

The objective of this study was to assess the population diversity of Pelian in the riparian ecosystems of Sabah from the perspective of conservation of the species and the subsequent establishment of Management Units and Conservation Units. This was achieved by the application of 12 microsatellite loci from published literature across ten river systems. There was a clear sub structuring of the populations based on geographic barriers that supports existing theories of speciation by isolation. The findings of this study will serve as a reference for monitoring of the populations and contribute to the development of a large scale conservation and breeding program in Sabah.

ACKNOWLEDGEMENTS

This research was funded by UMSGreat, grant number **GUG0166-02/2017** and Department of Fisheries Sabah, grant number **D28 0005 0024**.

REFERENCES

Abdul-Muneer, P. M. (2014). Application of Microsatellite Markers in Conservation Genetics and Fisheries Management: Recent Advances in Population Structure Analysis and Conservation Strategies. *Genetics Research International*, *2014*. https://doi.org/10.1155/2014/691759

AHMAD, A., TN-NEK, S. A. R., & AMBAK, MOHD. A. (2006). Preliminary study on fish diversity of ulu tungud, meliau range, sandakan, sabah. *Journal of Sustainability Science and Management*, *1*(2).

Allendorf, F. W. (2017). Genetics and the conservation of natural populations: allozymes to genomes. *Molecular Ecology*, *26*(2). https://doi.org/10.1111/mec.13948

Biun, H., Sade, A., Robert, R., & Rodrigues, K. F. (2021). Phylogeographic structure of freshwater tor sp. In river basins of sabah, Malaysia. *Fishes*, *6*(4). https://doi.org/10.3390/fishes6040044

Briñoccoli, Y. F., Jardim de Queiroz, L., Bogan, S., Paracampo, A., Posadas, P. E., Somoza, G. M., Montoya-Burgos, J. I., & Cardoso, Y. P. (2021). Processes that drive the population structuring of Jenynsia lineata (Cyprinidontiformes, Anablepidae) in the La Plata Basin. *Ecology and Evolution*, *11*(11). https://doi.org/10.1002/ece3.7427

Chapuis, M. P., & Estoup, A. (2007). Microsatellite null alleles and estimation of population differentiation. Molecular biology and evolution, 24(3), 621-631.

Crooijmans, R. P. M. A., Bierbooms, V. A. F., Komen, J., Van Der Poel, J. J., & Groenen, M. A. M. (1997). Microsatellite markers in common carp (Cyprinus carpio L.). *Animal Genetics*, *28*(2). https://doi.org/10.1111/j.1365-2052.1997.00097.x

De Queiroz, L. J., Torrente-Vilara, G., Quilodran, C., da Costa Doria, C. R., & Montoya-Burgos, J. I. (2017). Multifactorial genetic divergence processes drive the onset of speciation in an Amazonian fish. *PLoS ONE*, *12*(12). https://doi.org/10.1371/journal.pone.0189349

Dieringer, D., & Schlötterer, C. (2003). MICROSATELLITE ANALYSER (MSA): A platform independent analysis tool for large microsatellite data sets. *Molecular Ecology Notes*, *3*(1). https://doi.org/10.1046/j.1471-8286.2003.00351.x

Esa, Y. B., Siraj, S. S., Daud, S. K., Ryan, J. J. R., Rahim, K. A. A., & Tan, S. G. (2008). Molecular systematics of mahseers (Cyprinidae) in Malaysia inferred from sequencing of a mitochondrial Cytochrome C Oxidase I (COI) gene. *Pertanika Journal of Tropical Agricultural Science*, *31*(2).

Felsenstein, J. (1989). {PHYLIP} -- Phylogeny Inference Package ({V}ersion 3.2). *Cladistics*, *5*.

Freeland, J. R., Romualdi, C., & Okamura, B. (2000). Gene flow and genetic diversity: A comparison of freshwater bryozoan populations in Europe and North America. *Heredity*, *85*(5). https://doi.org/10.1046/j.1365-2540.2000.00780.x

Habera, J., & Moore, S. (2005). Managing southern Appalachian brook trout: A position statement. *Fisheries*, *30*(7).

Hallerman, E., & Hilsdorf, A. W. S. (2014). Conservation genetics of tilapias: Seeking to define appropriate units for management. *Israeli Journal of Aquaculture - Bamidgeh*, *66*. https://doi.org/10.46989/001c.20769

Haryani, G. S. (2022). Migratory freshwater fish in Indonesia: Threats and conservation efforts. *IOP Conference Series: Earth and Environmental Science*, *1062*(1). https://doi.org/10.1088/1755-1315/1062/1/012001

Hestirianoto, T., Sulistiono, Wildan, D. M., Simanjuntak, C. P. H., Rahardjo, M. F., Syafruddin, D., Nugroho, T., & Ismanto, A. J. (2021). Application of radiotelemetry in tracking the movement of mahseer fish (Tor spp.) in Batang Toru River, North Sumatera Province Indonesia. *IOP Conference Series: Earth and Environmental Science*, *744*(1). https://doi.org/10.1088/1755-1315/744/1/012028

Hutama, A., Dahruddin, H., Busson, F., Sauri, S., Keith, P., Hadiaty, R. K., Hanner, R., Suryobroto, B., & Hubert, N. (2017). Identifying spatially concordant evolutionary significant units across multiple species through DNA barcodes: Application to the conservation genetics of the freshwater fishes of Java and Bali. *Global Ecology and Conservation*,*12*. https://doi.org/10.1016/j.gecco.2017.11.005

Ingram, B., Sungan, S., Tinggi, D., Sim, S. Y., & De Silva, S. S. (2007). Breeding performance of Malaysian mahseer, Tor tambroides and T. douronensis broodfish in captivity. *Aquaculture Research*, *38*(8). https://doi.org/10.1111/j.1365-2109.2007.01716.x

Kalinowski, S. T., & Taper, M. L. (2006). Maximum likelihood estimation of the frequency of null alleles at microsatellite loci. In *Conservation Genetics* (Vol. 7, Issue 6). https://doi.org/10.1007/s10592-006-9134-9

Karjalainen, J., Sjövik, R., Väänänen, T., Sävilammi, T., Sundberg, L. R., Uusi-Heikkilä, S., & Marjomäki, T. J. (2022). Genetic-based evaluation of management units for sustainable vendace (Coregonus albula) fisheries in a large lake system. *Fisheries Research*, *246*.https://doi.org/10.1016/j.fishres.2021.106173

Larsen, P. F., Nielsen, E. E., Williams, T. D., Hemmer-Hansen, J., Chipman,J. K., Kruhøffer, M., Grønkjær, P., George, S. G., Dyrskjøt, L., & Loeschcke, V. (2007). Adaptive differences in gene expression in European flounder (Platichthys flesus). *Molecular Ecology*, *16*(22). https://doi.org/10.1111/j.1365-294X.2007.03530.x

Matschiner, M., & Salzburger, W. (2009). TANDEM: Integrating automated allele binning into genetics and genomics workflows. *Bioinformatics*, *25*(15). https://doi.org/10.1093/bioinformatics/btp303

Moritz, C. (1999). Conservation units and translocations: Strategies for conserving evolutionary processes. In *Hereditas* (Vol. 130, Issue 3). https://doi.org/10.1111/j.1601-5223.1999.00217.x

Nguyen, T., Baranski, M., Rourke, M., & McPartlan, H. (2007). Characterization of microsatellite DNA markers for a mahseer species, Tor tambroides (Cyprinidae) and cross-amplification in four congeners. *Molecular Ecology Notes*, *7*(1). https://doi.org/10.1111/j.1471-8286.2006.01546.x

Palsbøll, P. J., Bérubé, M., & Allendorf, F. W. (2007). Identification of management units using population genetic data. *Trends in Ecology and Evolution*, *22*(1). https://doi.org/10.1016/j.tree.2006.09.003

Pinder, A. C., Britton, J. R., Harrison, A. J., Nautiyal, P., Bower, S. D., Cooke, S. J., Lockett, S., Everard, M., Katwate, U., Ranjeet, K., Walton, S., Danylchuk, A. J., Dahanukar, N., & Raghavan, R. (2019). Mahseer (Tor spp.) fishes of the world: status, challenges and opportunities for conservation. In *Reviews in Fish Biology and Fisheries* (Vol. 29, Issue 2). https://doi.org/10.1007/s11160-019-09566-y

Rajkov, J., Weber, A. A. T., Salzburger, W., & Egger, B. (2018). Immigrant and extrinsic hybrid inviability contribute to reproductive isolation between lake and river cichlid ecotypes. *Evolution*, *72*(11). https://doi.org/10.1111/evo.13612

Raymond, M., & Rousset, F. (1995). GENEPOP (Version 1.2): Population Genetics Software for Exact Tests and Ecumenicism. *Journal of Heredity*, *86*(3). https://doi.org/10.1093/oxfordjournals.jhered.a111573

Rice, T. K., Schork, N. J., & Rao, D. C. (2008). Methods for Handling Multiple Testing. In *Advances in Genetics* (Vol. 60). https://doi.org/10.1016/S0065-2660(07)00412-9

Robert, R., Amit, N. H., Sukarno, N. M., Majapun, R. J., & Kumar, S. V. (2019). Population genetic structure of Asian snakehead fish (Channa striata) in North Borneo: Implications for conservation of local freshwater biodiversity. *Ecological Research*, *34*(1). https://doi.org/10.1111/1440-1703.1008

Slatkin, M. (1994). An exact test for neutrality based on the Ewens sampling distribution. *Genetical Research*, *64*(1). https://doi.org/10.1017/S0016672300032560

Takezaki, N., & Nei, M. (1996). Genetic distances and reconstruction of phylogenetic trees from microsatellite DNA. *Genetics*, *144*(1). https://doi.org/10.1093/genetics/144.1.389

Tsuji, S., Shibata, N., Sawada, H., & Watanabe, K. (2022). Differences in the genetic structure between and within two landlocked Ayu groups with different migration patterns in Lake Biwa revealed by environmental DNA analysis. *Environmental DNA*. https://doi.org/10.1002/edn3.345

Van Oosterhout, C., Hutchinson, W. F., Wills, D. P. M., & Shipley, P. (2004). MICRO-CHECKER: Software for identifying and correcting genotyping errors in microsatellite data. *Molecular Ecology Notes*, *4*(3). https://doi.org/10.1111/j.1471-8286.2004.00684.x

Walton, S. E., Gan, H. M., Raghavan, R., Pinder, A. C., & Ahmad, A. (2017). Disentangling the Taxonomy of the Mahseers (Tor spp.) of Malaysia: An Integrated Approach Using Morphology, Genetics and Historical Records. In *Reviews in Fisheries Science and Aquaculture* (Vol. 25, Issue 3). https://doi.org/10.1080/23308249.2016.1251391

Waples, R. S., & Allendorf, F. (2015). Testing for hardy-weinberg proportions: Have we lost the plot? In *Journal of Heredity* (Vol. 106, Issue 1). https://doi.org/10.1093/jhered/esu062

Borneo International Journal of Biotechnology
(BIJB) Vol. 5 (December 2025), 32-48.

e-ISSN 2716-697X

Thermal Diversity of Bacteria and Their Secrets to Cold Survival

Ching Xin Jie[1], Noor Hydayaty Md Yusuf[1], Clemente Michael Wong Vui Ling[1*]

Biotechnology Research Institute, Universiti Malaysia Sabah, 88400 Kota Kinabalu, Sabah, Malaysia.

[*]Corresponding author's email: michaelw@ums.edu.my

Received: 29 September 2025 | Accepted: 20 December 2025 | Published: 31 December 2025

ABSTRACT

Temperature is a critical physical factor influencing the survival, growth, and metabolic activity of organisms on Earth. Changes in temperature alter molecular kinetic energy, thereby affecting chemical reaction rates and essential cellular processes. While most organisms exhibit optimal growth within a narrow temperature range, many bacteria display remarkable adaptability across diverse thermal conditions. Exposure to sudden decreases in ambient temperature triggers cold shock responses that enable bacterial adaptation to new growth conditions. Previous studies have shown that bacteria share common cold-adaptation strategies, including the upregulation of cold stress genes encoding proteins that facilitate translation by preventing the formation of inhibitory mRNA secondary structures. In addition, bacteria modify the lipid composition of their cell membranes by adjusting fatty acid chain length, saturation, and cis–trans configuration to maintain membrane fluidity under cold stress. Genomic GC content has also been implicated in thermal adaptation, as it influences DNA stability and growth capacity at different temperatures. Importantly, psychrophilic and psychrotolerant bacteria produce cold-active enzymes that remain functional at low temperatures. This review highlights current knowledge on bacterial cold adaptation mechanisms and discusses future research opportunities enabled by advanced multi-omics technologies.

Keywords: Bacteria, Cold adaptation, Cold shock proteins, Extremophiles, GC content, Lipid membrane composition.

e-ISSN 2716-697X

INTRODUCTION

Organisms that can survive and thrive at extreme temperatures are termed extremophiles, along with those that can live in extreme pH, pressure, and radiation. Most of these temperature extremophiles are made up of bacteria and archaea; however, there are a few eukaryotes that have evolved to adapt towards extreme temperatures as well (Singh, 2013; Ahmad et al., 2025). Each extremophile has different traits to help it survive and grow optimally at temperatures that are either too high or too low for most organisms to endure, and those traits have been studied for the past few decades, since they could be a breakthrough that would eventually enhance and improve human life. In general, these extremophiles can be divided into two thermal groups, namely psychrophiles and thermophiles, whereas organisms that live at moderate temperatures are known as mesophiles (Schiraldi & De Rose, 2002; Ahmad et al., 2025). However, some researchers would further divide the psychrophiles into true psychrophiles and psychrotrophs, and thermophiles into hyperthermophiles and normal thermophiles, based on their optimal growth temperature, as shown in Figure 1.

The core strategy that most extremophiles adopted to adapt to extreme temperatures is the unique metabolic activities of extremophiles that lead to the production of special enzymes, proteins, or even primary and secondary products (extremolytes) that would help other essential enzymes to maintain proper functionality at extreme temperatures (Lentzen & Schwarz, 2006; Rajawat et al., 2022). Some of these extremolytes can even affect the physiological properties of the cells in different ways to adapt to high or low temperatures (Tronelli et al., 2007). Further research on these metabolic strategies and extremolytes would eventually lead to the development in the field of pharmaceuticals as well as for biotechnology (Sandle & Skinner, 2012), reducing environmental pollution (O'Driscoll et al., 2014; Chu et al., 2001; Hamdan, 2018), the discovery of new energy sources (Curvers et al., 2014; Hamdan, 2018), and boosting the commercial value of various industrial products such as sugar processing, milk production and alcohol production (Mehta et al., 2016).

e-ISSN 2716-697X

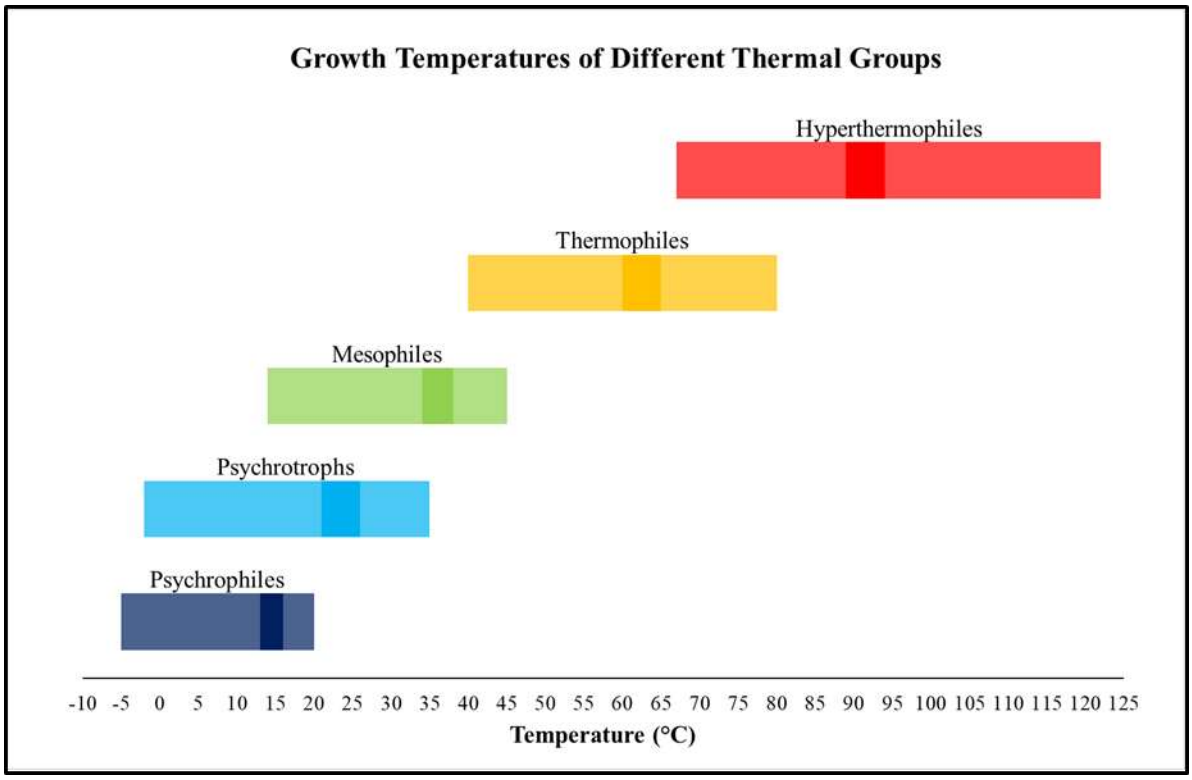

Figure 1: Growth temperature range for each thermal group. The darker region in each growth temperature bar represents the range of optimal growth temperature. Psychrophiles, including true psychrophiles and psychrotrophs, grow optimally at low temperatures, while thermophiles and hyperthermophiles have high optimal growth temperatures.

Psychrophiles, or cold-loving organisms, according to Morita (1975), are defined as "organisms having optimal temperature for growth at about 15 °C or lower, a maximal temperature for growth at about 20 °C, and a minimal temperature for growth at 0 °C or below". The cold environment made up the largest area on Earth. 70% of Earth is covered by the ocean with a temperature around 5 °C, whereas the polar region occupies another 15% (Singh, 2013).

One of the earliest studies on psychrophilic bacteria was reported in 1932 (Hampil, 1932). In 1959, Ingraham and Stokes came up with an article to discuss psychrophilic bacteria in detail, including ecology, physiology, and biochemistry of the bacteria (Ingraham & Stokes, 1959). The discovery of psychrophilic bacteria has provided insight into how life can be maintained under extreme cold. For example, Listeria monocytogenes, which can survive at refrigeration temperatures, is the main cause of food spoilage and contamination, even when foods are stored in cold temperatures (Farber & Peterkin, 1991). How the bacterium survives in such conditions leads to the study of cold adaptation in bacteria, to improve food quality and the health of consumers. Besides, further studies on psychrophilic bacteria led to the discovery of psychrophilic enzymes, which offer potential economic benefits (Feller & Gerday, 2003; Wang et

al., 2024). There is another thermal group of microorganisms that is always confused with psychrophiles, the psychrotrophs. Psychrotrophs are also referred to as facultative psychrophiles or psychrotolerant microorganisms. Psychrotrophs can grow at low temperatures, even down to 0°C (Gounot, 1986), but unlike true psychrophiles, they have optimal growth temperatures above 15°C (Moyer & Morita, 2007). Most of the psychrotrophs are determined as the main factor in food spoilage, particularly in the dairy industry (Champagne et al., 1994).

Organisms that live at intermediate temperatures are called mesophiles. They grow well at a moderate temperature ranging from 20°C to 45°C (Willey et al., 2008). When a mesophile is exposed to extreme temperature, its functional proteins or enzymes would either denature or turn inactive, which would lead to the mesophile's death. Most of the identified bacteria up until today are mesophilic bacteria. It is important to know that mesophilic bacteria have been involved in the preparation of beverages since ancient times, particularly in food fermentation. Mass production of beverages such as cheese, yoghurt, beers, and wine is possible thanks to the industrial application of bacteria. Mesophilic *Streptococci, Lactobacilli*, and *Bacilli*, for instance, can produce lactic acid (Rajvaidya & Markandey, 2006), which is particularly important in dairy products. *Escherichia coli* is probably the most important mesophilic bacterium to mankind. It is the most studied bacterium, and the understanding of it is much broader than that of other bacteria. Besides being economically valuable, *E. coli* is also very important in the field of research, such as bacteriology, biotechnology, and genetic engineering. Cloning technology involving *E. coli* is probably the most significant contribution of this bacterium in the realm of research (Lodish et al., 2000).

Despite being beneficial in many ways, some mesophilic bacteria are human pathogens. Since human body temperature is always around 37 °C, it makes a perfect place for the growth of most mesophilic bacteria, including pathogens. *Mycobacterium tuberculosis,* which grows best at around 35 °C to 37 °C is one of the most well-known mesophilic bacteria that are pathogenic to the mammalian respiratory system (Plorde, 2004).

A scorching environment can be found easily on Earth. Locations like hot springs, deserts, geothermal vents, and volcanic areas are extremely hot (Huber et al., 2000). These places are not habitable for most organisms, as heat will easily cause proteins and enzymes to denature, thus killing the organisms. However, thermophiles can adapt and survive in such environments with high temperatures. The term "thermophiles" generally denotes organisms that thrive at maximal growth temperatures between 70 °C and 80 °C. Only the hyperthermophiles reach and exceed 100°C, with 122°C being the current record for growth (Stetter, 2006; Madigan & Martino, 2006; De Maayer, 2022; Stetter, 2022).

Thermophilic bacteria have been identified to have optimum temperature from 55 °C to 105 °C, and many temperatures in between (Brock, 1986). *Thermus aquaticus* is the first thermophilic

bacterium to be discovered living in a hot spring in Yellowstone National Park, United States of America, by Brock (1997). Since then, thermophilic bacteria have been studied extensively due to their industrial potential. Taq polymerase, the crucial enzyme that makes polymerase chain reaction (PCR) amplification, is one of the successful products isolated from *T. aquaticus* (Chien et al., 1976).

Hyperthermophiles were once categorised as thermophiles. Like thermophiles, hyperthermophile lives in environments with high temperatures, except that the favoured temperatures are much higher than those tolerable by normal thermophiles. It is simply defined as an extreme thermophile, a bacterium that can live at a temperature higher than 90 °C (Brock, 2001). Although most of the hyperthermophiles are made up of Archaea, some non-Archaea bacteria can tolerate the extremely high temperature too. *Thermotoga maritime* is one of the most studied hyperthermophiles. It tolerates temperatures around 80 °C, which is too high for normal thermophilic bacteria to live in (Huber et al., 1986).

Cold Shock Response in Bacteria

Temperature is one of the best-defined environmental parameters that limit the activity, distribution, and survival of organisms. Temperature changes would affect biological systems, particularly in accelerating or decelerating the rate of biochemical reactions and shifting the reaction equilibrium in organisms (Rowbury, 2003; Wang et al., 2022). Proteins are one of the most important biomolecules that perform a vast array of functions in living organisms. However, the efficiency of proteins is greatly influenced by temperature. The high temperature would easily disrupt the non-covalent interactions that keep the protein in shape, leading to protein denaturation, while at low temperature, it would render most proteins inactive (Somero, 1995). Most organisms have evolved unique strategies to cope with different temperatures, for instance, by encoding proteins and enzymes that may withstand a range of temperatures or having isozymes that work at different temperatures (Vieille & Zeikus, 2001; Aouar et al., 2024; Ahmad et al., 2025). The adaptations are important to keep the function of the protein alive. Thermal stress occurs under heat or cold conditions; however, in this study, the focus is mainly on the response of bacteria under cold shock.

Cold Acclimation and Cold Adaptation

To successfully colonise low-temperature or high-temperature environments, living organisms have evolved at the molecular level, the whole cell, or even the ecosystem level. The process of these genetic and phenotypic change that accumulates over several generations in response to an organism's specific environmental niche is termed "adaptation" (Morgan-Kiss et al., 2006). Thermal adaptation refers to a prolonged period of exposure to a temperature above or below

the organism's optimal growth temperature, or the period of resumed exponential growth after a temperature shift (Frank et al., 2011; Dai et al., 2025). It takes a long time to achieve adaptation as it is part of an evolutionary process; however, changes in adaptation tend to be permanent, and the adaptive traits would be passed down to the offspring until the next adaptation happens.

Acclimation, in contrast to adaptation, which involves modification at the molecular level in response to environmental stress, refers to reversible, non-genetic changes in the phenotype of an organism that are induced by specific environmental conditions (Bennett & Lenski, 1997). It refers to temporary alterations, particularly physical reactions, that occur during a lifetime in response to transitory changes in surrounding conditions (Morgan-Kiss et al., 2006). It occurs during cold or heat shock, which is defined as the period immediately following a drop or rise in temperature of at least 10 °C until the organism re-enters the exponential stage of growth. Acclimation is often confused with the term "acclimatisation" (Barria et al., 2013). Both acclimation and acclimatisation refer to the same process; however, acclimation differs from acclimatisation in that, rather than the adaptive changes being induced by natural climate or environment, artificially induced environments are the ones that stimulate the modification or alteration.

Thermal adaptation and acclimation (or acclimatisation) are very crucial in the evolutionary process of bacteria. They work in continuation to ensure the survival of bacterial species during temperature shifts. Acclimation takes place right after an abrupt shift to a relatively low or high temperature, just to make sure that some of the bacteria survive the sudden temperature change. Then, adaptation starts working, generating some long-lasting adaptive traits that enable the bacteria to truly adapt to the new environment (Bradford, 2013). For instance, in response to cold shock, cold-induction protein, CIP, such as cold shock proteins, CSPs and cold acclimation proteins, CAPs will be highly expressed temporarily to sustain the viability of bacteria (Berger et al., 1996). Non-CIP would undergo some modification so that these proteins could function equally well at their optimal temperature. The process of adaptation will take some time, probably over several generations, to complete. CIP will then decrease gradually once bacteria have completely evolved the adaptive traits to adapt themselves towards the new temperature (Horn et al., 2007; Mittal et al., 2022).

Common Cold Stress Strategies in Bacteria

The fact that bacteria can thrive in such a wide range of temperatures shows that they have adopted some very effective strategies to cope with a sudden downshift in temperature. The three major thermal adaptations of bacteria include genomic Guanine (G) Cytosine (C) content, alteration of membrane lipids, and the production of extremolytes that could protect the bacteria from external stress (Russell, 1984).

e-ISSN 2716-697X

G+C content

The Guanine-Cytosine (GC) content varies widely, from as low as 16.5% to 75% in different bacterial species (Belozersky & Spirin, 1958), and several studies have proven that such an extreme range occurred due to mutational bias (Freese, 1962; Cox & Yanofsky, 1967). GC content in the genome has always been expected to be closely related to thermal adaptation in organisms, including bacteria (Musto et al., 2004; Zheng and Wu, 2010). For instance, when the samples were restricted to the Family level in prokaryotes, positive correlations were shown between genomic GC content and their respective optimal growth temperatures, supporting the idea of genomic base composition selection in response to different growth temperatures (Musto et al., 2004; Musto et al., 2006).

The speculation behind the selectionist hypothesis that GC content affects the growth temperature was established since the GC pair is bound by three hydrogen bonds, which confer higher thermal stability to the DNA itself (Yakovchuk et al., 2006; Aliperti et al., 2024), as well as higher-order structures of DNA and RNA transcripts (Biro, 2008). In another word, more energy or higher temperature is required to break the triple GC hydrogen bonds as compared to that of double bonds from Adenine-thymine base pairing, thus, genomes with higher GC content would tend to be thermally stable and the organisms itself is expected to be able to withstand higher growth temperature (Nishio et al., 2003; Musto et al., 2006). This thermodynamic hypothesis was further supported by a recent study involving 364 non-redundant bacterial genomes that shows evidence of a correlation between genomic GC content and optimal growth temperatures (Wu et al., 2012).

Despite all the studies supporting the correlation between genomic GC content and growth temperatures, this idea is still being debated by scientists. For instance, in 1997, Galtier and co-workers (1997) presented their findings, revealing that the correlation between GC content and optimal growth temperature is true only in ribosomal and transfer RNA stem, but not in the genomic DNA (Galtier & Lobry, 1997). These findings are then further strengthened in 2001, suggesting that only the GC content in structural RNA is strongly correlated with optimal temperature, while the genomic GC content and GC content in protein-coding genes (even at freely evolving sites) are not considered to take part in any form of thermal adaptation (Hurst & Merchant, 2001). Besides, a study in 2006 that reanalysed the data from Musto et al. (2004) proposed that the correlation is insignificant by claiming the use of more profound statistical methods rather than using a simple two-factor correlation analytical method (Wong et al., 2006). Furthermore, it is also proven that the GC content is also affected by multiple factors, including environment (Kembel & Jones 2022; Foerstner et al., 2005), nitrogen utilization (McEwan et al., 1998), the genome size (Heddi et al., 1998; Moran, 2002; Rocha & Danchin, 2002), aerobiosis (Naya et al., 2002), and state of free-living (Rocha and Danchin, 2002; Woolfit and Bromham, 2003), thus ruling out the idea that temperature alone can affect the G+C content in bacteria (Basak et al., 2005; Teng et al., 2023).

e-ISSN 2716-697X

Aid from cold stress proteins

While the correlation between G+C content at the whole-genome level and optimal growth temperature remains ambiguous, many studies have used G+C content as a preliminary indicator that certain genes do have a significant correlation with optimal growth temperatures (Galtier and Lobry, 1997; Zheng and Wu, 2010). The genomic G+C content in prokaryotes is mainly influenced by the G+C content of protein-coding sequences, which occupy the majority of the genome due to the absence of introns (Brocchieri, 2014). That is why looking closer into those specific genes in the genome separately would yield a different perspective of functional biology than just looking at the whole genome alone.

The fact that bacteria can thrive in such a wide range of temperatures suggests that they have adopted some very effective strategies to cope with the extremes in temperature, other than just modifying themselves. One of the major thermal adaptations of bacteria is the production of extremolytes that could protect the bacteria from external stress (Russell, 1984). These extremolytes are termed cold shock proteins, and they are highly produced after a rapid temperature shift, even though some of them are still being produced at relatively low levels under normal circumstances to regulate other biological functions.

Cold shock proteins (CSPs), or cold shock domains (CSDs), are protein domains of about 70 amino acids that have been found in prokaryotic and eukaryotic DNA-binding proteins (Doniger *et al*., 1992). The members of this CSP family are commonly found in the domain of eubacteria and appear to have various functions, such as transcriptional activators, RNA chaperones, and antifreeze protein (Graumann and Maraheil, 1998). Of all the CSPs, Csp-A-like protein (Csp-A) is the most common among bacteria, and its function is as an RNA chaperone (Yamanaka, 1999). This highlights the significance of CSPs as RNA chaperones as compared to other functions. CSPs are postulated to be one of the most important elements in the cold adaptation of bacteria, particularly psychrophiles and mesophiles (D'Amico et al., 2006; De Maayer et al., 2015). Normal cellular activities decreased at low temperatures due to the inactivation of the working proteins or enzymes. However, bacteria would induce CSPs, which could function normally to maintain their viability under cold conditions (De Maayer et al., 2015; Mittal et al., 2022).

Cold adaptation mechanisms of bacteria, especially psychrophilic bacteria, have always been of interest to researchers around the world. Many studies have been carried out, and several CSPs were identified and described in detail. For instance, CSPs from psychrophilic bacteria, *Shewanella livingstonensis* Ac10, were identified by different groups of researchers and were well described (Yoshimune et al., 2013). There are also a lot of studies on the CSPs from mesophilic bacteria. One of the earliest studies on mesophilic CSPs involved the induction of two classes of CSPs in *E. coli* (Jones et al., 1987). In 1997, *Enterococcus faecalis* JH2-2 was subjected to a cold-shock experiment, and results showed increased expression of 11 CSPs (Panoff et al., 1997). Expression CSPs do not just restrict to psychrophiles and mesophiles but are also demonstrated.

on thermophilic bacteria. Studies showed that thermophilic bacteria such as *Streptococcus thermophilic* (Wouters et al., 1999) and *Thermus aquaticus* (Jin et al., 2014) can produce CSPs as well.

Structural and dynamic features of CSPs have also been studied frequently to further investigate how the functional structure can affect the thermostability of CSPs of bacteria. As reported by Lee et al. in 2013, research on the Listeria monocytogenes (a psychrophilic bacterium) CspA (Lm-CspA) shows that it has a five-stranded β-barrel structure with hydrophobic core packing and two salt bridges. The study ended up concluding that the structural flexibility of Lm-CspA is one of the key factors that cause Lm-CspA to be less stable than mesophilic and thermophilic CSPs in terms of thermostability (Lee et al., 2013). However, there are no common CSPs except for CspA-like proteins that have been identified among bacteria so far, thus serving as a limitation to compare the functional structures of CSPs in different bacteria (Yamanaka, 1999).

Structural adaptation of cold-active enzymes

Most Antarctic psychrophiles and psychrotolerants that thrive at sub-zero temperatures need to continue to carry out cell function to survive and continue to grow. The main challenges for life at these temperatures are the exponential decrease in the chemical reaction rates. Hence, to maintain metabolic activities, they need to produce cold-active enzymes that exhibit high catalytic activities (k_{cat}) at low temperatures, often at a trade-off of thermal stability (Collins & Feller, 2023). The key structural adaptation to maintain high activity at low temperatures is to have increased conformational flexibility, to allow the enzymes to use a minimal amount of energy to carry out their tasks (Sarmiento et al., 2015). To achieve these, cold-adapted enzymes lower the number of salt bridges, hydrogen bonds, and ion pairs within the active site region, and harbour longer and more glycine-rich loops, which increase the local entropy and flexibility of the protein backbone (Collins & Feller, 2023). Those enzymes also undergo amino acid substitution to maintain their flexibility, for instance, by replacing large hydrophobic residues, such as isoleucine or phenylalanine, with smaller ones, namely, valine or alanine. This creates small internal cavities that increase the mobility of the internal groups, thereby reducing the enthalpy of activation for catalysis (Feller, 2013). All these adaptations allow them to have distinct thermodynamic profiles. Overall, cold-active enzymes, unlike enzymes from mesophilic and thermophilic counterparts, typically have a reduced $\Delta H^{\ddagger}$ and a greater negative activation entropy ($\Delta S^{\ddagger}$). Nonetheless, this frequently results in a reduction in substrate affinity (higher K_m), as the highly adaptable active site may not engage the substrate as firmly as a rigid one (Collins & Feller, 2023), but is sufficient to allow psychrophiles and psychrotolerants to adapt well to the extreme cold.

e-ISSN 2716-697X

Another mechanism adopted by bacteria to adapt to a cold environment is the alteration of membrane composition. The plasma membrane is a selective barrier made up of a phospholipid bilayer, which is susceptible to changes in environmental temperature (Mansilla et al., 2004). The effect of temperatures on membranes has been studied extensively to find out the role of membrane lipid composition in thermal adaptation. Previous studies suggested that bacteria, in general, can modulate membrane fluidity by altering their fatty acid composition (Chintalapati et al., 2004). Russell, in 1984, has described the interaction between bacterial membrane and temperature in detail (Russell, 1984).

These alterations of membrane composition mostly happen in the fatty acyl constituents of phospholipids and glycolipids (Russell, 1984). Although it happens less frequently, bacteria could also achieve the alteration by altering lipid head group, the protein content of the membrane, the length of fatty acid chain, the cis-trans proportion of fatty acid, and the synthesis of various carotenoids (Chintalapati et al., 2004).

Rapid temperature shift would lead to phase separation of a phospholipid, and thus, decrease membrane fluidity and increase permeability (Cao-Hoanget et al., 2010; Sun et al., 2025). For example, membrane fluidity of *Bacillus subtilis* at temperatures lower than its optimal growth temperature revealed two distinct adaptation mechanisms, including the increase in the ratio of anteiso- to iso- branched fatty acids, and rapid desaturation of phospholipids' fatty acid chains by fatty acid desaturase (Beranová et al., 2008). The membrane alteration process involves a chain reaction between sensor kinase DesK and response regulator DesR, which eventually induces synthesis of D5-desaturase (Beranová et al., 2008; Barria et al., 2013).

Studies on the membrane also found that temperature could affect the proteins embedded in the membrane as well. Investigation of 66 membrane proteins during cold shock suggested that there are changes in amino acid composition and hydrophobicity in these proteins (Kahlke & Thorvaldsen, 2012). The results undoubtedly linked the membrane proteins down to the amino acid level to the cold adaptation strategies of bacteria.

Cold Stress Response in Thermophiles

Although there are significantly fewer cold shock studies on thermophiles as compared to mesophiles and psychrophiles, cold stress responses were documented from a few thermophilic species (Ranawat & Rawat, 2017; De Maayer, 2022). Cold shock exposed on thermophilic bacterium *Thermoanaerobacter tengcogensis* MB4 revealed that the bacterium uses some of the above mentioned cold stress strategies, including maintenance of bacterial cell membrane fluidity by regulation of several fatty acids and glycerophospholipid biosynthesis genes, as well as high expression of CSP encoded by gene TteCspC which helped to regulate the expression of various genes while act as RNA chaperone to maintain transcriptional processes in the cell (Liu et al., 2014).

e-ISSN 2716-697X

Other than these common cold shock responses that can be seen in other thermal groups, the same study by Liu et al. (2014) further discovered several cellular processes that were involved in the thermophilic cold acclimation. These include DNA replication, recombination, and repair to defend against cold-induced damage, flagellar biosynthesis and motility as an escape attempt from the environmental stress, induction of signal transduction to detect, respond and adapt to cold stress, and increasing energy production to synthesise more specific proteins to cope with the cold stress. Besides, cold adaptation strategies such as endospore formation and natural competence were also reported as measures for long-term survival (Liu et al., 2014; Molle and Lemos, 2025). Similar responses were also reported on *Thermus* sp. GH5 and *Bacillus stearothermophilus* TLS33, where CSPs were related to signal transduction that would initiate bacterial sporulation (Topanurak et al., 2005), the energy metabolism pathway was reconfigured, and different amino acids were synthesised in response to different cold shock conditions (Yousefi-Nejad et al., 2011).

General Discussions

Bacteria play important roles as the primary agents for nutrient cycling in every corner of the earth, and this is even more important in the polar or cold region that lacks higher organisms, which are also important contributors to nutrient cycling. Thus, in the polar regions, the roles depend mainly on the lower organisms, especially the psychrophiles and psychrotolerants (Deming, 2002; Cavicchioli, 2006) that are well adapted to the local environments, and their ecological roles are vital for maintaining the polar biogeochemical balance. The above review provides an overview of bacteria from different thermal groups, their characteristics and how they adapt to their thermal niches, with and special focus on the psychrophiles and psychrotolerants. These adaptations are closely related to their dominance in the habitats they live in, and their active roles in the cycling of carbon, nitrogen, and other elements. At the same time, they also carry out decomposition of penguins, seals and birds' carcasses to enrich the nutrient-deficient terrestrial environments (Zdanowski, et al., 2005; Schaefer, et al., 2023; Zaini, et al., 2024). In summary, microbes, especially the bacteria that can withstand cold temperatures and perform decomposition and nutrient cycling, ensure that there are sufficient nutrients to sustain the life of microorganisms and some higher organisms, such as lichen and mosses, in the harsh Antarctic continent.

General Conclusion

Temperature is one of the most important environmental parameters that would affect the vitality of living organisms; thus, adaptation to different growth temperatures or sudden changes in surrounding temperature is crucial, especially for extremophiles (Barria et al., 2013). Besides the above common cold acclimation and cold adaptation strategies, many bacteria have also adopted their own unique strategies in order to cope with different cold stresses. Some of these strategies still remain undiscovered today, as many hypothetical proteins with unknown

functions were found to be involved in the process of cold adaptation (da Costa *et al*., 2018). Moreover, many genes might seem irrelevant to cold stress response, but they are involved in metabolism pathways that are actually part of the cold stress response as well. Bacterial cells comprise a complex metabolic network, but the interacting genes and metabolic reactions have been approached and studied as separate systems most of the time, despite knowing that many of these metabolic pathways are interdependent on one another.

The investigation of cold adaptation in bacteria requires a comprehensive multi-omics approach to encompass the complete intricacy of the biological response. While RNA-sequencing may offer a detailed perspective of the expressed genes, it needs collaborative information at proteomics and metabolomics levels to address post-transcriptional controls and actual metabolic fluxes. These will provide a holistic system biology coverage in revealing how the genome, transcriptome, and proteome interact to shift the metabolome toward a cold-adaptation state. These multi-omics are very important to resolve the functions of genes, especially in establishing the function of hypothetical genes and genes of unknown functions, considering that there are many genes involved in cold-adaptation that have yet to be discovered. Only through a multi-approach system biology analysis can we eventually understand the whole cold-adaptation strategies of the Antarctic microbes better (Govil et al., 2021). This multi-omics approach can also be capitalised to research on psychrophiles, especially obligate psychrophiles from deep-sea and sub-glacial environments that are currently difficult to culture. By combining the use of culture-independent metagenomic techniques, meta-proteomics, and metatranscriptomic and other new technologies, it is hoped that the adaptation mechanisms and strategies of obligate psychrophiles can be revealed and provide us with a better picture of how microscopic living things can live in a near-impossible cold place for many other organisms.

REFERENCES

Ahmad, S., Muflih, M. H., Al-Qadiri, H. M., & Hani, K. B. (2025). The extremophiles: Adaptation mechanisms and biotechnological applications. *Biology,* 14(4), 412.

Aliperti, L., Farfañuk, G., Couso, L. L., Soler-Bistué, A., Aptekmann, A. A., & Sánchez, I. E. (2024). r/K selection of GC content in prokaryotes. *Environmental Microbiology,* 26(2), e16511.

Aouar, B., Arrar, L., & Mezaache-Aichour, S. (2024). Advances in extremophile research: Biotechnological applications through isolation and identification techniques. *Microbiology Open,* 13(2), e1457

Barria, C., Malecki, M., & Arraiano, C.M. (2013). Bacterial adaptation to cold. *Microbiology,* 159, 2437-2443.

Basak, S., Mandal, S., & Ghosh, T.C. (2005). Correlations between genomic GC levels and optimal growth temperatures: some comments. *Biochemical and Biophysical Research Communications,* 327(4), 969-970.

Belozersky, A.N. & Spirin, A.S. 1958. A correlation between composition of deoxyribonucleic and ribonucleic acid. *Nature,* 182, 111-112.

Bennett, A.F. & Lenski, R.E. (1997). Evolutionary adaptation to temperature. VI. Phenotypic acclimation and its evolution in *Escherichia coli*. *Evolution,* 51(1), 36-44.

Beranová, J., Jemioła-Rzemińska, M., Elhottová, D. et al. (2008). Metabolic control of the membrane fluidity in *Bacillus subtilis* during cold adaptation. *Biochimica et Biophysica Acta – Biomembranes,* 1778(2), 445-453.

Berger, F., Morellet, N., Menu, F. et al. (1996). Cold shock and cold acclimation proteins in the psychrotrophic bacterium *Arthrobacter globiformis* SI55. *Journal of Bacteriology,* 178(11), 2999-3007.

Cao-Hoang, L., Dumont, F., Marechal, P.A. et al. (2010). Inactivation of *Escherichia coli* & *Lactobacillus plantarum* in relation to membrane permeabilization due to rapid chilling followed by cold storage. *Archives of Microbiology,* 192, 299-305.

Cavicchioli, R. (2006). Cold-adapted archaea. *Nature Reviews Microbiology*, 4(5), 331-343.

Champagne, C.P., Laing, R.R., Roy, D. et al. (1994). Psychrotrophs in dairy products: their effects and their control. *Critical Reviews in Food Science and Nutrition,* 34(1), 1-30.

Chien, A., Edgar, D.B., & Trela, J.M. (1976). Deoxyribonucleic acid polymerase from the extreme thermophile *Thermus aquaticus*. *Journal of Bacteriology,* 128(3), 1550-1557.

Dai, R., Sun, X., Zhu, J., Geng, J., & Wang, W. (2025). Metabolic rearrangement enables adaptation of microbial growth rate to temperature shifts. *Nature Microbiology,* 10(3), 856–867.

D'Amico, S., Collins, T., Marx, J. et al. (2006). Psychrophilic microorganisms: challenges for life. *EMBO Reports,* 7(4), 385-389.

Da Costa, W.L.O., de Aragão Araújo, C.L., Dias, L.M. et al. (2018). Functional annotation of hypothetical proteins from the *Exiguobacterium antarcticum* strain B7 reveals proteins involved in adaptation to extreme environments, including arsenic resistance. *PLoS One,* 13(6), e0198965.

Deming, J. W. (2002). Psychrophiles and polar regions. *Current Opinion in Microbiology*, 5(3), 301-309.

De Maayer, P., Anderson, D., Cary, C. et al. (2015). Some like it cold: understanding the survival strategies of psychrophiles. *EMBO Reports,* 15(5), 508-517.

De Maayer, P. (2022). Freezing" Thermophiles: From One Temperature Extreme to Another**.** *Microorganisms,* 10(12), 2417.

Doniger, J., Landsman, D., Gonda, M.A., et al. (1992). The product of unr, the highly conserved gene upstream of N-ras, contains multiple repeats similar to the col-shock domain (CSD), a putative DNA binding motif. *The New Biologist,* 4(4), 389-395.

Farber, J.M. & Peterkin, P.I. (1991). *Listeria monocytogenes*, a food-borne pathogen. *Microbiology Review,* 55(3), 476-511.

Feller, G. (2013). Psychrophilic enzymes: from folding to function and biotechnology. Scientifica, 2013(1), 512840.

Freese, E. (1962). On the evolution of the base composition of DNA. *Journal of Theoretical Biology,* 3(1), 82-101.

Galtier, N. & Lobry, J.R. (1997). Relationships between genomic G+C content, RNA secondary structures, and optimal growth temperature in prokaryotes. *Journal of Molecular Evolution,* 44(6), 632-636.

Gounot, A.M. (1986). Psychrophilic and psychrotrophic microorganisms. *Experientia,* 42(11), 1192-1197.

Govil, T., Sharma, W., Salem, D. R., & Sani, R. K. (2021). Multi-omics approaches for extremophilic microbial, genetic, and metabolic diversity. In *Extreme Environments* (pp. 311-329). CRC Press.

Graumann, P. & Marahiel, M.A. (1998). A superfamily of proteins that contain the cold-shock domain. *Trends in Biochemical Sciences,* 23, 286-290.

Hamdan, A. (2018). Psychrophiles: ecological significance and potential industrial application. *South African Journal of Science,* 114(5-6), 1-6.

Hampil, B. (1932). The influence of temperature on the life processes and death of bacteria. *The Quarterly Review of Biology,* **7**(2), 172-196.

Heddi, A., Charles, H., Khatchadourian, C., et al. (1998). Molecular characterization of the principal symbiotic bacteria of the weevil *Sitophilus oryzae*: a peculiar G+C content of an endocytobiotic DNA. *Journal of Molecular Evolution,* 47(1), 52-61.

Horn, G., Hofweber, R., Kremer, W. et al. (2007). Structure and function of bacterial cold shock proteins. *Cellular and Molecular Life Sciences,* 64(12), 1457-1470.

Huber, R., Huber, H., & Stetter, K.O. (2000). Towards the ecology of hyperthermophiles: biotopes, new isolation strategies and novel metabolic properties. *FEMS Microbiology Reviews,* 24, 615-623.

Huber, R., Langworthy, T.A., König, H. et al. (1986). *Thermotoga maritime sp. nov.* represents a new genus of unique extremely thermophilic eubacteria growing up to 90^{O}C. *Archives of Microbiology,* 144(4), 324-333.

Hurst, L.D. & Merchant, A.R. (2001). High guanine-cytosine content is not an adaptation to high temperature: a comparative analysis amongst prokaryotes. *Proceedings of the Royal Society B: Biological Sciences,* 268(1466), 493-497.

Ingraham, J.L. & Stokes, J.L. (1959). Psychrophilic Bacteria. *Bacteriological Reviews,* 23, 97-108.

Jin, B., Jeong, K.W., & Kim, Y. (2014). Structure and flexibility of the thermophilic cold-shock protein of *Thermus aquaticus*. *Biochemical and Biophysical Research Communications,* 451(3), 402-407.

Jones, P.G., VanBogelen, R.A., & Neidhardt, F.C. (1987). Induction of proteins in response to low temperature in *Escherichia coli*. *Journal of Bacteriology,* 169, 2092-2095.

Kahlke, T. & Thorvaldsen, S. (2012). Molecular characterization of cold adaptation of membrane proteins in the *Vibrionaceae* core-genome. *PLoS One,* 7(12), e51761.

Kembel, S. W., & Jones, A. E. (2022). Soil, ocean, hot spring, and host-associated environments reveal unique selection pressures on genomic features of bacteria in microbial communities. *Nature Ecology and Evolution,* 7(4), 570–580.

Lee, J., Jeong, K.W., Jin, B. et al. (2013). Structural and dynamic features of cold-shock proteins of *Listeria monocytogenes*, a psychrophilic bacterium. *Biochemistry,* 52(14), 2492-2504.

Lentzen, G. & Schwarz, T. (2006). Extremolytes: natural compounds from extremophiles for versatile applications. *Applied Microbiology and Biotechnology,* 72(4), 623-634.

Liu, B., Zhang, Y.H., & Zhang, W. (2014). RNA-Seq-based analysis of cold shock response in *Thermoanaerobacter tengcogensis*, a bacterium harboring a single cold shock protein encoding gene. *PLoS One,* 9(3), e93289.

Lodish, H., Berk, A., Zipursky, S.L., et al. (2000). *Molecular Cell Biology*. New York: W.H. Freeman Publisher.

Madigan, M.T. & Martino, J.W. (2006). *Brook Biology of Microorganisms* (11th ed.). New Pearson Prentice Hall, New York.

Mansilla, M.C., Cybulski, L.E., Albanesi, D. et al. (2004). Control of membrane lipid fluidity by molecular thermosensors. *Journal of* Moyer, C.L. & Morita, R.Y. (2007). *Psychrophiles and Psychrotrophs*. New Jersey: John Wiley & Sons Ltd.

Musto, H., Naya, H., Zavala, A., et al. (2004). Correlations between genomic GC levels and optimal growth temperatures in prokaryotes. *FEBS Letters,* 573(1-3), 73-77.

Musto, H., Naya, H., Zavala, A., et al. (2006). Genomic GC level, optimal growth temperature, and genome size in prokaryotes. *Biochemical and Biophysical Research Communications,* 347(1), 1-3.

Naya, H., Romero, H., Zavala, A. et al. (2002). Aerobiosis increases the genomic guanine plus cytosine content (GC%) in prokaryotes. *Journal of Molecular Evolution,* 55(3), 260-264.

Nishio, Y., Nakamura, Y., Kawarabayasi, Y. et al. (2003). Comparative complete genome sequence analysis of the amino acid replacements responsible for the thermostability of *Corynebacterium efficiens*. *Genome Research,* 13, 1572-1579.

O'Driscoll, K., Princeton, N.J., Sambrotoo, R. et al. (2014). Bioremediation of persistent organic pollutants using thermophilic bacteria. US 2014/0042087 A1.

Panoff, J.M., Corroler, D., Thammavongs, B. et al. (1997). Differentiation between cold shock proteins and cold acclimation proteins in a mesophilic Gram-positive bacterium, *Enterococcus faecalis* JH2-2. *Journal of Bacteriology,* 179(13), 4451-4454.

Plorde, J.J. (2004). Mycobacteria. In: *Sherris Medical Microbiology* (Ryan, K.J. & Ray, C.G., eds.), pp 439-456. McGraw-Hill Medical Publishing Division, New York.

Rajvaidya, N. & Markandey, D.K. (2006). *Industrial Applications of Microbiology*. A P H Publishing Corp, New Delhi.

Rajawat, A., Singh, A., & Gupta, P. (2022). Perspectives on the microorganism of extreme environments and their applications. *Microbial Cell Factories,* 21(1), 143.

Ranawat, P. & Rawat, S. (2017). Stress response physiology of thermophiles. *Archive of Microbiology,* 199, 391-414.

Russell, N.J. (1984). Mechanisms of thermal adaptation in bacteria: blueprints for survival. *Trends in Biochemical Sciences,* 9(3), 108-112.

Sandle, T. & Skinner, K. (2012). Study of psychrophilic and psychrotolerant micro-organisms isolated in cold rooms used for pharmaceutical processing. *Journal of Applied Microbiology,* 114(4), 1166-1174.

Stetter, K. O. (2022). A brief history of the discovery of hyperthermophilic life. *Extremophiles,* 26(6), 1-13.

Sun, B., Fan, C., Shi, X., Hu, Z., and Chen, J. (2025). Cold stress enhances cryotolerance in Lacticaseibacillus rhamnosus B6 via membrane lipid remodeling and differential protein expression. *Current Research in Microbial Sciences,* 9, 100453.

Teng, W., Liao, B., Chen, M., Shu, W., & Faucher, S. P. (2023). Genomic legacies of ancient adaptation illuminate GC-content evolution in bacteria. *Microbiology Spectrum,* 11(1), Article e02145-22.

Topanurak, S., Sinchaikul, S., Sookkheo, B. et al. 2005. Functional proteomics and correlated signaling pathway of the thermophilic bacterium *Bacillus stearothermophilus* TLS33 under cold-shock stress. *Proteomics,* 5(17), 4456-4471.

Tronelli, D., Maugini, E., Bossa, F. et al. (2007). Structural adaptation to low temperatures – analysis of the subunit interface of oligomeric psychrophilic enzymes. *The FEBS Journal,* 274(17), 4595-4608.

Vieille, C. & Zeikus, G.J. (2001). Hyperthermophilic enzymes: sources, uses, and molecular mechanisms for thermostability. *Microbiology and Molecular Biology Reviews,* 65(1), 1-43.

Wang, H., Dell, A. I., Sinsabaugh, R. L., & Gittelson, O. D. (2022). A general theory for temperature dependence in biology. *Proceedings of the National Academy of Sciences,* 119(31), e2120058119.

Wu, H., Zhang., Z., Hu, S., et al. (2012). On the molecular mechanism of GC content variation among eubacterial genomes. *Biology Direct,* 7, 2.

Yakovchuk, P., Protozanova, E., & Frank-Kamenetskii, M.D. (2006). Base-stacking and base-pairing contributions into thermal stability of the DNA double helix. *Nucleic Acid Research,* 34(2), 564-574.

Yamanaka, K. (1999). Cold shock respsonse in *Escherichia coli*. *Journal of Molecular Microbiology and Biotechnology,* 1(2), 193-202.

Yoshimune, K., Kawamoto, J., & Kurihara, T. 2013. Proteins involved in cold adaptation. In: *Cold-adapted Microorganisms* (Yumoto, I. ed.), pp. 97-107. National Institute of Advanced Industrial Science and Technology, Japan.

Yousefi-Nejad, M., Naderi-Manesh, H., & Khajeh, K. (2011). Proteomics of early and late cold shock stress of thermophilic bacterium, *Thermus* sp. GH5. *Journal of Proteomics,* 74(10), 2100-2111.

Zaini, N. A., Ismail, S. S., Low, V. L., Mahmud, M. H., Houssaini, J., Lee, W. Y., & Heo, C. C. (2024). Soil chemical properties associated with penguin carrion in Barton Peninsula, King George Island, Antarctica. *Polar Biology*, 47(7), 681-691.

Zdanowski, M. K., Zmuda, M. J., & Zwolska, I. (2005). Bacterial role in the decomposition of marine-derived material (penguin guano) in the terrestrial maritime Antarctic. *Soil Biology and Biochemistry*, 37(3), 581-595.

Zheng, H. & Wu, H. (2010). Gene-centric association analysis for the correlation between the guanine-cytosine content levels and temperature range conditions of prokaryotic species. *BioMed Central Bioinfomatics,* 11(11), S7.

Borneo International Journal of Biotechnology (BIJB) Vol. 5 (December 2025), 49-63.

e-ISSN 2716-697X

Antioxidant and Hepatoprotective Potential of *Hedyotis diffusa*: A Sabah Native Plant

Gilbert Ringgit[1], Robin Jacobson Laurduraj[1], Mohammad Iqbal[1]*

Biotechnology Research Institute, Universiti Malaysia Sabah, Jalan UMS, 88400 Kota Kinabalu, Sabah, Malaysia
*Corresponding author's email: miqbal@ums.edu.my

Received: 9 October 2025 | Accepted: 20 December 2025 | Published: 31 December 2025

ABSTRACT

Hedyotis diffusa is a medicinal plant recognized for its potential as an alternative natural drug due to its rich polyphenol content. These compounds are known to possess antioxidant and hepatoprotective activities, which may be beneficial in treating liver diseases—a major cause of human mortality worldwide. This research was conducted to determine the phenolic compounds and their scavenging activity in *Hedyotis diffusa*. Additionally, *in vivo* experiments using Sprague-Dawley rats were performed to evaluate the hepatoprotective effects through serum and liver analysis based on CCl_4-induced model, a hepatotoxic agent (mimic free radical). The *Hedyotis diffusa* aqueous extract exhibited a phenolic content (90.22 ± 0.10 mg GAE/g) and scavenging activity (IC_{50} = 1540 µg/mL). In the animal study using Sprague-Dawley rats, treatment with *Hedyotis diffusa* at 150 mg/kg (HD150) and 300 mg/kg (HD300) significantly reduced AST (HD150 = 31.8%; HD300 = 49.4%), ALT (HD150 = 35.8%; HD300 = 48.6%), and MDA (HD150 = 10.6%; HD300 = 26.6%) levels, while increasing GSH levels (HD150 = 18.8%; HD300 = 36.4%) against CCl_4-induced oxidative stress. These findings demonstrate that *Hedyotis diffusa* possesses significant hepatoprotective effects against carbon tetrachloride-induced hepatotoxicity.

Keywords: *Hedyotis diffusa*, Antioxidant, Hepatoprotective, Polyphenol, AST, ALT, MDA, GSH

e-ISSN 2716-697X

INTRODUCTION

Sabah is one of the states in Malaysia, located in the northern region of Borneo Island. It shares borders with Sarawak (Malaysia), Brunei, Kalimantan (Indonesia), and the Philippines. Borneo Island is endowed with rich biodiversity due to its extensive rainforests and tropical climate, with temperatures ranging from approximately 23–32°C. The indigenous people of Sabah traditionally use medicinal plants in their daily lives (Kulip, 2003). *Hedyotis diffusa* is one of medicinal plant, traditionally used for treating hepatitis, tonsillitis, appendicitis, pneumonia, mastitis, urethral infections, and tumours affecting the liver, lungs, and stomach (Z. Liang et al., 2008). *Hedyotis diffusa* belongs to Rubiaceae family and has been scientifically validated for its pharmacological properties, including anticancer (Chen et al., 2008), antifungal (Li et al., 2005), anti-inflammatory, antioxidant, immunoregulatory, and neuroprotective activities (Ahmad et al., 2005). However, the potential of *Hedyotis diffusa* as an antioxidant and hepatoprotective agent in Sabah remains unexplored. Therefore, investigating its bioactive properties could contribute significantly to scientific research and pharmaceutical drug development.

The liver is important organ that responsible for metabolism, secretion, and storage (Gutiérrez and Solís, 2009). According to (Shakya & Shukla, 2011), the liver diseases can be caused by toxic chemicals, excessive alcohol consumption, infections, and autoimmune disorders. Hepatotoxic chemicals such as carbon tetrachloride (CCl_4) induce liver cell damage through lipid peroxidation and oxidative stress (Fox et al., 1996). Alternative natural drugs with antioxidant and hepatoprotective properties is crucial in liver research through *in vitro* and *in vivo* experiments.

Polyphenols have garnered significant attention from researchers and the pharmaceutical industry due to their well-established antioxidant properties. They preventing diseases associated with oxidative stress, including cardiovascular and neurodegenerative diseases, as well as cancer (Manach et al., 2004; Rasmussen et al., 2005). Phenolic compounds are secondary metabolites characterized by aromatic rings with one or more hydroxyl groups (Djeridane et al., 2006). Phenolic compounds in *Hedyotis diffusa* have demonstrated hepatoprotective activity through various mechanisms, including immunotherapeutic pathways (Zheng et al., 2025), enzymatic regulation involving superoxide dismutase and NADPH oxidase (Y. Liang et al., 2021) and studies using a zebrafish model (Wang et al., 2023).

Given the limited data on *Hedyotis diffusa* that integrates both *in vitro* and *in vivo* evaluation, a comprehensive investigation is necessary to provide complete pharmaceutical data, especially on its efficacy against free radicals. Research information will provide essential data for identifying a novel antioxidant source, offering a comprehensive assessment through both chemical reactions and animal models.

e-ISSN 2716-697X

MATERIALS AND METHODS

Chemicals

Plant Collection and Extraction

Hedyotis diffusa samples were obtained from local herb suppliers in Kota Kinabalu, Sabah. The whole plants were washed and air-dried at 20°C ± 0.5°C of room temperature for one day, followed by oven drying at 37°C ± 0.5°C for three days (Thermo Scientific, Waltham, MA, USA). Heavy duty blender (Waring Commercial, PA, USA) was performed to ground sample into fine powder using a. Extraction was carried out based on the method by Maghrani et al. (2003), with modifications. In brief, 100 g powdered sample was mixed with 1000 mL boiled water on a hot plate with magnetic stirring for 10 minutes. The solids were removed from the mixture using Whatman filter paper and a chimney flask. The extract was kept for further analysis under temperature of -20°C ± 0.5°C.

Total Phenolic Content (TPC) Determination

Total phenolic content conducted based on Ringgit et al. (2024;2025) with some modifications. A 1 mL of 1:10 (v/v) Folin and Ciocalteu's phenol reagent (R&M Chemicals, Kumpulan Saintifik F.E. Sdn. Bhd., Selangor, Malaysia) mixed with 0.3 mL sample for 10 minutes dark incubation. Next, 1.2 mL of 7.5% (w/v) sodium carbonate (CNa_2O_3 (HmbG Chemicals, Hamburg, Germany) mixed with mixture for 30 minutes further dark incubation. The spectrophotometer (SP-3000 nano, Optima, Tokyo, Japan) performed to evaluate the activity under 743 nm and standard is gallic acid, $C_6H_2(OH)_3COOH•H_2O$ (Nacalai Tesque, Kyoto, Japan). The result expresses as milligrams of gallic acid equivalent per gram (mg GAE/g).

DPPH Radical Scavenging Activity

Antioxidant activity following Hatano et al. (1988) method with modifications. A 0.1M DPPH (2,2-diphenyl-1-picrylhydrazyl hydrate; $C_{18}H_{12}N_5O_6$) (TCI, Tokyo, Japan) was dissolved in methanol. Then, 2.7 mL of the DPPH solution was mixed with 300 µL of the sample extract. Ascorbic acid (HmbG Chemicals, Hamburg, Germany) was used as the standard. The mixture was kept in the dark for one hour. Absorbance was measured at 517 nm using a spectrophotometer, and antioxidant activity was expressed as the percentage of radical scavenging activity (%RSA) using the following equation:

$$\%RSA = [(A_{standard} - A_{sample})/A_{standard}] \times 100\%$$

$A_{standard}$ and A_{sample} are absorbance readings of ascorbic acid and sample with DPPH, respectively. The % RSA graph was constructed and the IC_{50} was obtained.

Animal Experiment

The animal experiments were carried out in strict adherence to ethical guidelines, university standards, and federal legislation pertaining to animal experimentation (UMS/IP7.5/M3/4-2012). Sixteen adult male Sprague-Dawley rats (4–8 weeks old), weighing 150–200 g, were obtained from in-house breeding at the Animal Facility, Faculty of Food Science and Nutrition, Universiti Malaysia Sabah. The rats were acclimatized for one week under controlled conditions: room temperature (20°C ± 0.5°C), humidity (50% ± 5%), and a 12-hour light/dark cycle. The animals were randomly divided into four groups. The control group I (CG; n = 4) received normal saline. The group II (CT; n = 4) was administered carbon tetrachloride at 1.2 mL/kg body weight by gavage on days 13 and 14. Groups III and IV received Hedyotis diffusa at 150 mg/kg (HD150; n = 4) and 300 mg/kg (HD300; n = 4), respectively, for 14 days by gavage, in addition to carbon tetrachloride at 1.2 mL/kg body weight on days 13 and 14. Hedyotis diffusa was dissolved in distilled water daily prior to oral administration. Carbon tetrachloride was dissolved in 1:1 corn oil. All rats had free access to water. After 24 hr of administration of last dose of carbon tetrachloride, the animals were killed by cervical dislocation, blood and liver samples were collected and stored in ice-cold saline (0.85% w/v sodium chloride) for biochemical and hematological analysis.

Post-mitochondrial Supernatant Preparation

A 1 g liver tissue was homogenized in 10 mL of chilled phosphate buffer (0.1 M, pH 7.4) containing 1.17% (w/v) potassium chloride (KCl) using a homogenizer (Polytron PT 1200E, Switzerland). The homogenate was first centrifuged at 2000 rpm for 10 minutes at 4°C ± 0.5°C using a refrigerated centrifuge (Avanti J-E, Brea, California, USA) to remove nuclear debris. The resulting supernatant was then centrifuged at 10,000 rpm for 30 minutes at 4°C ± 0.5°C to obtain the post-mitochondrial supernatant, which was used to determine malondialdehyde (MDA) and reduced glutathione levels.

Serum Alanine Aminotransferase (ALT) and Aspartate Aminotransferase (AST) Determination

Serum levels of alanine aminotransferase (ALT) and aspartate aminotransferase (AST) were measured using the method of Reitman and Frankel (1957), with slight modifications. Briefly, 0.5 mL of substrate containing 2 mM α-ketoglutarate and 200 mM D,L-aspartate for ALT, or 2 mM α-ketoglutarate and 200 mM D,L-alanine for AST-was mixed with 0.05 mL of serum and 1.55 mL of phosphate buffer (pH 7.5). The mixture was incubated in a water bath at 37°C ± 0.5°C for 15 minutes. To stop the reaction, 0.5 mL of 1 mM 2,4-dinitrophenylhydrazine (DNPH) was added. After 20 minutes, 5 mL of 0.4 N NaOH was added, and absorbance was measured at 510 nm after 30 minutes using a blank as reference.

Lipid Peroxidation (MDA) Determination

Lipid peroxidation in the post-mitochondrial supernatant was evaluated following the method of Buege and Aust (1978), with modifications by Iqbal et al. (1999). One volume of the supernatant was mixed with 0.5 volumes of 10% (w/v) trichloroacetic acid and centrifuged at 8000 × g for 30 minutes at 4°C ± 0.5°C. The resulting supernatant (1 mL) was combined with 1 mL of 0.67% (w/v) thiobarbituric acid and incubated in a boiling water bath for 30 minutes. After cooling in an ice bath, the mixture was centrifuged at 14,000 × g using a refrigerated centrifuge. Absorbance was measured at 535 nm using a spectrophotometer at 37°C ± 0.5°C. Results were expressed as the amount of malondialdehyde (MDA) formed.

Glutathione Reduced (GSH) Determination

Reduced glutathione levels in the liver were determined following the method of Jollow et al. (1974), with modifications. Briefly, 0.1 mL of hepatic post-mitochondrial supernatant (10% w/v) was mixed with 1 mL of 4% (w/v) sulfosalicylic acid and kept at 4°C ± 0.5°C for one hour. The mixture was then centrifuged at 3000 × g for 30 minutes. For analysis, 0.1 mL of the clear supernatant was added to 2.7 mL of phosphate buffer (0.1 M, pH 7.4) and 0.2 mL of DTNB solution (4 mg/mL in 0.1 M phosphate buffer, pH 7.4). Absorbance was measured at 412 nm, and results were expressed as micromoles of reduced glutathione per gram of tissue.

Statistical analysis

All data were obtained from expression of standard deviation (S.D) from triplicate of number of sample (n = 3). Graph was plotted to determine the the IC_{50} value from standard calibration curve (y= mx + C) and regression (r^2 = 0.999 0.1) from Microsoft excel software.

RESULTS AND DISCUSSION

Total Phenolic Content (TPC)

The phenolic content of *Hedyotis diffusa* was determined from its aqueous extract using a standard calibration curve (y = 0.0057x – 0.0026, r^2 = 0.9999) based on gallic acid. According to the standard curve, 100 g of *Hedyotis diffusa* in aqueous extract contained 90.22 ± 0.10 mg GAE/g (see Table 1).

e-ISSN 2716-697X

Table 1 Total phenolic content of *Hedyotis diffusa*

Sample	TPC (mg GAE/g)
Hedyotis diffusa	90.22 □ 0.10

Milligrams of gallic acid weight, mg GAE/g.

Antioxidant Activity (DPPH)

Antioxidant activity of *Hedyotis diffusa* extract evaluated using DPPH assay, which measures the extract's ability to capture free radicals with IC_{50} value of 1540 □g/mL obtained. In this study, the concentration of 2400 µg/mL was prepared and subsequently diluted in a serial manner to a final concentration of 25 µg/mL. Based on this serial dilution, seven concentrations were obtained: 2400, 1200, 600, 300, 150, 75, and 25 µg/mL. Each of these concentrations from the extraction yield of *Hedyotis diffusa* and was dissolved in the presence of DPPH radicals. The same DPPH concentration was used in all treatments of scavenging activity with respective extract concentrations (see Table 2). The relationship between the plant extract and DPPH radicals was evaluated by measuring absorbance using a spectrophotometer. Fig. 1 illustrates the plant extract effects in the presence of DPPH radicals. The highest point on the graph corresponds to the highest scavenging activity, while the lowest point indicates minimal activity (y-axis). Based on the graph, the scavenging activity of *Hedyotis diffusa* extract increasing with increasing concentration treatment. The maximum activity could reach up to 80% scavenging activity with maximum concentration of 2400 µg/mL than the lowest concentration of 25 µg/mL (5% scavenging activity).

Table 2 Antioxidant activity of *Hedyotis diffusa*

Parameter	Sample	IC_{50} (□g/mL)
DPPH	*Hedyotis diffusa*	1540
	Ascorbic acid	75

Half inhibition concentration, IC_{50}.

e-ISSN 2716-697X

Fig. 1 Scavenging activity of *Hedyotis diffusa* extract against DPPH radicals (n = 3).

In vivo Hepatoprotective Activity

Serum Analysis (AST and ALT)

In this study, CCl_4 treatment performed to evaluate the hepatoprotective effects of *Hedyotis diffusa* extract in mitigating liver inflammation, as indicated by changes in ALT and AST levels. Elevated ALT (1.7 μmol/min/dL10^{-3}) and AST (1.5 μmol/min/dL10^{-3}) levels in the animal model are indicative of liver inflammation (*p≤0.05). To address this condition, *Hedyotis diffusa* extract was administered with the objective of reducing ALT and AST levels. Fig. 2 illustrates the effect of *Hedyotis diffusa* extract on serum AST and ALT levels in rats subjected to CCl_4 treatment. The control group exhibited significantly lower serum AST (0.5 μmol/min/dL10^{-3}) and ALT (0.7 μmol/min/dL10^{-3}) levels compared to the CCl_4-treated group, as well as the groups receiving *Hedyotis diffusa* extract at doses of 150 mg/kg (HD150 group) (ALT = 1.1 μmol/min/dL10^{-3} and AST = 1.08 μmol/min/ dL10^{-3} ; **p≤0.05), and 300 mg/kg (HD300 group) (ALT = 0.9 μmol/min/dL10^{-3} and AST = 0.8 μmol/min/ dL10^{-3}; **p≤0.05).

e-ISSN 2716-697X

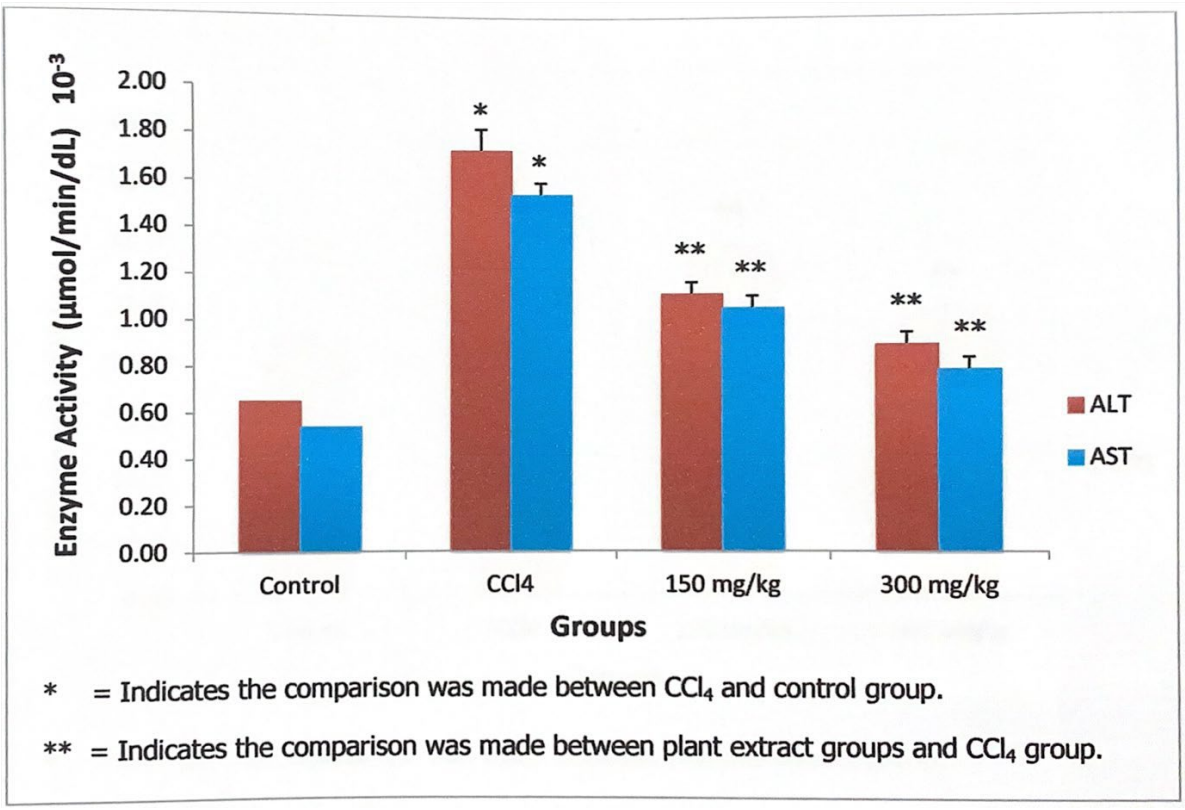

Fig. 2 Effects of Hedyotis diffusa on serum ALT and AST levels in the presence of CCl_4 radicals (n = 4).

* Indicates a statistically significant difference between CCl4 and control group ($p \leq 0.05$).

** Indicates a statistically significant difference between plant extract groups and CCl_4 group ($p \leq 0.05$).

Liver Analysis (MDA and GSH)

The presence of CCl_4 radicals in rats resulted a significant elevated levels of lipid peroxidation (LOP) and malondialdehyde (MDA) (*$p \leq 0.05$) as shown in figure 3. However, these levels decreased significantly following treatment with *Hedyotis diffusa* extract at doses of 150 mg/kg and 300 mg/kg in the animal model (**$p \leq 0.05$). A higher extract concentration (300 mg/kg) led to a greater reduction in LOP and MDA levels compared to the 150 mg/kg treatment (**$p \leq 0.05$). As shown in the figure 4, hepatic reduced glutathione (GSH) levels were markedly decreased in the CCl_4-treated group compared with the control group (*$p \leq 0.05$), indicating oxidative stress induced by CCl_4 administration. Pretreatment with the *Hedyotis diffusa* extract significantly restored GSH levels in a dose-dependent manner. Animals receiving 150 mg/kg of the *Hedyotis*

diffusa extract showed a significant increase in GSH levels compared with the CCl_4 group (**p≤0.05), while the 300 mg/kg dose produced a more pronounced elevation, bringing GSH levels close to those of the control group (**p≤0.05 vs. CCl_4). These findings suggest that the *Hedyotis diffusa* extract effectively attenuates CCl_4-induced depletion of GSH, with greater protection observed at the higher dose.

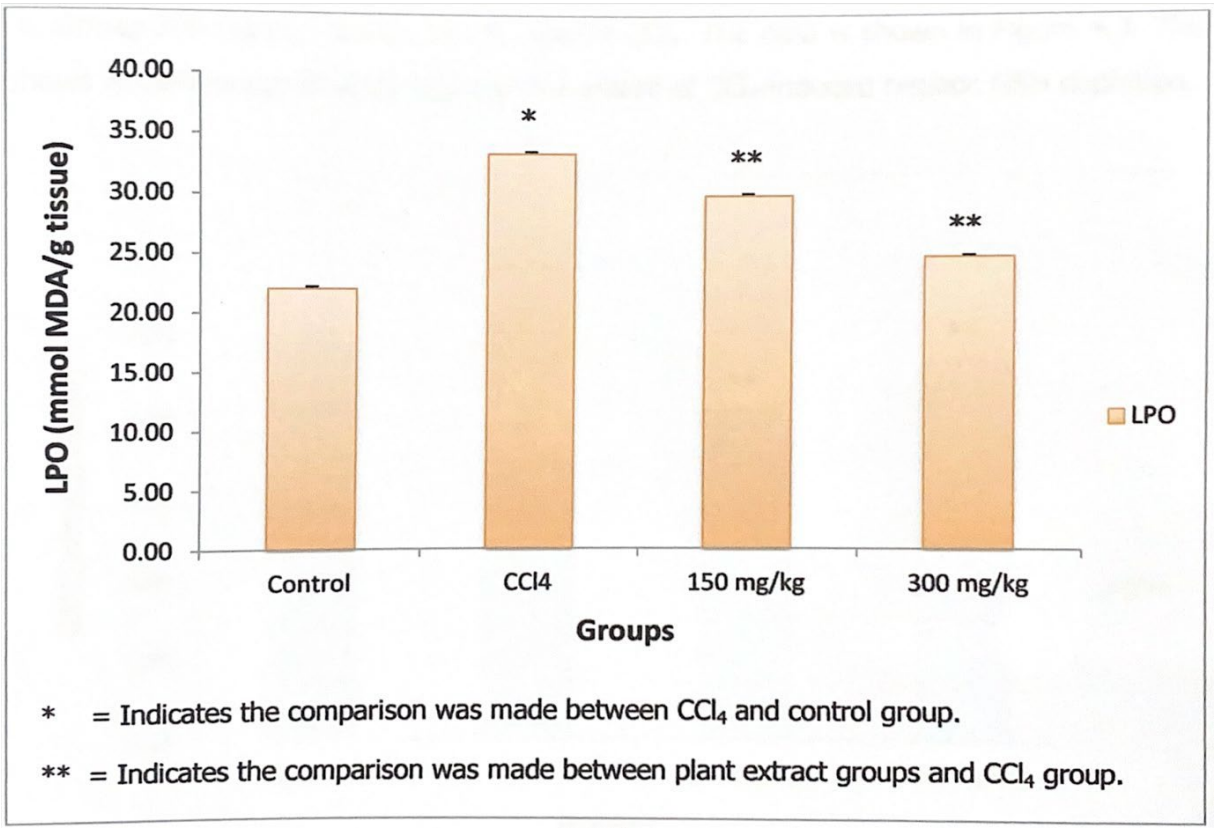

Fig. 3 Effects of *Hedyotis diffusa* on MDA levels in the presence of CCl_4 radicals (n = 4).
* Indicates a statistically significant difference between CCl_4 and control group (p≤0.05).
** Indicates a statistically significant difference between plant extract groups and CCl_4 group (p≤0.05).

e-ISSN 2716-697X

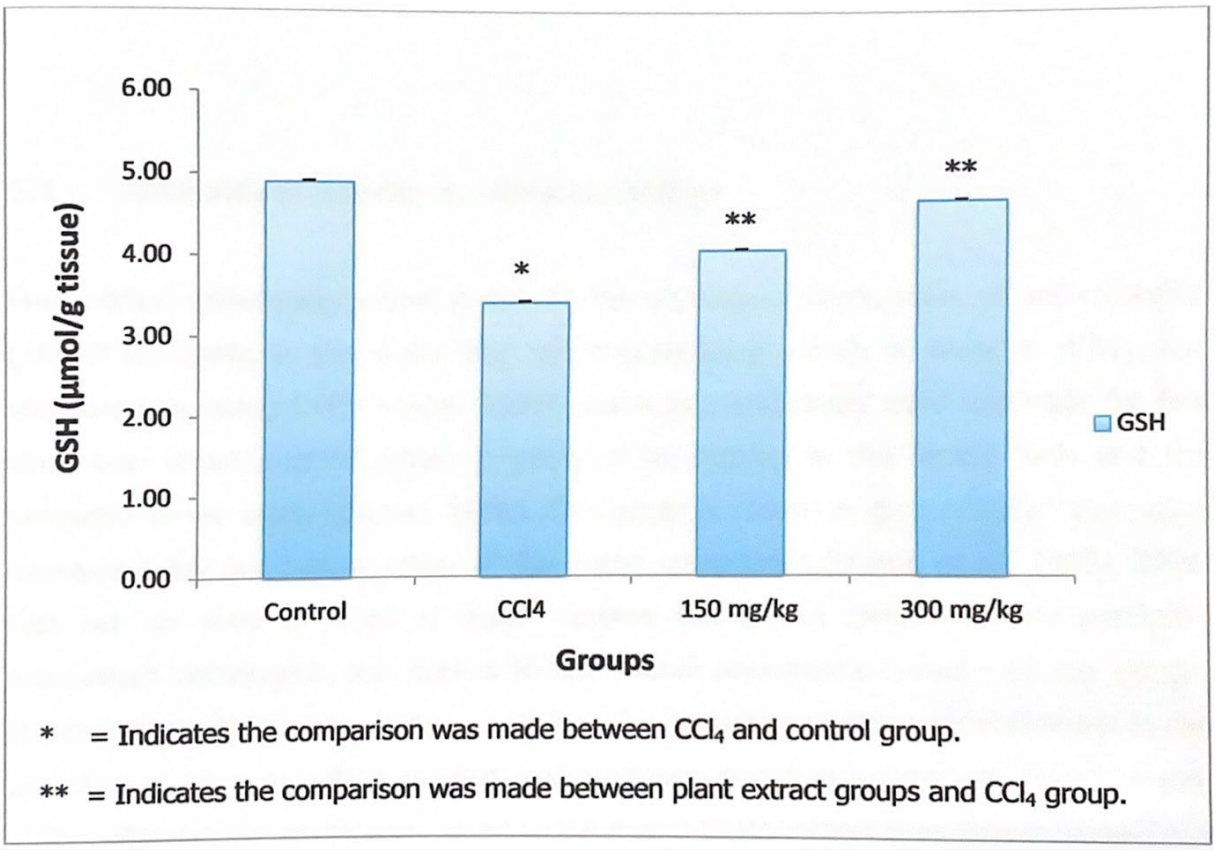

Fig. 4 Effects of *Hedyotis diffusa* on GSH levels in the presence of CCl4 radicals (n = 4).
* Indicates a statistically significant difference between CCl4 and control group ($p \leq 0.05$).
** Indicates a statistically significant difference between plant extract groups and CCl4 group ($p \leq 0.05$).

In this study, the extraction process yielded approximately 0.09% of the initial weight (100 g) using aqueous extraction. The findings suggest that *Hedyotis diffusa* comprises approximately 0.09% phenolic compounds when extracted with a polar solvent such as water. Although the phenolic content appears relatively low, it is higher compared to previous findings. A prior study by Zheng et al. (2024) reported that *Hedyotis diffusa* aqueous extract contained a higher phenolic content than that extracted using 30% ethanol (6.47 ± 1.16 mg GAE/g). The phenolic content reported was lower a recent study by Gull et al. (2024), which used 80% ethanol (52.423 mg GAE/10 mg or 5242.3 mg GAE/g). These comparative studies indicate that solvent polarity and concentration significantly influence the extraction efficiency of phenolic compounds from *Hedyotis diffusa*. Highly polar solvents tend to extract higher amounts of phenolic content, as demonstrated in the present study. Since water is a more polar solvent than ethanol, reducing the ethanol concentration from 80% to 30% resulted in a decrease in phenolic content. This observation suggests that *Hedyotis diffusa* aqueous extract may contain a high proportion of phenolic hydroxyl groups. The principal detection mechanism is attributed to the reducing

power of phenolic hydroxyl groups and their interaction with the phosphotungstic-phosphomolybdic complex (Yu et al., 2000; Singleton et al., 1965).

The DPPH trend observed in the graph suggests a positive correlation between extract concentration and scavenging activity (%). The scavenging activity increased with increasing extract concentration, reaching approximately 80% at 2400 µg/mL of *Hedyotis diffusa* aqueous extract. From these data, the half-maximal inhibitory concentration (IC_{50}) was determined by interpolating the scavenging activity (%) to identify the specific extract concentration (µg/mL) required to inhibit 50% of radical activity. At 50% scavenging activity (y-axis), the IC_{50} value of *Hedyotis diffusa* aqueous extract was found to be approximately 1540 µg/mL, with significantly higher than standard antioxidant, ascorbic acid. As shown in Table 2, ascorbic acid exhibited radical scavenging activity at a minimum concentration as low as 75 µg/mL. In terms of effectiveness, a lower IC_{50} value indicates a more potent radical-scavenging ability. For instance, ascorbic acid required only 75 µg/mL to achieve significant radical scavenging, whereas *Hedyotis diffusa* aqueous extract required over 20-fold higher concentration (1540 µg/mL) for a comparable effect. Based on these results, it was estimated that *Hedyotis diffusa* aqueous extract contained approximately 4.87% essential antioxidant compounds at the IC_{50} value, in comparison to ascorbic acid (assuming 75 µg/mL corresponds to 100% scavenging activity). The IC_{50} value obtained in this study (1540 µg/mL) was higher than that reported in a previous study (268.1 µg/mL) by Zheng et al. (2024), suggesting that *Hedyotis diffusa* in aqueous extract contains phenolic hydroxyl groups with potent scavenging activity. The primary detection mechanism is attributed to the reducing power of phenolic hydroxyl groups and their interaction with the phosphotungstic-phosphomolybdic complex (Yu et al., 2000; Singleton et al., 1965).

Additionally, *Hedyotis diffusa* extract demonstrated the ability to scavenge free radicals and terminate reactions generated by radical chain processes (Duh et al., 1997). According to the mechanism proposed by Larson (1988), antioxidants (AH) donate a hydrogen atom to DPPH radicals, forming a stable, non-radical DPPH-H, as illustrated below.

$$DPPH + AH \rightarrow DPPH\text{-}H + A$$

Previously, the potential antioxidants capable of donating a hydrogen atom include cysteine, glutathione, ascorbic acid, tocopherol, and polyhydroxyl aromatic compounds such as pyrogallol and gallic acid (Sini and Devi, 2004).

In the CCl_4-treated group, radical exposure led to an increase in AST and ALT levels above 1.60 µM/min/d (*$p \leq 0.05$). However, the administration of *Hedyotis diffusa* extract at 150 mg/kg and 300 mg/kg resulted in a dose-dependent reduction in AST and ALT activity (**$p \leq 0.05$).The underlying mechanism involves the formation of trichloromethyl free radicals ($\bullet CCl_3$), which react with oxygen to generate trichloromethyl peroxy radicals ($\bullet CCl_3O_2$). These radicals attack membrane polyunsaturated fatty acids, triggering lipid peroxidation, which in turn leads to liver

injury and impaired membrane function (Krishna et al., 2009; Yang et al., 2010). Based on the results, treatment with *Hedyotis diffusa* extract at 150 mg/kg and 300 mg/kg resulted in a reduction of serum AST by 31.8% and 49.4%, respectively (**p≤0.05). while serum ALT levels decreased by 35.8% and 48.6%, respectively (**p≤0.05). The observed decrease in ALT and AST levels with increasing extract concentration suggests that *Hedyotis diffusa* extract exerts a protective effect against liver damage.

Fig. 3 illustrates the inhibitory effect of *Hedyotis diffusa* extract on MDA formation, an indicator of lipid peroxidation induced by CCl_4 radicals (Yang et al., 2010). The results indicate that 150 mg/kg treatment *Hedyotis diffusa* significantly reduced MDA levels by 10.6%, while the 300 mg/kg *Hedyotis diffusa* treatment achieved a significantly greater reduction of MDA 26.6% in liver tissue (**p≤0.05).. The treated groups exhibited significantly lower MDA levels compared to the CCl_4 group (**p≤0.05)., suggesting that *Hedyotis diffusa* possesses antioxidant properties that mitigate lipid peroxidation by scavenging free radicals. Fig. 4 presents the effect of CCl_4 treatment on glutathione (GSH) levels, along with the impact of *Hedyotis diffusa* extract at 150 mg/kg and 300 mg/kg. The results indicate that a higher dose of 300 mg/kg increased GSH levels by 36.4% in response to CCl_4 exposure, whereas the 150 mg/kg dose led to an 18.8% increase (**p≤0.05). GSH levels serve as a critical biomarker for liver health, as oxidative stress depletes GSH due to its consumption by glutathione-related enzymes, leading to cellular intoxication (Sen et al., 1996). The significant elevation of GSH (**p≤0.05) levels following *Hedyotis diffusa* extract treatment suggests that this plant exhibits hepatoprotective properties by counteracting free radical-induced oxidative damage.

CONCLUSION

Hedyotis diffusa is rich in phenolic compounds with potent antioxidant activity. Polyphenols derived from this plant mitigate the elevated levels of AST and ALT and restore the levels of MDA and GSH, which are associated with hepatoprotective effects. Notably, *Hedyotis diffusa* sourced locally exhibits high scavenging activity (IC_{50} = 1540 µg/mL) and effectively inhibits lipid peroxidation, as demonstrated through both in vitro and in vivo assays. This study provides a valuable reference for the potential discovery of novel hepatoprotective compounds derived from *Hedyotis diffusa* with minimal side effects. Future studies should focus on the bioassay-guided isolation of the specific phenolic compounds responsible for this activity and evaluation of the extract's efficacy in chronic liver disease models.

their suitability as feed. Microalgae must fall within an optimal size range and shape for ingestion by the target species, especially during larval stages (Annamalai et al., 2021). Mota et al. (2023) demonstrated that when the physical characteristics of microalgae correspond to the

ACKNOWLEDGMENTS

The authors sincerely appreciate the Universiti Malaysia Sabah Research Grant Priority Area Scheme, Ministry of Higher Education, Malaysia, for supporting this work through grant No. SBK0027-SKK-2012. Special thanks are extended to Prof. Dr. Jualang Azlan Gansau, Director of the BRI at UMS, for her invaluable guidance and support.

AUTHOR CONTRIBUTIONS

Gilbert Ringgit prepared the manuscript. Robin Jacobson Laurduraj conducted the experiment. Associate Professor Dr. Mohammad Iqbal helped in designing the experiment and proofread the manuscript.

DECLARATION OF COMPETING INTEREST

The authors ensure that the work presented in this article is free of financial interests or personal relationships that may have influenced its outcome.

REFERENCES

Ahmad R, Ali AM, Israf DA, Ismail NH, Shaari K, Lajis NH. Antioxidant, radical-scavenging, anti-inflammatory, cytotoxic and antibacterial activities of methanolic extracts of some *Hedyotis species*. Life Sciences, 76(17):1953–1964 (2005).

Buege JA, Aust SD. Microsomal lipid peroxidation. In Methods in Enzymology. 52: 302–310 (1978).

Chen XH, Gao RL, Qian XD, Wang X, Tan P L, Yin L M, Zhou YH. Inhibition effect of hedyotis diffusa wild injection on HL-60 cells and its mechanism. Zhongguo Shi Yan Xue Ye Xue Za Zhi. 16(5): 1035–1038 (2008).

Djeridane A, Yousfi M, Nadjemi B, Boutassouna D, Stocker P, Vidal N. Antioxidant activity of some algerian medicinal plants extracts containing phenolic compounds. Food Chemistry. 97(4): 654–660 (2006).

Fox VL, Cohen MB, Whitington PF, Colletti RB. Outpatient liver biopsy in children: a medical position statement of the North American Society for Pediatric Gastroenterology and Nutrition. Journal of Pediatric Gastroenterology and Nutrition. 23(3): 213–216 (1996).

Gull S, Tasneem F, Ahmed I, Aslam MA, Tayyeb A, Abid L, Arshad MI, Shahzad N. Ethanolic extract of *Euphorbia royleana* Boiss. reduces metastasis of breast cancer cells and inhibits tumor progression in vivo. Medical Oncology. 41(6): 1–16 (2024).

Gutiérrez RMP, Solís RV. Hepatoprotective and inhibition of oxidative stress in liver of *Prostechea michuacana*. Records of Natural Products. 3(1): 46–51 (2009).

Iqbal M, Giri U, Giri DK, Alam MS, Athar M. Age-dependent renal accumulation of 4-hydroxy-2-nonenal (HNE)-modified proteins following parenteral administration of ferric nitrilotriacetate commensurate with its differential toxicity: Implications for the involvement of HNE-protein adducts in oxidative stress and carcinogenesis. Archives of Biochemistry and Biophysics. 365(1): 101–112 (1999).

Jollow DJ, Mitchell JR, Zampaglione NA, Gillette JR. Bromobenzene-induced liver necrosis. Protective role of glutathione and evidence for 3, 4-bromobenzene oxide as the hepatotoxic metabolite. Pharmacology. 11(3): 151–169 (1974).

Krishna KL, Mruthunjay K, Patel JA. Antioxidant and hepatoprotective activity of leaf extract of *Justicia gendarussa* Burm. International Journal of Biological Chemistry. 3(3): 9–11 (2009).

Kulip J. An ethnobotanical survey of medicinal and other useful plants of Muruts in Sabah, Malaysia. Telopea. 10(1): 81–98 (2003).

Larson RA. Review Article Number 30 the Antioxidants of Higher Plants. Phytochemistry. 27(4): 969–1988 (1988).

Li H, Qing C, Zhang Y, Zhao Z. Screening for endophytic fungi with antitumour and antifungal activities from Chinese medicinal plants. World Journal of Microbiology and Biotechnology. 21(8–9): 1515–1519 (2005).

Liang Y, Niu QQ, Zhao YH. Pharmacological research progress of ursolic acid for the treatment of liver diseases. Traditional Medicine Research. 6(4): 38 (2021).

Liang Z, He M, Fong W, Jiang Z, Zhao Z. A comparable, chemical and pharmacological analysis of the traditional Chinese medicinal herbs *Oldenlandia diffusa* and *O. corymbosa* and a new valuation of their biological potential. Phytomedicine. 15(4): 259–267 (2008).

Maghrani M, Lemhadri A, Jouad H, Michel JB, Eddouks M. Effect of the desert plant *Retama raetam* on glycaemia in normal and streptozotocin-induced diabetic rats. Journal of Ethnopharmacology. 87(1): 21–25 (2003).

Manach C, Scalbert A, Morand C, Rémésy C, Jiménez L. Polyphenols: Food sources and bioavailability. American Journal of Clinical Nutrition. 79(5): 727–747 (2004).

Rasmussen SE, Frederiksen H, Krogholm KS, Poulsen L. Dietary proanthocyanidins: Occurrence, dietary intake, bioavailability, and protection against cardiovascular disease. Molecular Nutrition and Food Research. 49(2): 159–174 (2005).

Reitman S, Frankel S. A colorimetric method for the determination of serum glutamic oxalacetic and glutamic pyruvic transaminases. American Journal of Clinical Pathology. 28(1): 56–63 (1957).

Ringgit G, Cheong BE, Shah MD, Siddiquee S. Phenols, flavonoids and anthocyanins in *Solanum lasiocarpum* from Borneo: In vitro antioxidant activity and phytochemical profiling *via* LCMS Q-TOF. Food Bioscience. 61: 104966 (2024).

Ringgit G, Cheong BE, Shah MD, Siddiquee S. Phytochemical composition and antioxidant properties of *Canarium odontophyllum* (Sarawak Olive): A seasonal fruit from Borneo, East Malaysia. Phytomedicine Plus 5(1): 100703 (2025).

Sen CK, Packer L. Antioxidant and redox regulation of gene transcription. The FASEB Journal. 10(7): 709–720 (1996).

Shakya AK, Shukla S. Evaluation of hepatoprotective efficacy of Majoon-e-Dabeed-ul-ward against acetaminophen-induced liver damage: A Unani herbal formulation. Drug Development Research. 72(4):346-52 (2011).

Singleton VL, Rossi JA. Colorimetry of Total Phenolics with Phosphomolybdic-Phosphotungstic Acid Reagents. American Journal of Enology and Viticulture. 16(3): 144–158 (1965).

Wang X, Zhao J, Zhang R, Liu X, Ma C, Cao G, Wei Y, Yang P. Protective effect of Hedyotis diffusa Willd. ethanol extract on isoniazid-induced liver injury in the Zebrafish Model. Drug Design, Development and Therapy. 1995-2015 (2023).

Yang J, Li Y, Wang F, Wu C. Hepatoprotective effects of apple polyphenols on CCl4-induced acute liver damage in mice. Journal of Agricultural and Food Chemistry. 50(10): 6525–6531 (2010).

Yu Z, Dahlgren RA. Evaluation of methods for measuring polyphenols in conifer foliage. Journal of Chemical Ecology. 26(9): 2119–2140 (2000).

Zheng Q, Jin X, Nguyen TT M, Yi EJ, Park SJ, Yi GS, Yang SJ, Yi TH. Autophagy-Enhancing Properties of *Hedyotis diffusa* Extracts in HaCaT Keratinocytes: Potential as an Anti-Photoaging Cosmetic Ingredient. Molecules. 30(2): 1–18 (2025).

Zheng Q, Wu X, Peng S. The immunotherapy mechanism of *Hedyotis Diffusae* Herba in treating liver cancer: a study based on network pharmacology, bioinformatics, and experimental validation. Naunyn-Schmiedeberg's Archives of Pharmacology. 398(1): 951–965 (2024).

Borneo International Journal of Biotechnology (BIJB)
Vol. 5 (December 2025), 64-79.

e-ISSN 2716-697X

Characterization of Lipase-Immobilized Polymethacrylate-based Monolith at Different Porogen Contents, Diameter, and Number of Holes for the Immobilization Process

Eryati Derman[1], Rahmath Abdulla[2], Clarence M. Ongkudon[1]*

[1]Biotechnology Research Institute, Universiti Malaysia Sabah, Jalan UMS, 88400, Kota Kinabalu, Sabah, Malaysia [2]BioAgriTech Research Group, Faculty of Science and Technology, Universiti Malaysia Sabah, Jalan UMS, 88400, Kota Kinabalu, Sabah, Malaysia
*Corresponding email: clarence@ums.edu.my
Received: 16 October 2025 | Accepted: 20 December 2025 | Published: 31 December 2025

ABSTRACT

Polymethacrylate-based monoliths have attracted a lot of attention due to their exceptional properties, such as reusability, solvent tolerance, and higher stability. This study investigates the physical characteristics and immobilization yield of lipase on polymethacrylate-based monoliths fabricated with varying porogen contents, hole diameters, and hole numbers. By systemically altering these structural parameters, this study aimed to elucidate their influence on monolith morphology, surface area, and pore architecture, which are critical for enzyme loading and catalytic performance. Immobilization yield was quantified via protein loading. Results revealed that the highest immobilization yield was achieved at 60% porogen concentration when varying the diameter and number of holes, with a yield of 58.67 ± 0.69%. At a diameter of 0.4 mm (18 holes) under varied porogen concentrations, immobilization yields of 57.50 ± 0.95% were obtained. In comparison, the simulation data predicted that the highest immobilization yield at a diameter of 0.3 mm (24 holes) with varied porogen concentration, yielding 55.90 ± 1.12% and immobilization yield of 58.90 ± 0.31% at 60% porogen content with different diameters and numbers of holes. These findings are crucial as they provide valuable insights into the design of tailored monolithic supports for biocatalytic applications, particularly in sustainable biodiesel production.

Keywords: Diameter; immobilization; lipase; polymethacrylate-based monoliths; porogen concentration;

e-ISSN 2716-697X

INTRODUCTION

Enzyme immobilization has been widely applied in biocatalysis due to its practicality, enhanced stability, and reusability, making it a valuable strategy for industrial processes (Parandi et al., 2022). Compared to free enzymes or other catalysts, immobilised enzymes offer improved selectivity, thermal and chemical stability, ease of recovery, and consistent activity under diverse reaction conditions (Rajnish et al., 2021; Xie & Huang, 2020). The choice of support material plays a critical role in ensuring enzyme stability and reusability, thereby determining the overall efficiency of the immobilization process.

Traditionally, supports such as silica, polymer beads, and nanomaterials have been employed, often fabricated as millimeter-sized particles with catalytic agents distributed on their surfaces or within internal pores (Trubac et al., 2001; Zhao et al., 2021). These micromaterials, polymers, and nanomaterials have been gaining a lot of attention for their potential in immobilizing enzymes for industrial applications (Rajnish et al., 2021). While effective, these particulate supports are limited by mass transfer constraints, flow dynamics, and mechanical stability, which can hinder large-scale applications pressure (Santos et al., 2020; Trubac et al., 2001). Optimal reactor performance requires supports with sufficient surface area, tailored pore structures, and mechanical robustness to sustain catalytic activity under industrial conditions (Afandizadeh & Foumeny, 2001). By understanding the underlying factors, engineers can design an optimal system with the prescribed conditions.

To overcome these limitations, monolithic supports have emerged as promising alternatives. Porous carbon monoliths with tunable porosity are more promising for various applications, such as adsorption and energy storage. A large quantity of enzymes is much easier to immobilize in a porous structure compared to a flat surface support (Gustafsson, 2012). The pore dimension of a monolith can be tailored by varying the polymerization or synthesis conditions accordingly. However, the synthesis of carbons with controlled porosity and monolithic shape is often expensive and timeconsuming. Enzymes can be immobilized on a wide variety of synthetic and natural supports (carriers) through covalent or ionic bonding, adsorption, carrier-free cross-linked enzymes, and affinity binding (Sheldon et al., 2021). However, different applications need completely different technical requirements in terms of the carrier size, materials, configuration, and method of immobilization for the production process.

Polymethacrylate-based monoliths are attractive as a lipase carrier as they can enhance the lipase enzymes' catalytic activity due to their unique properties, which can be modified so that they can have high enzyme loading capacity and high surface-to-volume ratio, inertness against microbial and chemical degradation, biocompatibility with any enzymes, and also easy to separate at the end of the process (Haghighi et al., 2024). The monoliths are also much easier to recover and manipulate in an industrial process (Zhao et al., 2021. Their adaptability makes them particularly suitable for lipase immobilization, where enhanced catalytic activity and reusability

e-ISSN 2716-697X

are critical for cost-effective biodiesel production. The use of novel carriers with highly porous properties, with much easier separation in the final production process, will be very beneficial to the industry.

In this study, we prepared and modified polymethacrylate-based monoliths to serve as lipase carriers in a continuous flow system using an NGC Chromatography setup. We investigated the influence of porogen content, holes diameter, and number of holes on lipase immobilization efficiency and catalytic performance. These modifications aim to optimize monolith design for industrial applications requiring stable, reusable, and high-performance biocatalysts in continuous processes

MATERIALS & METHODS

Chemicals and materials

A Azobisisobutyronitrile (AIBN, Mw of 164.21, 98%), Cyclohexanol 99% (Mw of 100.16), ethylene glycol dimethacrylate (EDMA, 98%, Mw of 198.22), glycidyl methacrylate (GMA, 97%, Mw of 142.15), methanol AR grade ≥ 99.5%, Bradford protein assay and Candida rugosa lipase enzymes (L1754, BCCJ3778, type VII, hydrolytic activity 1070 U/mg, ≥700 units/mg solid) were purchased from Sigma-Aldrich, USA through Next Gene Scientific Sdn Bhd (Malaysia). Reagents such as sodium phosphate dibasic heptahydrate and sodium phosphate monobasic monohydrate were supplied by ACCVA Solutions Sdn Bhd. All other reagents and solvents were of analytical grade and used as received, without any additional purification step.

Polymethacrylate-based Monolith Preparation

The polymethacrylate-based monolith was prepared based on a study by (Simbas & Ongkudon, 2019) methods with slight modifications. The polymethacrylate-based monolith polymerization mixture was prepared, which consisted of the initiator (AIBN), monomer (EDMA and GMA), and porogen (cyclohexanol). The mixture was sonicated for 15 minutes and placed in a water bath for 1 hour at 55 °C. Then the monoliths were washed with both methanol and deionized water overnight.

e-ISSN 2716-697X

Physical Modification

A mechanical drilling into the surface of the polymethacrylate-based monolith was done using a High-Speed Steel (HSS) Twist Drill (Model DM-240, GUNAISI, China). The diameters of the drill used were 0.3 mm, 0.4 mm, 0.5 mm, and 0.6 mm. The number of holes drilled into the monoliths was related to the diameter of the drill. In this study, we were focused on finding the ideal average total surface area of holes for each of the drill bits based on the diameter chosen. This was determined by the number of holes that can be drilled into the monolith without any cracks occurring on the monolith's surface. The total surface area chosen specified the number of holes that were drilled into the monolith. Each diameter will have a different number of holes, but with a constant average total surface area of holes for each drill bit. The calculation was adapted from a general equation and modelling approaches for immobilization on porous materials (Kar, 2025; Maghraby et al., 2023). The calculation was expressed as follows:

$$\text{Average total surface area of holes} = 2\pi r \times t \times h$$

Where r is the radius of the holes drilled into the monolith (if the diameter of the drill is 0.3 mm, the radius is 0.15 mm), t is the thickness of the monolith (10 mm), and h is the number of holes. All analyses were performed in triplicate.

Lipase Immobilization Process

According to the process described by (Coutinho, 2020) with some modifications, Candida rugosa lipase enzymes were immobilized to the polymethacrylate-based monolith at 30 °C, 150 rpm for 72 hours (Aghabeigi et al., 2023). The immobilization methods selected for this study were adsorption to the hydrophobic surface. The monoliths were immersed in 10 mL of 0.1 M sodium phosphate buffer solution at pH 7 with a lipase concentration of 10 mg/mL. After 72 hours, the monoliths were washed with the buffer three times to remove loosely bound enzymes. The residual enzyme solution from the immobilization process was removed and stored for analysis. The filtrates or the washing solutions were collected for protein analysis, which was determined by the Bradford protein assay using the enzyme lipase as a standard reference to build the calibration curve based on the method by (Cheng et al., 2019; Luangon et al., 2012; Silva et al., 2023). The protein concentration in the supernatant is measured using the Bradford method. Lastly, the immobilization yield (%) for each sample was calculated based on study by (Zhang et al., 2023) and (Boudrant et al., 2020)using the following formula:

$$\text{Immobilization yield (\%)} = [\text{Immobilized enzyme} / \text{Initial amount of enzyme}] \times 100\%$$

e-ISSN 2716-697X

Experimental Design

This study employed a two-stage experimental approach. First, a One-Factor-at-a-Time (OFAT) design was used to evaluate the individual effects of porogen concentration and hole diameter on lipase immobilization yield. This preliminary screening established practical ranges and identified significant factors influencing immobilization efficiency (Parandi et al., 2023). Subsequently, Response Surface Methodology (RSM) was applied to simulate and optimize the combined effects of porogen concentration, hole diameter, and number of holes. Historical Data Design of RSM was used as a statistical design to estimate and study the correlation between the porogen concentration, diameter, and amount of lipase immobilized during the immobilization process (Zulqarnain et al., 2023). The independent variables were the porogen concentration and diameter of the polymethacrylate monolith, while the immobilization efficiency was selected as the response parameter. Each experiment was performed in triplicate to reduce the chance of error (Sajjad et al., 2022). Therefore, the OFAT results served as the foundation for defining variable ranges in the RSM model.

The relationship between the independent variables and immobilization yield was described using a second-order polynomial regression equation. The regression model was evaluated using coefficient of determination (R^2) and adjusted R^2 to assess model fit. Analysis of variance (ANOVA) was also used to confirm the overall significance of the regression. All statistical analyses were performed using Design-Expert version 7.0 software (Dharmegowda et al., 2022; Panakkal et al., 2021). The model parameters and statistical outputs are reported in the Results section.

RESULTS & DISCUSSION

Polymethacrylate-based monolith synthesis

The material interface is the key factor that determines the rate of a reaction or a process (Yeh et al., 2016). Optimizing the synthesis and fabrication of the polymethacrylate monolith will be very beneficial in increasing the productivity and maximizing the production results of the biodiesel yield in future research. The monoliths were fabricated from 0% to 60% porogen concentration to evaluate the pore morphology and mechanical stability. This preliminary screening facilitated the selection of monolith types most suitable for lipase immobilization and column drilling, ensuring reproducibility and structural integrity in subsequent experiments.

Figure 1 shown that the polymethacrylate monolith prepared has a different color and disposition according to the porogen content. After thoroughly washing with methanol and deionized water, the wall of the monolith surface and color can be differentiated. Fabricated monolith with 0% and 20% porogen concentration has a glass, opaque surface, while the monoliths with higher porogen content at 40% and 60% were white in color and

more solid. However, polymethacrylate-based monoliths at higher porogen concentration were easier to break apart. This was seen during the washing steps as the wall surface of the monolith crumbled and cracked. The monoliths are washed with methanol to remove the unreacted inert porogen and monomeric reagents, and further washing with deionized water causes the samples to become firmer and solid when left to dry (Kamin et al., 2020). Methanol also has the lowest capability to dissolve the monomers, resulting in the formation of large pores and a highly porous surface for the polymethacrylate-based monolith (Hermawan et al., 2021).

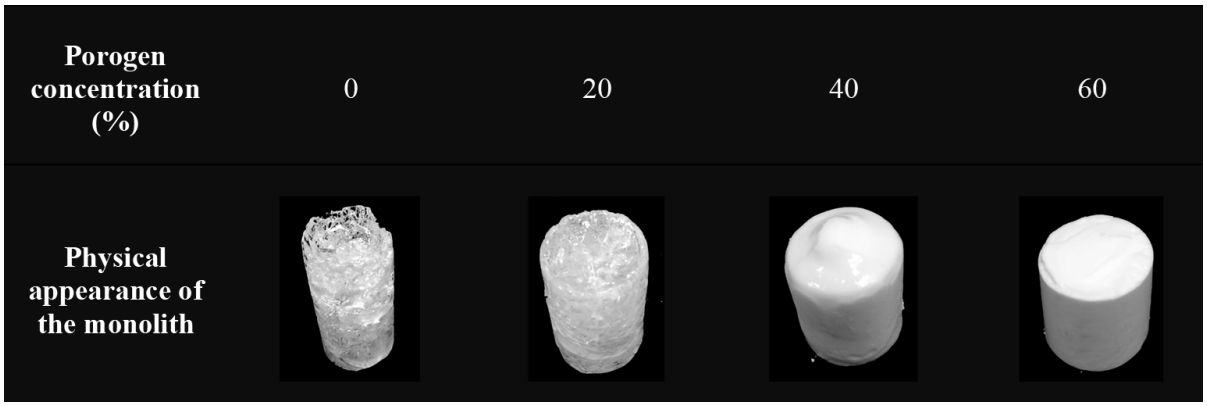

Figure 1 Polymethacrylate-based monoliths prepared at different porogen concentrations.

Physical modification of the polymethacrylate-based monoliths through mechanical drilling

The polymethacrylate-based monoliths undergo physical modification through drilling using HSS Twist drills at several diameters. The number of holes drilled into the monolith was selected and determined by drilling each of the monoliths according to the previous Table 1. From the table, the greatest number of holes that can be drilled into the monoliths without causing a crack on the surface of the monoliths (Figure 2) was using 0.3 mm with 24 holes. Therefore, the average total surface area of holes for each drill bit chosen was 226.22 mm^2. Figure 2 shows some of the images of the cracked polymethacrylate-based monoliths during the drilling process. According to a study by Rahman et al., too much porogen content during polymethacrylatebased monolith preparation can cause brittle polymers that are prone to cracking and have low impact resistance (Rahman et al., 2018). As shown in Figure 2, drilling at 60% porogen concentration with a 0.3 mm bit and 28 holes resulted in visible cracks in the monolith structure. In contrast, Figure 3 illustrates monoliths prepared under the same conditions with 23 holes, where no cracks were observed. This comparison highlights the importance of porogen concentration and drilling parameters in maintaining monolith integrity for subsequent lipase immobilization.

e-ISSN 2716-697X

Table 1 Different diameters and numbers of holes of the polymethacrylate-based monoliths

Diameter (mm)	Number of holes					
0.3	20	22	24	26	28	30
0.4	15	17	18	20	21	23
0.5	12	13	14	16	17	18
0.6	10	11	12	13	14	15
Total surface area of monolith (mm^2)	188.52	207.37	226.22	245.08	263.98	282.78

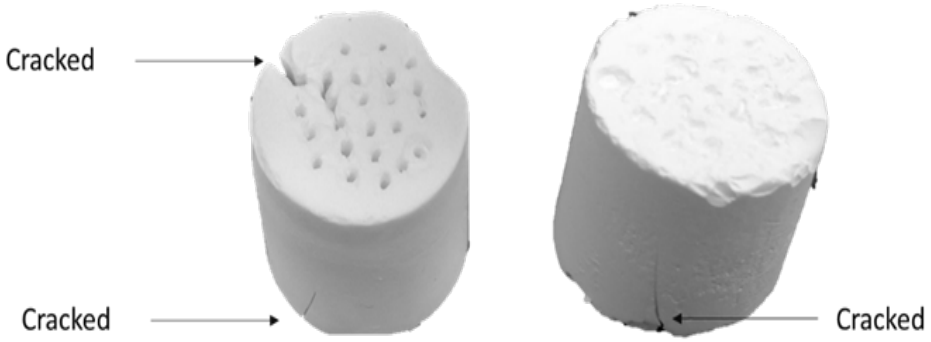

Figure 2 The cracked polymethacrylate monoliths fabricated at 60% porogen concentration during the drilling process using a 0.3 mm diameter drill bit with 28 holes.

e-ISSN 2716-697X

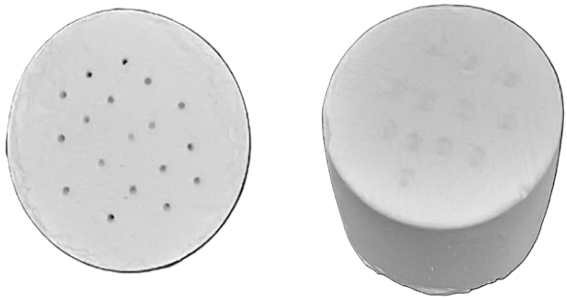

Figure 3 The polymethacrylate monoliths fabricated at 60% porogen concentration, drilled using 0.3 mm diameter drill bits without cracks, with 23 holes.

Experimental and simulation investigations of lipase immobilization process

The polymethacrylate-based monoliths were immobilized with the Candida rugosa lipase enzymes to study their immobilization yield after the monoliths underwent physical modification through drilling. The lipase immobilization process was performed on polymethacrylate at 30%, 40%, 50% and 60% porogen concentrations with diameters of 0.3 mm, 0.4 mm, 0.5 mm, and 0.6 mm. The 30%, 40%, 50% and 60% porogen content were selected for the immobilization process based on their physical surface, which is more suitable for the immobilization process. This is because at higher porogen content (>60%), monoliths produced were brittle and often collapsed into powder form during fabrication screening. The immobilization process can cause structural changes in the support material; therefore, choosing the right support was crucial (Cornejo, 2021).

The immobilization yield at different porogen concentrations and diameters, based on experimental results and predicted simulation values from RSM analysis for the immobilization process, is shown in Figure 4. The highest immobilization yield was obtained at 60% porogen contents under varied diameter and number of holes, with a yield of 58.67 ± 0.69%. At a diameter of 0.4 mm (18 holes) when varying the porogen concentration, immobilization yields of 57.50 ± 0.95% were achieved. In comparison, the simulation predicted the highest immobilization yield at a drill diameter of 0.3 mm with 24 holes, resulting in 55.90 ± 1.12%. At 60% porogen concentration, the model further indicated an immobilization yield of 58.90 ± 0.31% across different diameters and hole numbers.

e-ISSN 2716-697X

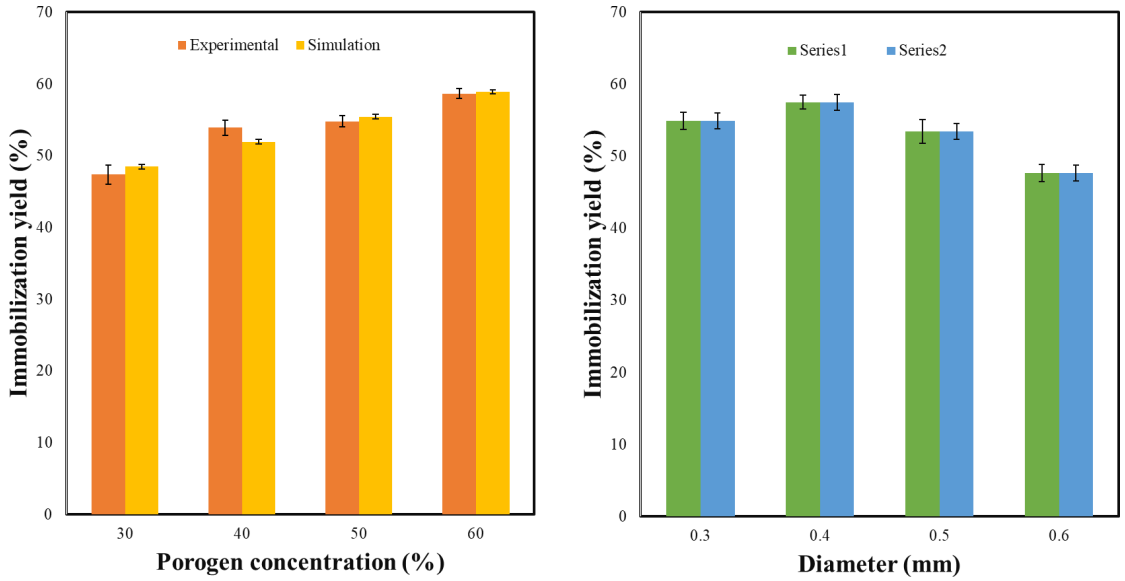

Figure 4 The immobilization yield at different (A) porogen concentration and (B) Diameter based on the experimental results and predicted simulation value from RSM analysis for the immobilization process.

In this study, Design Expert and Response Surface Methodology (RSM) data analysis were adopted to analyze the interaction between parameters and investigate the immobilization efficiency of lipase enzymes attached to the polymethacrylate-based monolith (Table 2 and Figure 5). From the analysis of variance (ANOVA) analysis in Table 2, the Model F-value of 4.76 implies that the model is significant, in which there is only a 1.48% chance that the a "Model F-Value" this large could occur due to noise. Linear model was suggested as the model because the p-value was statistically significant with p-value of <0.001. RSM is used to analyze and evaluate the input variables based on the confidence level and the coefficient of determination (Dharmegowda et al., 2022). In this model, significance of each parameter was also determined using the p-value. From the table, only parameter A, the porogen concentration is significant. Different porogen concentrations can changed the overall polymerization kinetics resulted in distinct pore structures (Chan et al., 2017). Table 2 shows that the predicted R2 of 0.1880 is in reasonable agreement with the adjusted R2 of 0.3723. The interaction of input and output parameters for a process is the most critical parameters which affect the response of that particular process (Zulqarnain et al., 2023). Hence, experimental responses and the prediction value are essential for an accurate optimum conditions' prediction of the immobilization process.

e-ISSN 2716-697X

Table 2 Analysis of Variance (ANOVA)

Source	Sum of Squares	Df	Mean square	F value	p-value (Prob> F)
Model	340.42	3	113.47	4.76	0.0148
A	301.50	1	301.50	12.64	0.0026
B	0.46	1	0.46	0.019	0.8917
C	0.79	1	0.79	0.033	0.8583
Residual	381.73	16	23.86		
Cor Total	722.15	19			
Standard Deviation		4.88	R-Squared		0.4714
Mean		53.69	Adj R-Squared		0.3723
C. V. %		9.10	Pred R-Squared		0.1880
PRESS		586.40	Adeq precision		6.587

Regression Equation (Model: Linear)

Immobilization yield = 53.91 + 5.21 (A, porogen concentration) + 0.86 (B, holes diameter) + 1.12 (C, number of holes)

Figure 5 (A and B) shows that the highest immobilization yield was achieved at 0.30 mm diameter and 60% porogen concentration, with 57.96%. Meanwhile, for the interaction of the number of holes and diameter, predicted that the highest immobilization yield of 60.45% at a higher number of holes with a smaller diameter of 0.3 mm (Figure 5, C and D). Lastly, the interaction of the number of holes and porogen concentration in Figure 5 (E and F) shows the highest immobilization yield at 24 holes and 60% porogen concentration, with 58.14%. These findings highlight that 60% porogen concentration with diameters of 0.3 mm and a number of holes of 24 constantly yields the highest immobilization yield for the lipase immobilization process.

The higher the porogen concentration, the larger the pore size and porosity of the polymethacrylate-based monolith (Hermawan et al., 2021). Thus, this allows unrestricted interaction of a lipase enzyme with the surface of the monolithic material, which leads to a higher immobilization yield (Volokitina et al., 2017). The pores must have a large enough size to

e-ISSN 2716-697X

allow the binding of the lipase enzymes inside and outside the monolithic material. The polymethacrylate-based monolith with higher porogen content forms a more porous matrix with increased surface area and interconnected pore networks, which facilitates the enzyme binding and diffusion (Bié et al., 2022; Serial et al., 2026). A greater number of micropores increases the total available surface area. Therefore, enzymes can spread more evenly, which reduces crowding and steric hindrance during the immobilization process

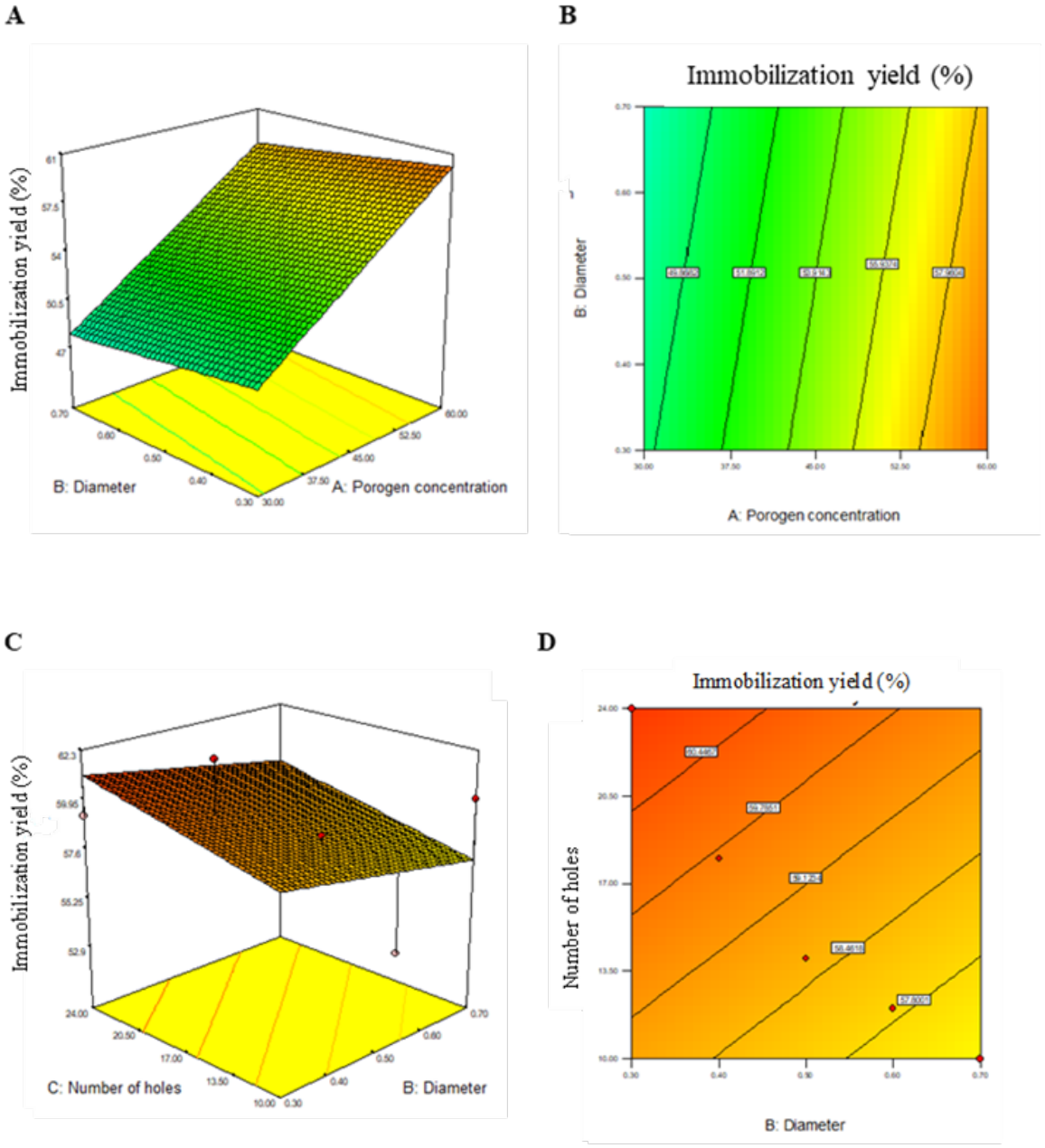

e-ISSN 2716-697X

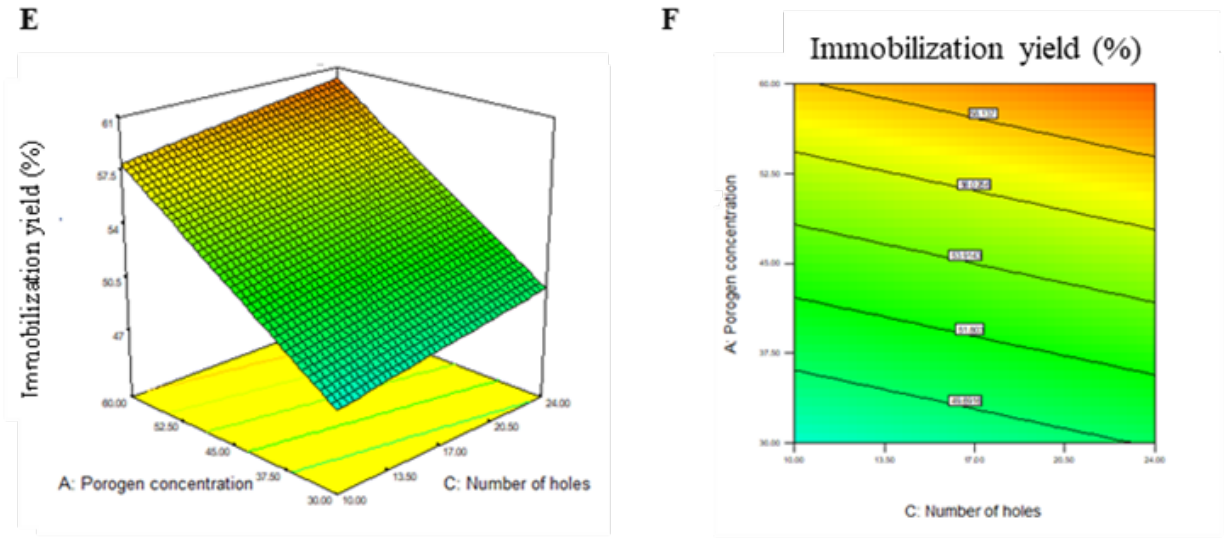

Figure 5 The 3-D surface and contour plot of the immobilization yield, (A-B) interaction between diameter and porogen concentration, (C-D) interaction between diameter and number of holes, and (E-F) interaction between porogen concentration and number of holes after the lipase immobilization process.

CONCLUSION

This study underscores the pivotal role of structural parameters, such as porogen concentration and monolith diameter (corresponding to the number of holes), in optimizing the lipase immobilization process on porous polymethacrylate-based monoliths. The experimental and simulation results consistently highlight that 60% porogen concentration is the most favorable condition, with diameters of 0.4 mm and 0.3 mm yielding the highest immobilization yield for the experimental and simulation data. The immobilization yield increases with smaller pore diameters, a higher number of holes, and greater porogen contents because of the improved surface area and accessibility for lipase enzyme attachment, enhancing the loading efficiency. These findings not only validate the tunability of monolith architecture for enhanced enzyme loading but also pave the way for designing robust biocatalytic platforms tailored for industrial applications such as biodiesel production. By continuing to refine the polymethacrylate-based monolith design and expanding its application scope, this research makes a meaningful contribution to the advancement of eco-friendly and efficient biocatalytic technologies.

e-ISSN 2716-697X

ACKNOWLEDGEMENTS

This research is funded by Fundamental Research Grant Scheme (FRGS) FRG0583-1/2022 from the Ministry of Higher Education, Malaysia.

REFERENCES

Afandizadeh, S., & Foumeny, E. A. (2001). *Design of packed bed reactors :guides to catalyst shape , size , and loading selection*. *21*.

Aghabeigi, F., Nikkhah, H., Zilouei, H., & Bazarganipour, M. (2023). Immobilization of lipase on the graphene oxides magnetized with NiFe2O4 nanoparticles for biodiesel production from microalgae lipids. *Process Biochemistry*, *126*(January), 171–185. https://doi.org/10.1016/j.procbio.2023.01.012

Bié, J., Sepodes, B., Fernandes, P. C. B., & Ribeiro, M. H. L. (2022). Enzyme Immobilization and Co-Immobilization: Main Framework, Advances and Some Applications. In *Processes* (Vol. 10, Issue 3). https://doi.org/10.3390/pr10030494

Boudrant, J., Woodley, J. M., & Fernandez-Lafuente, R. (2020). Parameters necessary to define an immobilized enzyme preparation. *Process Biochemistry*, *90*, 66–80. https://doi.org/10.1016/j.procbio.2019.11.026

Chan, Y. W., Kansil, T., & Ongkudon, C. M. (2017). Analytical and preparative polymethacrylate monolith fabrication: effect of porogen content and column size on pore morphology. *Colloid Polymer Science*, *295*, 2373–2382.

Cheng, W., Li, Y., Li, X., Bai, W., & Liang, Y. (2019). Preparation and characterization of PDA/SiO2 nanofilm constructed macroporous monolith and its application in lipase immobilization. *Journal of the Taiwan Institute of Chemical Engineers*, *104*, 351–359. https://doi.org/10.1016/j.jtice.2019.09.013

Cornejo, I. (2021). A model for correcting the pressure drop between two monoliths. *Catalysts*, *11*(11), 1–13. https://doi.org/10.3390/catal11111314

Coutinho, T. C. (2020). Immobilization of enzymes of agroindustrial interest on hydroxyapatite nanoparticles: β-glucosidase, xylase and phytase. In *Federal University of São Carlos, Graduate Program of Chemical Engineering*. https://repositorio.ufscar.br/handle/ufscar/12468

Dharmegowda, I. Y., Muniyappa, L. M., Siddalingaiah, P., Suresh, A. B., Chandrashekarappa, M. P. G., & Prakash, C. (2022). MgO Nano-Catalyzed Biodiesel Production from Waste Coconut Oil and Fish Oil Using Response Surface Methodology and Grasshopper Optimization. *Sustainability*, *14*, 11132.

Gustafsson, H. (2012). *Enzyme Immobilization in Mesoporous Silica*. Chalmers University of Technology.

Haghighi, F. H., Binaymotlagh, R., Palocci, C., & Chronopoulou, L. (2024). Magnetic Iron Oxide Nanomaterials for Lipase Immobilization: Promising Industrial Catalysts for Biodiesel Production. *Catalysis Today*, *14*, 336.

Hermawan, B. A., Mutakin, & Hasanah, A. N. (2021). Role of porogenic solvent type on the performance of a monolithic imprinted column. *Chemical Papers*, *75*(4), 1301–1311. https://doi.org/10.1007/s11696-020-01399-5

Kamin, Z., Abdulrahim, N., Misson, M., Chel Ken, C., Sarbatly, R., Krishnaiah, D., & Bono, A. (2020). Melt blown polypropylene nanofiber template for homogenous pore channels monoliths. *IOP Conference Series: Materials Science and Engineering*, *736*(5), 052006. https://doi.org/10.1088/1757-899X/736/5/052006

Kar, R. K. (2025). Introduction to Metabolic Engineering and Application. Biologically-Inspired Systems Springer, Cham. https://doi.org/10.1007/978-3-031-93189-5_4.

In D. Lahiri, M. Nag, D. Bhattacharya, & S. Ghosh (Eds.), *Introduction to Metabolic Engineering and Application. Biologically-Inspired Systems* (pp. 105–119). Springer Cham. https://doi.org/10.1007/978-3-031-93189-5

Luangon, B., Siyasukh, A., Winayanuwattikun, P., Tanthapanichakoon, W., & Tonanon, N. (2012). Flow-through immobilization of Candida rugosa lipase on hierarchical micro-/macroporous carbon monolith. *Journal of Molecular Catalysis B: Enzymatic*, *75*, 80–85. https://doi.org/10.1016/j.molcatb.2011.11.017

Maghraby, Y. R., El-Shabasy, R. M., Ibrahim, A. H., & Azzazy, H. M. E. (2023). Enzyme Immobilization Technologies and Industrial Applications. *ACS Omega*, *8*, 5184–5196. https://doi.org/10.1021/acsomega.2c07560

Panakkal, E. J., Cheenkachorn, K., Gundupalli, M. P., Kitiborwornkul, N., & Sriariyanun, M. (2021). Impact of sulfuric acid pretreatment of durian peel on the production of fermentable sugar and ethanol. *Journal of the Indian Chemical Society*, *98*(12), 100264. https://doi.org/10.1016/j.jics.2021.100264

Parandi, E., Mousavi, M., Kiani, H., Rashidi Nodeh, H., Cho, J., & Rezania, S. (2023). Optimization of microreactor-intensified transesterification reaction of sesame cake oil (sesame waste) for biodiesel production using magnetically immobilized lipase nano-biocatalyst. *Energy Conversion and Management*, *295*(September). https://doi.org/10.1016/j.enconman.2023.117616

Parandi, E., Safaripour, M., Abdellattif, M. H., Saidi, M., Bozorgian, A., Rashidi Nodeh, H., & Rezania, S. (2022). Biodiesel production from waste cooking oil using a novel biocatalyst of lipase enzyme immobilized magnetic nanocomposite. *Fuel*, *313*(December 2021), 123057. https://doi.org/10.1016/j.fuel.2021.123057

Rahman, S. K. A., Yusof, N. A., Abdullah, A. H., Mohammad, F., Idris, A., & Al-lohedan, H. A. (2018). Evaluation of porogen factors for the preparation of ion imprinted polymer monoliths used in mercury removal. *PLoS ONE*, *13*(4), 1–14. https://doi.org/10.1371/journal.pone.0195546

Rajnish, K. N., Samuel, M. S., J, A. J., Datta, S., Chandrasekar, N., Balaji, R., Jose, S., & Selvarajan, E. (2021). Immobilization of cellulase enzymes on nano and micro-materials for breakdown of cellulose for biofuel production-a narrative review. *International Journal of Biological Macromolecules*, *182*, 1793–1802. https://doi.org/10.1016/j.ijbiomac.2021.05.176

Sajjad, N., Orfali, R., Perveen, S., Rehman, S., Sultan, A., Akhtar, T., Nazir, A., Muhammad, G., Mehmood, T., Ghaffar, S., Al-taweel, A., Jilani, M. I., & Iqbal, M. (2022). Biodiesel Production from Alkali-Catalyzed Transesterification of Tamarindus indica Seed Oil and Optimization of Process Conditions. *Molecules*, *27*, 3230.

Santos, S., Puna, J., & Gomes, J. (2020). A Review on Bio-Based Catalysts (Immobilized Enzymes) Used for Biodiesel Production. *Energies*, *13*, 3013.

Serial, M. R., Schmidt, L., Adrian, M., Brauckmann, G., Benders, S., Bueschler, V., Liese, A., & Penn, A. (2026). A novel method for quantifying enzyme immobilization in porous carriers using simple NMR relaxometry. *Biochemical Engineering Journal*, *225*, 109909. https://doi.org/10.1016/j.bej.2025.109909

Sheldon, R. A., Basso, A., & Brady, D. (2021). New frontiers in enzyme immobilisation: robust biocatalysts for a circular bio-based economy. *Royal Society 0f Chemistry: Chem Soc Rev*, *50*, 5850–5862. https://doi.org/10.1039/d1cs00015b

Silva, J. M. F., dos Santos, K. P., dos Santos, E. S., Rios, N. S., & Gonçalves, L. R. B. (2023). Immobilization of Thermomyces lanuginosus lipase on a new hydrophobic support (Streamline phenyl^{TM}): Strategies to improve stability and reusability. *Enzyme and Microbial Technology*, *163*, 110166. https://doi.org/10.1016/j.enzmictec.2022.110166

Simbas, A. F., & Ongkudon, C. M. (2019). Parametric Studies of Polymethacrylate-based Monolith Fabrication. *Transactions on Science and Technology*, *6*(3), 304–309.

Trubac, R. E., Dautzenberg, F. M., Griffin, T. A., Paikert, B., Schmidt, V. R., & Overbeek, R. A. (2001). *Micro-engineered catalyst systems : ABB ' s advancement in structured catalytic packings*. *69*, 17–24.

Volokitina, M. V., Nikitina, A. V., Tennikova, T. B., & Korzhikova-Vlakh, E. G. (2017). Immobilized enzyme reactors based on monoliths: Effect of pore size and enzyme loading on biocatalytic process. *Electrophoresis*, *38*(22–23), 2931–2939. https://doi.org/10.1002/elps.201700210

Xie, W., & Huang, M. (2020). Fabrication of immobilized Candida rugosa lipase on magnetic Fe3O4-poly(glycidyl methacrylate-co-methacrylic acid) composite as an efficient and recyclable biocatalyst for enzymatic production of biodiesel. *Renewable Energy*, *158*, 474–486. https://doi.org/10.1016/j.renene.2020.05.172

Yeh, S. I., Huang, Y. C., Cheng, C. H., Cheng, C. M., & Yang, J. T. (2016). Development of a millimetrically scaled biodiesel transesterification device that relies on droplet-based co-axial fluidics. *Nature Publishing Group*, *101*, 1–7. https://doi.org/10.1038/srep29288

Zhang, H., Zhu, R., Shi, Y., Yu, X., Zhang, L., Li, Y., & Shi, G. (2023). Lipase immobilization using scalable and biocompatible lignin-based material as a carrier. *Industrial Crops and Products*, *193*, 116241. https://doi.org/10.1016/j.indcrop.2023.116241

Zhao, F., Zhang, H., Zhang, Z., & Liang, Y. (2021). Preparation of mesoporous nanofilm constructed millimeter-sized macroporous SiO2 for lipase immobilization. *Microporous and Mesoporous Materials*, *323*(May), 111227. https://doi.org/10.1016/j.micromeso.2021.111227

Zulqarnain, Mohd Yusoff, M. H., Nazir, M. H., Rahman, M. F. A., Yaqoob, H., Rashid, T., Hai, I. U., & Sher, F. (2023). Hybrid valorization of biodiesel production using sustainable mixed alcohol solvent. *Environmental Technology & Innovation*, *29*, 102963. https://doi.org/10.1016/j.eti.2022.102963

Borneo International Journal of Biotechnology (BIJB)
Vol. 5 (December 2025), 80-111

e-ISSN 2716-697X

Microalgae as Functional Feed in Fish Larval Rearing: Nutritional Value, Ecological Functions, and Future Prospects for Sustainable Aquaculture

Ignatia Justine[1], Mailin Misson[1]*, Ching Fui Fui[2], Wilson Thau Lym Yong[1,3], Grace Joy Wei Lie Chin[1]

[1]Biotechnology Research Institute, University Malaysia Sabah, Jalan UMS, 88400 Kota Kinabalu, Sabah, Malaysia. [2]Higher Institution Centres of Excellence, Borneo Marine Research Institute, Universiti Malaysia Sabah, 88400, Kota Kinabalu, Sabah, Malaysia
[3]Seaweed Research Unit, Faculty of Science and Natural Resources, University Malaysia Sabah, Jalan UMS, 88400 Kota Kinabalu, Sabah, Malaysia.
*Corresponding email: mailin@ums.edu.my
Received: 24 October 2025 | Accepted: 20 December 2025 | Published: 31 December 2025

ABSTRACT

As global fish stocks decline and aquaculture expansion intensifies, sustainable larval rearing remains a critical challenge due to the high dependency on live feed such as rotifers and *Artemia*. Microalgae, as the foundational feed component, play a pivotal role in supporting larval nutrition, health, and water stability. While numerous reviews have discussed microalgae as nutritional supplements or live feed, few have comprehensively analyzed their multifunctional role as both nutritional and ecological components within larval rearing systems. This review uniquely integrates current understanding on microalgae's biochemical composition, functional bioactivity, and ecosystem-level interactions that enhance larval survival, immunity, and water quality. It emphasizes the dual role of microalgae in nutrition and bioremediation, presenting an updated synthesis of species-specific applications and their suitability based on biochemical and physiological traits. Additionally, this review identifies emerging technological and bioprocessing innovations such as strain improvement, cell-wall modification, and integration with biofloc and circular bioeconomy systems that address limitations of cost, digestibility, and biochemical variability. By bridging nutritional, physiological, and environmental perspectives, this paper offers a holistic and practice-oriented framework for using microalgae as functional feed to enhance larval growth, health, and rearing sustainability in aquaculture.

Keywords: Microalgae, Phytoplankton, Sustainable Aquaculture, Health benefit, Aquafeed, Fish Larvae Nutrition

e-ISSN 2716-697X

INTRODUCTION

The global population continues to increase rapidly, driving a growing demand for food, especially high-quality protein sources. According to the Food and Agriculture Organization (FAO, 2024), global food demand is projected to rise from approximately 2.1 billion tonnes to nearly 3 billion tonnes by 2050. As capture fisheries have reached their maximum sustainable yield, aquaculture has become one of the fastest growing food production sectors, providing nearly half of the fish consumed worldwide. This expansion, however, has intensified the need for sustainable, nutritionally balanced, and cost-effective feeds to support the growing aquaculture industry (Sarker, 2023). In 2022, global aquafeed production reached 52.9 million tonnes, accounting for about 4.2% of total compound feed production, with China, Vietnam, India, Norway, and Indonesia ranking among the top producers (Dikel and Demirkale, 2024).

Traditionally, aquaculture has relied heavily on fishmeal and fish oil derived from wild caught fish as primary feed ingredients. Fishmeal is valued for its high protein content (60 to 72%), excellent digestibility, and balanced amino acid profile, while fish oil provides essential long chain polyunsaturated fatty acids (LC PUFAs), particularly eicosapentaenoic acid (EPA) and docosahexaenoic acid (DHA), which are critical for fish growth, reproduction, and immunity (Siddik et al., 2024). Despite their nutritional superiority, the increasing use of fishmeal and fish oil poses major sustainability concerns due to overexploitation of marine resources, fluctuating prices, and ecological impacts associated with their harvesting and processing (Boyd and McNevin 2022). It is essential to identify alternative feed ingredients that can deliver comparable nutritional value while minimizing environmental impact and production cost to ensure the future sustainability of aquaculture.

Among the most critical stages in aquaculture production is larval rearing, which often determines the overall success of hatchery operations (El-Sayed et al., 2024). Fish larvae, such as those of the Asian seabass (*Lates calcarifer*), are highly vulnerable during early development due to their small size, limited mouth gape, and immature digestive systems (Islam et al., 2024). Consequently, recent study by Safiin et al. (2021) stated that the Asian seabass are unable to ingest or efficiently digest conventional formulated feeds and instead depend on live feeds such as rotifers (*Brachionus plicatilis*) and *Artemia nauplii*. Although these live feeds remain indispensable in larval culture, they present several limitations, including variable nutritional composition, the need for enrichment with essential fatty acids, susceptibility to contamination, and high production costs. Moreover, their culture can be labor intensive and environmentally sensitive, often leading to inconsistent supply. These challenges underscore the urgent need for alternative or supplementary feed resources that can improve larval survival, growth, and overall hatchery efficiency.

Microalgae play a critical ecological role in larval rearing systems through the greenwater effect. This phenomenon refers to the presence of suspended microalgae in rearing tanks which improves water quality by stabilizing dissolved oxygen, reducing harmful nitrogen compounds, and promoting beneficial microbial communities that outcompete pathogenic bacteria (Pascon et al., 2021). The green coloration of the water also diffuses light intensity, reducing visual stress and improving feeding behavior in fish larvae with transparent bodies (El-Sayed et al., 2024). Furthermore, microalgae can secrete extracellular compounds with antibacterial and antioxidant properties, enhancing larval stress tolerance and immunity (Fan et al., 2022). Besides, these effects contribute to improved larval survival, growth, and overall system stability, making microalgae a multifunctional component of sustainable hatchery management (Ma and Hu, 2024).

The effectiveness of microalgae in larval nutrition and health has been supported by numerous studies demonstrating their ability to enhance growth performance, feed utilization, pigmentation, and immune response in various fish species. For instance, enrichment of live feeds with microalgae such as *Nannochloropsis*, *Isochrysis*, *Tetraselmis*, and *Chlorella* has been shown to improve their fatty acid profiles, thereby enhancing the nutritional quality of feed consumed by larvae (Siddik et al., 2024). Direct feeding of microalgae to larvae has also yielded positive outcomes, particularly in early stages where microalgal cells can be ingested whole (de Moraes et al., 2022). These findings highlight the potential of microalgae as both a primary and supplementary feed source for larval rearing, providing not only essential nutrients but also bioactive metabolites that promote overall larval fitness.

Despite these benefits, several challenges remain in the large-scale application of microalgae for aquaculture feed. Production costs, nutrient variability among strains, and limitations in digestibility due to rigid cell walls are among the key barriers (Machado et al., 2022). However, advances in biotechnology and bioprocessing such as strain improvement, cell wall modification, and integration of microalgae cultivation into biofloc or circular bioeconomy systems offer promising solutions to enhance efficiency and reduce costs (Ahmad et al., 2022; Zimmermann et al., 2023). Furthermore, comprehensive biochemical characterization and performance evaluation of different microalgal species are essential to identify optimal strains for specific aquaculture applications (Zhang et al., 2023).

Therefore, this review provides a comprehensive synthesis of current knowledge on the functional role of microalgae as feed in fish larval rearing. It discusses their nutritional value, bioactive properties, and ecological contributions to larval culture systems, with emphasis on the greenwater effect and species-specific applications. The review also highlights technological advances and future directions for improving microalgae utilization, aiming to strengthen the foundation for sustainable and resilient aquaculture practices.

e-ISSN 2716-697X

Aquaculture and Sustainable Feed

The global population is projected to increase by 2.3 billion people between 2009 and 2050, leading to a sharp rise in food demand, including cereals (FAO, 2024). In line with this, aquaculture has become the fastest-growing food production sector. According to the FAO (2024), global aquaculture production reached 130.9 million tonnes in 2022, consisting of 94.4 million tonnes of aquatic animals and 37.8 million tonnes of algae, surpassing capture fisheries for the first time in history. This shift highlights the increasing reliance on aquaculture to meet global protein demand while alleviating pressure on overexploited wild fish stocks.

As summarised in Table 1, global aquaculture production is largely dominated by freshwater species such as carps and tilapia, while marine species like salmon and seabass contribute substantially to high-value markets. Carps remain vital for ensuring global food security, especially in Asia, while tilapia continues to expand due to its resilience, fast growth, and cost-effectiveness. Meanwhile, salmon and seabass farming continues to grow, driven by technological and genetic advancements in aquaculture operations in regions such as Norway, Chile, and the Mediterranean (Næve et al., 2022; Zoli et al., 2023; FAO, 2024; Meurer et al., 2025). These trends point to an increasing need for high-quality, species-specific feeds capable of supporting optimal growth and health in intensively farmed fish.

The sustainability of aquaculture depends heavily on the development of nutritionally balanced and environmentally friendly feed sources (Tacon et al., 2022). Traditionally, fishmeal and fish oil have served as the primary protein and lipid sources in aquafeeds (Kousoulaki et al., 2022). However, the rising cost, limited availability, and ecological concerns associated with these ingredients have intensified the search for alternative feed components, including microalgae (Gao et al., 2024). Microalgae, in particular, offer a promising solution because they can simultaneously provide essential nutrients and contribute to environmental sustainability through carbon sequestration and minimal reliance on arable land or freshwater resources.

Microalgae are microscopic photosynthetic organisms that play a crucial role in aquatic ecosystems and are regarded as a promising sustainable feed resource (Sarıtaş et al., 2024). The term "algae" broadly encompasses diverse eukaryotic organisms capable of oxygenic photosynthesis, excluding higher plants (Barsanti and Gualtieri, 2022). Marine microalgae typically thrive in seawater environments, whereas freshwater species inhabit lakes, rivers, and ponds (Ramlee et al., 2021) as described in Figure 1.

e-ISSN 2716-697X

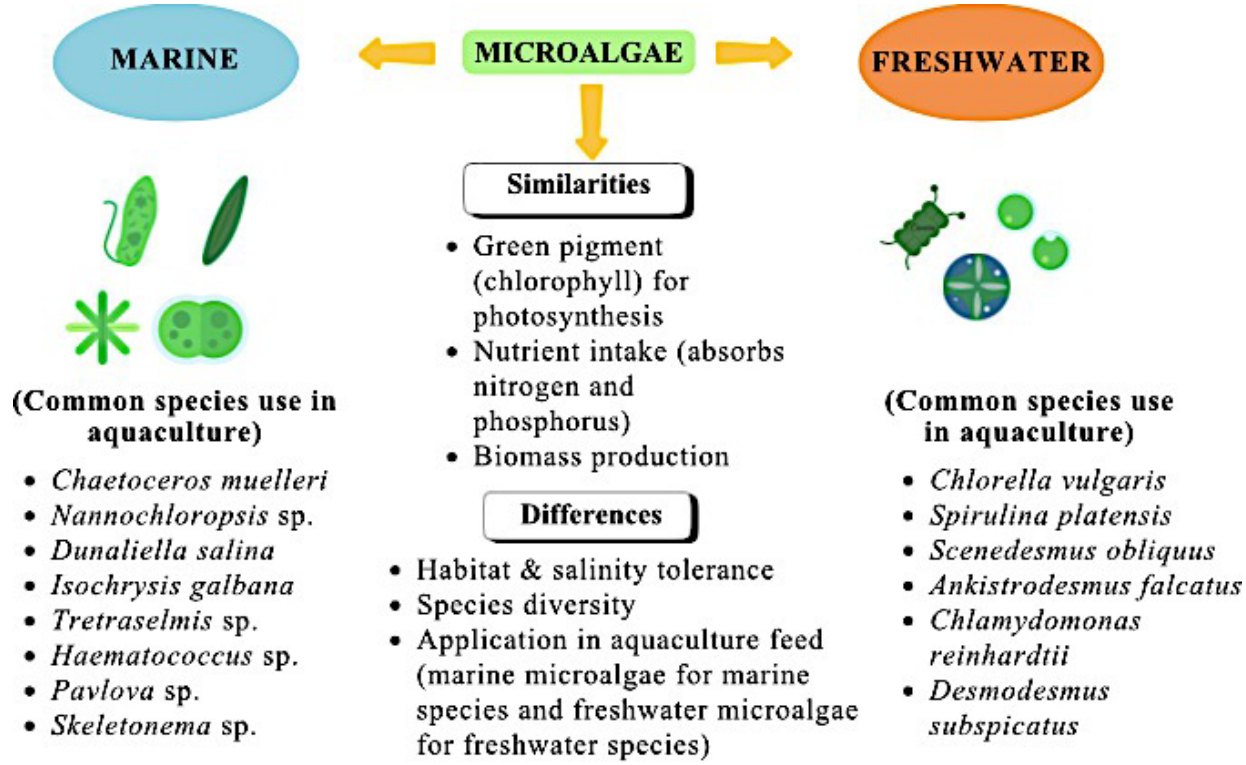

Figure 1 Different species of microalgae based on their respective habitats.

In aquaculture, species such as *Nannochloropsis sp.*, *Isochrysis sp.*, *Tetraselmis sp.*, and *Chaetoceros sp.* are commonly used due to their high nutritional value and suitability as live feeds or as components in formulated diets for various aquatic organisms (Batista et al., 2020). These species provide essential nutrients, including proteins, lipids, pigments, and bioactive compounds, that not only enhance growth, immunity, and survival of fish larvae but also contribute to water quality and ecosystem stability in rearing systems. Collectively, these attributes position microalgae as a multifunctional, sustainable feed component capable of addressing both nutritional and environmental challenges in modern aquaculture.

e-ISSN 2716-697X

Table 1 Most Frequently Farmed Shellfish and Fish

Species Group	Top Species	Production	Ref.
Freshwater Finfish (carps)	Silver carp (*Hypophthalmichthys molitrix*) and grass carp (*Ctenopharyngodon idellus*)	The largest overall output, leading in global freshwater production, particularly in Asia (China, India). Essential for ensuring global food security.	FAO. (2024)
Freshwater finfish (Tilapia)	Nile Tilapia (Oreochromis niloticus)	Ranked as the third most cultivated finfish species worldwide. Known for its resilience, rapid growth, and cost-effectiveness in various markets.	Meurer et al., (2025)
Marine finfish (Salmonids)	Atlantic salmon (*Salmo salar*)	Mainly cultivated in Chile and Norway. The strong demand propels ongoing advancements in genetics and operations.	Næve et al., (2022)
Marine Finfish (Asian Seabass)	Asian Seabass (*Lates calcarifer*), European Sea Bass (*Dicentrarchus labrax*)	High-value, high-end market species. Notable growth in Asia (Asian Seabass) and the Mediterranean region (European Sea Bass).	Zoli et al., (2023)

e-ISSN 2716-697X

Nutritional Requirement of Fish Larval

Fish life cycle progresses from eggs, embryo, larvae, juvenile and adult stages as stated in Figure 2. Among these stages, the larval phase is the most critical and vulnerable, with high mortality rates often limiting overall aquaculture productivity. The early developmental stages of fish larvae and juveniles require highly digestible and nutritionally balanced diets due to rapid organ formation, intense growth, and high metabolic activity (Joly et al., 2021). Compared to adult fish, larvae possess an immature digestive system, which makes the nutrient composition and physical presentation of feed crucial for ensuring efficient digestion and nutrient absorption (Ribeiro et al., 2022). Feed inefficiency at this stage not only affects growth but can also compromise immune function and long-term survival, demonstrating the importance of precision nutrition in larval rearing systems. Many studies have emphasized the importance of three major macronutrients, proteins, lipids, and carbohydrates, in supporting larval development, although the optimal proportions vary among species and developmental stages (Li et al., 2021; Meurer et al., 2025).

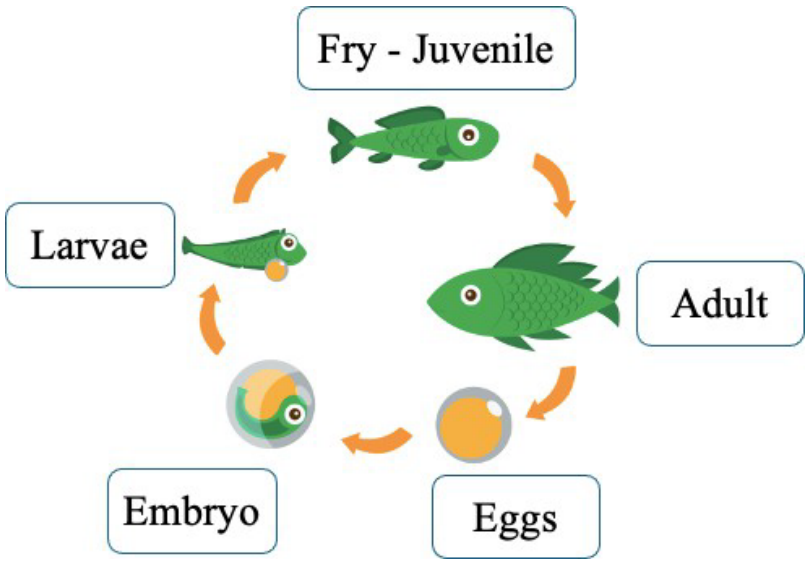

Figure 2 Fish development from early phase until adult.

Protein is the main dietary component influencing larval growth, muscle development, and tissue synthesis. Research suggests that crude protein requirements generally range from 45 to 55 percent, with attention to a balanced amino acid profile that includes essential amino acids such as lysine and methionine (Zhang et al., 2022; Jang et al., 2022). Insufficient or imbalanced protein can impair growth, reduce survival, and increase susceptibility to stress and disease.

Lipids serve as a critical energy source and provide essential fatty acids such as eicosapentaenoic acid (EPA) and docosahexaenoic acid (DHA), which are important for neural development, visual function, and cell membrane integrity (Mejri et al., 2021; Koven et al., 2024). Recommended lipid inclusion levels between 10 and 20 percent have been shown to support optimal energy metabolism and larval growth (Hossain et al., 2023; Figueroa et al., 2025). Moreover, the balance between n-3 and n-6 fatty acids can influence stress tolerance, inflammatory responses, and long-term performance in aquaculture species.

Carbohydrate utilization, on the other hand, remains limited due to low amylase activity in larvae, and excessive intake may lead to poor digestion and liver glycogen accumulation. Therefore, carbohydrate levels are typically maintained below 20 percent in larval diets (Zhao et al., 2022; Zheng et al., 2023). However, carbohydrates can provide readily available energy when formulated appropriately with other macronutrients. This emphasizes the importance of diet formulation tailored to species-specific digestive capacities.

In addition to macronutrients, micronutrients such as vitamins and minerals are critical for maintaining larval health and supporting metabolic functions. Vitamin C supports collagen synthesis and acts as an antioxidant, while vitamin E protects cell membranes from oxidative damage caused by the breakdown of highly unsaturated fatty acids (El-Sayed et al., 2022; Medagoda et al., 2023). Deficiencies in these vitamins may result in skeletal deformities, poor wound healing, and reduced stress tolerance (Singh et al., 2021; Mourad et al., 2022; Dey et al., 2025). Likewise, minerals such as phosphorus, zinc, copper, and selenium play important roles in bone formation, enzyme function, and antioxidant defense. Inadequate intake of these minerals often leads to growth retardation, cataracts, and skeletal abnormalities (Fraser et al., 2019; Lall and Kaushik, 2021; Martínez et al., 2024). The precise balance and bioavailability of these micronutrients are increasingly recognized as essential for optimizing larval performance and resilience, particularly under intensive aquaculture conditions.

Overall, the literature indicates that while significant progress has been made in understanding the nutrient requirements of fish larvae, inter-species variation, developmental stage-specific needs, and limited knowledge of nutrient interactions continue to present challenges for formulating efficient, balanced, and cost-effective larval diets. Emerging strategies such as functional feed additives, microalgae

supplementation, and live feed enrichment are showing promise in addressing these challenges.

Feeding Limitation in Larval Rearing

Feeding during the early stages of larval rearing remains one of the most critical challenges in aquaculture nutrition. Numerous studies have highlighted that first-feeding larvae exhibit limited success when reared solely on conventional microdiets such as formulated, finely ground, or microencapsulated dry feeds (Melaku et al., 2024). Given their impact on growth, survival, and long-term development, these limitations bring attention to the critical need for feeding strategies tailored to the specific nutritional and physiological requirements of larvae. As shown in Figure 3, these limitations are broadly categorized into morphological, physiological, and physical constraints that collectively restrict nutrient intake, assimilation, and survival rates.

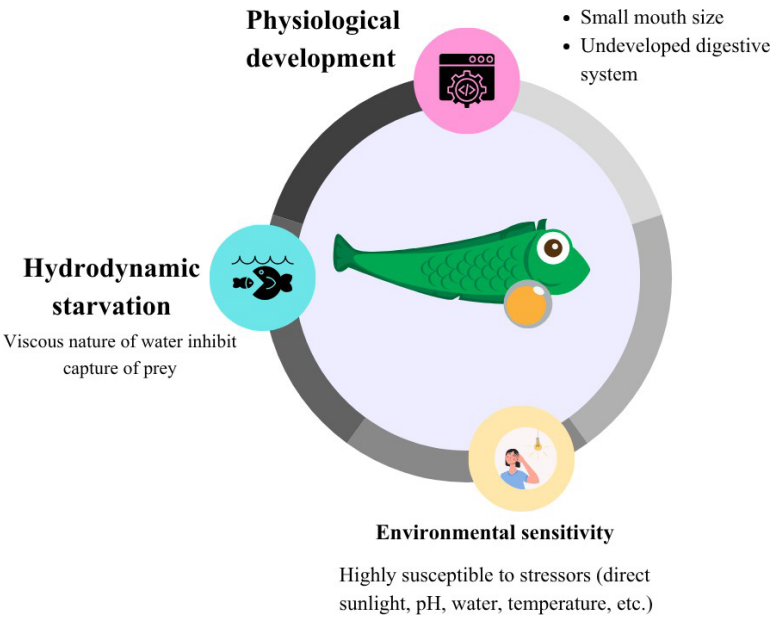

Figure 3 Feeding limitation in larval rearing.

Pepin (2023) reported that morphological constraints are mainly due to the extremely small mouth opening (gape size) of newly hatched larvae, which limits their ability to ingest even finely ground or sieved feeds. Similarly, Lahnsteiner et al. (2023) demonstrated that the particle size of most commercial microdiets still exceeds larval ingestion capacity, leading to starvation and high mortality during the first-feeding stage. This is the reason why live feeds such as *Brachionus* (rotifers) and *Artemia nauplii* remain essential in early larval culture as they offer optimal particle size, motility, and digestibility. These attributes directly improve feed intake, nutrient assimilation, and survival, despite the higher production costs and labor requirements (Syukri et al., 2022; Melaku et al., 2024).

Physiological limitations further compound feeding challenges, as larval fish possess underdeveloped digestive organs and enzyme systems compared to juveniles and adults (Joly et al., 2021). Many marine species exhibit agastric larval stages where the stomach and associated acid-secreting glands are not yet functional, preventing the secretion of pepsin and hydrochloric acid necessary for effective protein digestion (Goodrich, 2025). As a result, conventional diets containing complex proteins, such as those derived from fish meal, are poorly digested (El-Sayed et al., 2024; Molinari et al., 2025).

Larvae also rely heavily on exogenous enzymes from live prey and on limited pancreatic enzymes such as trypsin and chymotrypsin (Arenas et al., 2024; Khan and Rahman, 2025). Diets lacking pre-digested or hydrolyzed protein sources can therefore lead to poor nutrient absorption, intestinal inflammation, and hepatic stress (Li et al., 2021; Melaku et al., 2024). In addition, Lall and Kaushik (2021) highlighted that larval livers have limited biosynthetic capacity for essential nutrients such as phospholipids and docosahexaenoic acid (DHA). These nutrients are critical for neural and visual development (Ranard and Appel, 2024, Ramena et al. (2025)**.** In order to promote healthy organ development and physiological maturation, feed formulation must take into account both the macronutrient content and the bioavailability of critical functional chemicals.

Physical and behavioral constraints also play a significant role in feed inefficiency. Nutrient leaching from water-soluble compounds such as vitamins and amino acids occurs rapidly once dry microdiets are immersed, leading to nutrient loss and deterioration of water quality due to uneaten particles (Simon et al., 2021; Chuang, 2024; El-Sayed et al., 2024). Furthermore, feed buoyancy and sinking rates often fail to match larval feeding behavior, resulting in low ingestion rates and reduced feed utilization (Melaku et al., 2024). In contrast, live prey remain suspended in the water column and provide visual and chemical cues that stimulate active feeding. The absence of such cues in inert diets not only reduces palatability but also exacerbates feed wastage and environmental stress, highlighting the dual nutritional and ecological roles that live or functional feeds play in early larval rearing (Murray, 2023; Yu et al., 2023; Lim et al., 2024).

Functional Role of Microalgae in Larval Rearing System

Microalgae perform multiple integrated roles that make them a critical component of successful larval rearing systems (Figure 4). Beyond providing high-quality protein, essential PUFAs, DHA, EPA, and other key nutrients that support rapid growth microalgae contribute to maintaining optimal water quality by assimilating toxic nitrogenous wastes (ammonia and nitrite) and stabilizing oxygen and pH levels. The "Greenwater" effect amplifies these benefits, promoting larval survival and disease resistance through behavioral stability, shading, and the provision of bioactive compounds such as antioxidants and prebiotics. These multifunctional roles demonstrate that microalgae are not simply a feed supplement but a foundational ecological and physiological agent, integrating nutritional support, environmental regulation, and immunological modulation to enhance both larval performance and the sustainability of aquaculture systems.

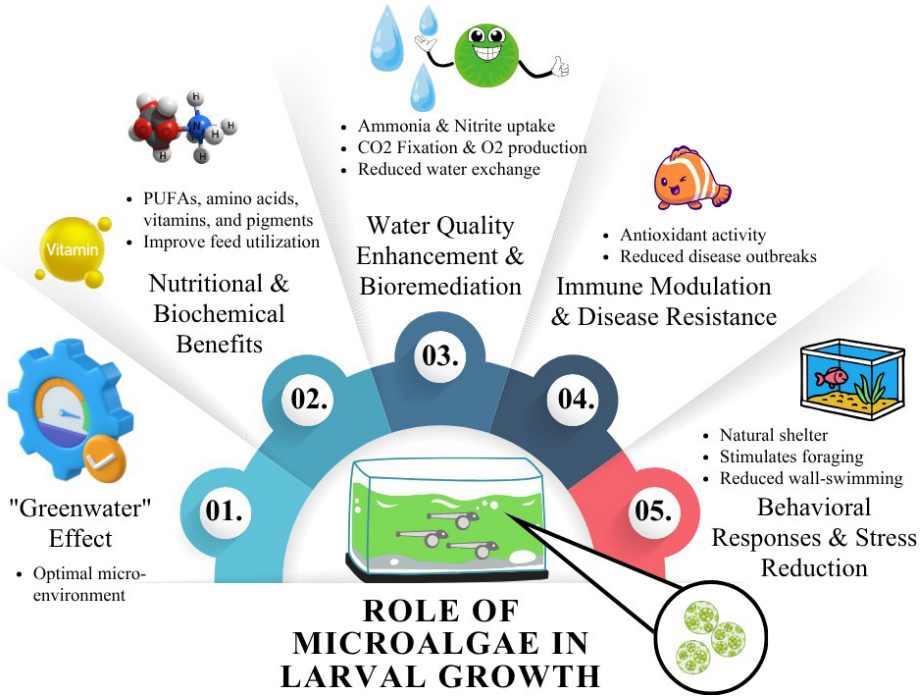

Figure 4 Role of microalgae in larval rearing system.

e-ISSN 2716-697X

The "Greenwater" Effect in Larvae Rearing

According to Ma and Hu (2023), the inclusion of microalgae in larval rearing systems plays a vital role in the successful cultivation of aquatic species with small planktonic larvae such as marine fish and crustaceans. This practice, widely known as the greenwater technique, involves maintaining microalgae, typically species from the genera *Nannochloropsis*, *Isochrysis*, or *Chlorella*, within the rearing tanks at low to moderate densities (Zanella et al., 2020; Mathew et al., 2021; Sales et al., 2022). The resulting greenwater effect offers both nutritional and ecological benefits to the larvae and their live prey, including rotifers and Artemia (Sultana et al., 2025).

Several studies have reported that the greenwater condition enhances larval survival, growth, and health by improving environmental stability and water quality (Basford et al., 2021). Microalgae help assimilate toxic nitrogenous compounds such as ammonia and nitrite, thereby reducing the need for frequent water exchange and maintaining a stable rearing environment (Zhu et al., 2024). Furthermore, the presence of microalgae contributes to microbial balance by promoting beneficial bacterial communities and suppressing harmful pathogens such as Vibrio species, either through competitive exclusion or the release of antimicrobial compounds (Jusidin et al., 2022).

In addition to these water quality and microbial effects, the greenwater condition provides optical and behavioral benefits. The suspended algal cells create a mild turbidity that reduces excessive light penetration, offering visual comfort and minimizing stress and cannibalism among light-sensitive larvae (Chen and Zeng, 2021). The greenwater effect exhibits that microalgae serve not only as a nutritional source but also as a dynamic ecological regulator, stabilizing water quality, supporting beneficial microbial communities, and mitigating environmental stressors. Integrating these ecological principles into larval rearing strategies is therefore essential for enhancing survival, growth, and overall system resilience in aquaculture.

Nutritional and Biochemical Benefits

Microalgae play a significant role in larval rearing systems by providing a consistent and readily available source of essential nutrients, including proteins, lipids, vitamins, minerals, and immunostimulants (Bahi et al., 2023). Table 2 summarized different microalgae species based on their respective nutritional and biochemical compositions. The figures displayed indicate ranges or representative data obtained in earlier studies because the biochemical composition of microalgae can vary based on species, strain, growth circumstances, and culture phase. Their continuous presence within the culture environment not only supports direct larval nutrition but also benefits zooplankton prey such as rotifers and *Artemia*, thereby enhancing the overall nutritional dynamics of the system.

According to Wang et al. (2021), microalgae contain 40 to 60 percent protein on a dry weight basis and exhibit a balanced essential amino acid profile comparable to fishmeal, making them an effective protein substitute in formulated diets. Their lipid fractions are rich in long-chain polyunsaturated fatty acids (PUFAs), particularly eicosapentaenoic acid (EPA, 20:5n-3) and docosahexaenoic acid (DHA, 22:6n-3), which are crucial for neural and retinal development in fish and shrimp larvae (Remize et al., 2021; Soto et al., 2023). These fatty acids also promote higher larval survival, improved growth rates, and better stress resistance.

Beyond their macronutrient composition, microalgae provide several biochemical compounds that contribute functional benefits to larval health. Pigments such as astaxanthin from *Haematococcus pluvialis* act as strong antioxidants that help neutralize free radicals and enhance immunity, thereby improving resistance to diseases (Eldessouki et al., 2024). These pigments also contribute to the desirable coloration of salmonids and ornamental species, increasing their market value (Yaqoob et al., 2021). Additionally, microalgal polysaccharides, including β-glucans, function as natural immunomodulators and prebiotics that support gut health and nutrient absorption (Bahi et al., 2023).

However, not all microalgae are equally digestible. Species such as *Chlorella* possess rigid cell walls that can reduce nutrient bioavailability (Wang et al., 2024). To overcome this limitation, cell wall–disrupted or enzymatically treated microalgal products have been developed to improve digestibility and nutrient release, particularly for early larval stages or non-grazing species (Prates, 2025). Overall, the balanced composition of proteins, essential fatty acids, vitamins (including B12, C, and E), and minerals positions microalgae as a sustainable and functional alternative to conventional fishmeal and fish oil in larval rearing systems (Annamalai et al., 2021; Ahmad et al., 2022)

e-ISSN 2716-697X

Table 2 Common species microalgae species with their respective nutritional profiles.

Microalgae species	Lipid	Protein	Carbohydrate	Ref.
Chlorella sp.	23.4%	45.3%	34.79%	Nagappan *et al.*, 2021
Chlamydomonas nivalis	52.0%	-	10.4%	Hounslow *et al.*, 2021
Porphyridium sp.	2.23%	14.58 ± 0.35 pg/cell	23-52%	Tounsi *et al.*, 2024
Tetraselmis subcordiformis	57%	-	-	Saadaoui *et al.*, 2024
Chlorella vulgaris	31.33%	50.8%	-	Liu *et al.*, 2022
Haematococcus pluvialis	40.3-51.31%	29-45%	15-17%	Tosuner & Urek, 2021
Isochrysis sp.	-	17.1-23.2%	42.7-56.7%	Singh *et al.*, 2021
Nannochloropsis sp.	36.0±0.32%	54.0±1.05%	24.0±2.51%	Hossain *et al.*, 2022
Chlamydomonas rheinhardtii	18.1±0.6%	49.7±0.9%	21.7±0.5%	López *et al.*, 2023
Spirulina sp.	6.2±0.2%	66.0±0.8%	18.1±0.6%	de Morais *et al.*, 2022
Tetraselmis sp.	16.3±0.8%	34.1±1.4%	29.1±1.1%	Dammak *et al.*, 2022
Tisochrysis sp.	29.3 ± 0.3%	42.0 ± 2.5%	12.6 ± 0.7%	Pagnini *et al.*, 2023

e-ISSN 2716-697X

Water Quality Enhancement and Bioremediation

Microalgae play a vital role in maintaining water quality within larval rearing systems through their photosynthetic and nutrient uptake activities. During photosynthesis, microalgae absorb carbon dioxide and release oxygen, contributing to stable dissolved oxygen levels that are essential for larval survival and microbial balance. According to Han et al. (2019), microalgae buffer water pH and maintain alkalinity by utilizing carbon dioxide and acidic compounds, hence reducing the risk of sudden fluctuations commonly observed in intensive rearing environments.

Beyond gas regulation, microalgae act as natural biofilters by assimilating nitrogenous wastes such as ammonia and nitrite, both of which are toxic even at low concentrations (Markou et al., 2023). This nutrient uptake not only improves water quality but also promotes algal growth, creating a self-regulating system that supports a more sustainable culture environment. Additionally, microalgae release dissolved organic compounds that stimulate the growth of beneficial bacteria. These bacteria contribute to a balanced microbial community capable of outcompeting pathogenic species through a process known as competitive exclusion, thereby reducing the risk of disease outbreaks and maintaining a stable and healthy aquatic ecosystem (Smahajcsik et al., 2025).

Immune Modulation and Disease Resistance

The immunostimulatory potential of microalgae in larval aquaculture also has been highlighted. Polysaccharides such as β-glucans found in microalgal cell walls can activate the innate immune responses of fish larvae, enhancing their defense mechanisms against pathogens (Shochicha et al., 2025). Pigments including phycocyanin and carotenoids such as astaxanthin further contribute to immune protection by acting as powerful antioxidants that neutralize oxidative stress and promote overall physiological resilience (Zittelli et al., 2023). In addition to these bioactive compounds, larvae consuming microalgae may also ingest beneficial bacteria associated with the algal surface. These bacteria behave similarly to probiotics by strengthening the intestinal barrier, promoting the establishment of a healthy gut microbiota, and inhibiting the colonization of harmful microorganisms (Anjaly et al., 2025). Some microalgae and their symbiotic bacteria also secrete antimicrobial metabolites that suppress pathogenic species within the digestive tract (Smahajcsik et al., 2025). Collectively, these interactions contribute to disease resistance and maintain the microbial equilibrium characteristic of the greenwater system, reducing infection risks and enhancing larval survival.

e-ISSN 2716-697X

Behavioral Responses and Stress Reduction

The optical and physical characteristics of microalgae in greenwater systems influence larval behavior and welfare. The green coloration caused by suspended algal cells reduces water transparency, creating a visually comfortable environment that facilitates prey detection and capture. This improved visibility helps larvae efficiently locate live feed such as rotifers and *Artemia*, leading to better feeding performance and more uniform growth (Chen and Zeng, 2021). Furthermore, the slight turbidity in greenwater mimics natural shaded habitats where larvae typically seek refuge, thereby reducing stress and aggressive behaviors such as cannibalism. A calmer rearing environment minimizes energy expenditure on escape responses and allows larvae to focus on feeding and development. As a result, improved feeding efficiency, enhanced stress tolerance, and better overall health have been observed in larvae reared under greenwater conditions (Pratama et al., 2024).

Selection Criteria of Microalgae as Aquaculture Feed

The selection of suitable microalgae species for aquaculture feed is a critical step that determines not only the nutritional quality of the rearing system but also its overall operational and economic feasibility. As illustrated in Figure 5, this selection involves a combination of biological and practical factors that together determine feed efficiency and sustainability. These factors include physical properties (such as cell size, motility, and water stability), nutritional composition (including protein content, essential fatty acids, vitamins, and minerals), biological characteristics (such as digestibility and palatability), and visual attributes (such as colour contrast, which enhances feed visibility for larvae). Table 3 provides a summary of the microalgae species' biological characteristics and their uses

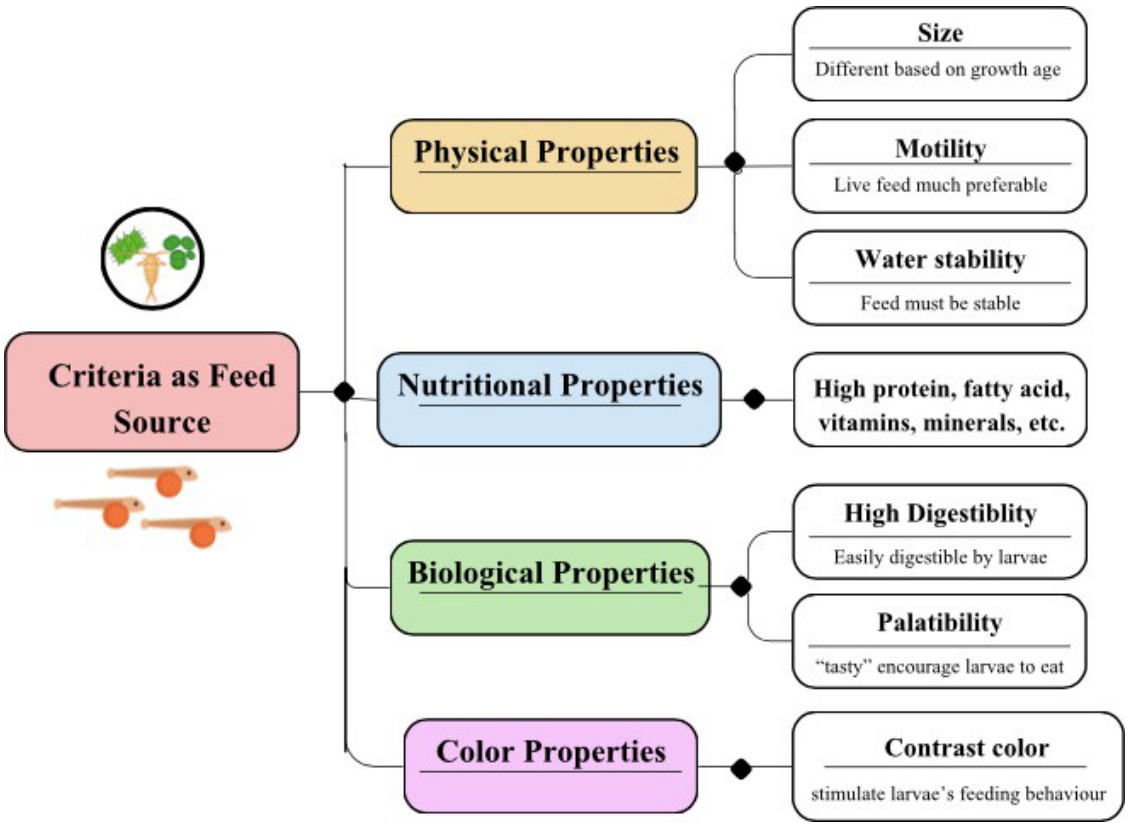

Figure 5 Feed source criteria for larvae.

The biological properties of microalgae, including cell size, morphology, digestibility and biochemical composition**,** are fundamental in determining their suitability as feed. Microalgae must fall within an optimal size range and shape for ingestion by the target species, especially during larval stages (Annamalai et al., 2021). Mota et al. (2023) demonstrated that when the physical characteristics of microalgae correspond to the developmental stage of fish larvae, feed intake and growth performance are significantly improved. Nutritionally, superior microalgae strains provide high protein content (40–60% dry weight) with a balanced essential amino acid profile comparable to fishmeal (Wang et al., 2021). In addition, microalgae are rich sources of long-chain polyunsaturated fatty acids (PUFAs) such as eicosapentaenoic acid (EPA, 20:5n-3) and docosahexaenoic acid (DHA, 22:6n-3), which are essential for the growth, neural, and retinal development of fish and shrimp larvae (Santin et al., 2021; Soto et al., 2023These biochemical qualities position microalgae as an effective and sustainable replacement for traditional fishmeal and fish oil.

In addition to nutritional composition, practical and economic factors play a key role in selecting microalgae species for large-scale production. Ideal strains should exhibit rapid growth and high biomass yield to meet the continuous demand of aquaculture operations (Ma and Hu, 2024). Cultivation feasibility is enhanced when the strain demonstrates resilience to fluctuating environmental conditions such as light intensity, temperature, salinity, and pH (Ansari et al., 2021). The selected microalgae should also be non-toxic, compatible with the target species, and palatable enough to promote consistent feed intake, particularly when used in live feed enrichment for *Artemia* and rotifers (Ma and Hu, 2024).

Several microalgae species have been widely adopted as industry standards due to their proven nutritional efficacy and cultivation advantages. *Nannochloropsis* and *Isochrysis* are particularly valued for their high polyunsaturated fatty acid content, serving as primary sources of EPA and DHA, respectively (Siddik et al., 2024). Asghari et al. (2025) reported that combining *Nannochloropsis oculata* and *Isochrysis galbana* in a biofloc-algal system enhanced PUFA deposition, particularly EPA and DHA, in fish fillets, suggesting synergistic nutritional benefits. *Tetraselmis* species are also frequently preferred for their high protein content, robust growth, and tolerance to environmental fluctuations, making them ideal candidates for large-scale cultivation (Nezafatian et al., 2023). *Tetraselmis tetrathele*, for example, demonstrates exceptional resistance to high ammonium nitrogen concentrations and is commonly used for bioremediation in aquaculture systems, contributing to both water quality improvement and cost reduction (Farahin et al., 2021). Similarly, the diatom *Chaetoceros* has been recognized for its appropriate cell size and balanced nutritional composition, which make it suitable as live feed for mollusk and shrimp larvae (Bhattacharjya et al., 2024). Moreover, the cyanobacterium *Arthrospira platensis* (commonly known as *Spirulina*) is often incorporated as a feed additive to enhance immunity and pigmentation in fish and shrimp diets (Reham et al., 2025

Overall, selecting an ideal microalgal species requires a balance between biological suitability and production efficiency. Species that combine high nutritional value, environmental resilience, and ease of cultivation hold the greatest potential to serve as sustainable alternatives to traditional aquaculture feed components.

e-ISSN 2716-697X

Table 3 Different microalgae species based on biological properites and potential applications

Microalgae species	Biological properties	Potential applications	Ref.
Chlorella sp.	1. Photosynthetic pigments (chlorophyll, carotenoids (astaxanthin) 2. Polysaccharides 3. Fatty acids 4. Antioxidants	1. Health and Biomedical Sector (wound healing, drug delivery) 2. Environmental and Energy Sustainability (wastewater treatment, biofuel production) 3. Food and agriculture	Abreu *et al.*, 2023
Chlamydomonas nivalis	1. Carbon shifting (turns its carbon into fat (lipids) to survive)	1. Biofuel 2. Salt-water farming 3. Genetic engineering	Hounslow *et al.*, 2021
Porphyridium sp.	1. No cell wall. 2. Exopolysaccharides 3. B-Phycoerythrin (B-PE) pigment 4. LC-PUFAs fatty acid	1. Live feed (aquaculture) 2. Cosmetics 3. Health supplement 4. Medical diagnostic	Bayu *et al.*, 2023
Tetraselmis subcordiformis	1. Outdoor resilience 2. Lipid diversity (polar and neutral lipids)	1. Biofuel 2. Aquaculture feed 3. Nutraceuticals	Saadaoui *et al.*, 2024
Chlorella vulgaris	1. Detoxification 2. Pigment (lutein and chlorophyll)	1. Food supplement 2. Animal feed 3. Medicine/cosmetics	
Haematococcus pluvialis	1. Antioxidants 2. Survival mechanism (red pigment)	1. Health supplements 2. Fish feed 3. Skin care 4. Medicine	
Isochrysis sp.	1. ACE Inhibition 2. Antioxidant 3. High digestibility	1. Heart-health (anti-hypertension) 2. Anti-aging 3. Food industry	
Nannochloropsis sp.	1. Digestibility 2. Bioactive peptides 3. Lipid quality (EPA) 4. Antihypertensive activity	1. General nutrition 2. Heart health 3. Chronic disease prevention	

Chlamydomonas rheinhardtii	1. Pigment (Lutein, B-carotene)	1. Nutraceuticals 2. Medicine 3. Vision health 4. Food industry	Masi *et al.*, 2023
Spirulina sp.	1. Pigment (C-Phycocyanin (C-PC)) 2. Antihyperlipidemic	1. Pharma/Food industry 2. Heart health 3. Brain health	Bortolini *et al.*, 2022
Tetraselmis sp.	1. Antioxidant 2. Antimicrobial 3. Enzymatic (Superoxide Dismutase (SOD))	1. Natural preservative 2. Food industry 3. Nutraceuticals	Carrillo & Anchundi a, 2024
Tisochrysis sp.	1. DHA Powerhouse 2. Pigment (Fucoxanthin) 3. Morphological Flexibility (cells changed their size and shape during co-cultivation to optimize nutrient uptake.)	1. Brain health 2. Infant formula 3. Weight management	Maglie *et al.*, 2021

CHALLENGERS

Despite the promising nutritional and functional benefits discussed in previous sections, the widespread commercial application of microalgae as an aquaculture feed ingredient remains constrained by several biological, technical, and economic challenges**.** While microalgae offer exceptional protein content, balanced amino acids, and valuable PUFAs such as EPA and DHA, their large-scale production and consistent nutritional delivery are yet to reach full industrial maturity

e-ISSN 2716-697X

Current Limitations and Technical Barriers

One of the most pressing limitations lies in the high production cost associated with large-scale cultivation, harvesting, and downstream processing. Compared with conventional fishmeal-based feeds, microalgal biomass production remains energy-intensive, particularly in closed photobioreactor systems that require stringent environmental control (Ma and Hu, 2024). Furthermore, batch-to-batch variability in biochemical composition is a major constraint. Since nutrient profiles are strongly influenced by light intensity, nutrient availability, and temperature, the resulting inconsistency can affect the feed's nutritional reliability and larval performance. Another significant challenge is cell wall rigidity in certain microalgae, such as *Chlorella*, which reduces digestibility and nutrient bioavailability to fish larvae (Wang et al., 2024). Similarly, the oxidative instability of essential PUFAs during storage leads to rapid degradation, compromising both feed quality and larval health. The risk of biological contamination, particularly by competing algal species or harmful microorganisms, also complicates mass culture operations and poses potential biosecurity risks for aquaculture systems. Addressing these barriers requires not only process optimization but also an understanding of species-specific physiology and biochemical dynamics to ensure consistent feed quality and larval performance.

FUTURE PROSPECTS

Technological and Biological Innovations

Addressing these limitations will require technological advancements and strategic innovation across multiple fronts. Ongoing research in genetic engineering, strain improvement, and metabolic optimization holds significant potential for producing microalgae with enhanced digestibility, faster growth, and higher yields of target compounds such as DHA, EPA, and pigments (Prates, 2025). Selective breeding and omics-based approaches can further identify resilient strains capable of maintaining stable nutrient profiles under variable culture conditions. Moreover, the use of low-cost and sustainable culture media, such as wastewater, agricultural runoff, or aquaculture effluent, offers a dual advantage of bioremediation and cost reduction (Farahin et al., 2021). Integrating microalgae cultivation into circular bioeconomy frameworks could transform waste management challenges into value-generating systems, simultaneously improving environmental sustainability and production efficiency. These innovations highlight the dual potential of microalgae as both a high-quality feed ingredient and a tool for environmental management, demonstrating that technological and biological solutions must be synergistically applied to overcome current production constraints.

e-ISSN 2716-697X

Future Directions and Collaborative Frameworks

The successful industrial adoption of microalgae-based feeds hinges on coordinated efforts among researchers, industry stakeholders, and policymakers. Establishing standardized cultivation protocols, ensuring feed safety, and developing clear regulatory frameworks are essential steps for achieving reliable large-scale production and market acceptance. Collaboration between academia, commercial producers, and government agencies can accelerate technology transfer, encourage innovation-driven investment, and foster the development of resilient supply chains. Technological advancements, including automation, AI-assisted monitoring, and bioprocess engineering, are expected to optimize production efficiency, reduce operational costs, and maintain consistent nutritional quality. By integrating these innovations with strategic policy and industry frameworks, microalgae can transition from a supplementary feed to a core functional ingredient, offering a renewable, nutrient-rich, and environmentally responsible alternative to conventional fishmeal. This positions microalgae not merely as a nutritional resource but as a strategic tool for advancing resilient, resource-efficient, and sustainable aquaculture systems, capable of meeting the growing global demand for high-quality aquatic products.

CONCLUSION

In summary, microalgae play a crucial functional role in fish larval rearing systems as both nutritional and ecological components that support sustainable aquaculture. Through the greenwater effect, microalgae enhance water quality, reduce toxic nitrogen compounds, and promote the growth of beneficial microbial communities. They also supply essential nutrients such as proteins, polyunsaturated fatty acids, vitamins, and bioactive compounds that strengthen larval health, immunity, and feeding efficiency. As aquaculture continues to expand, addressing challenges related to large-scale cultivation, nutrient variability, and digestibility remains critical. Future progress in strain improvement, bioprocess optimization, and circular bioeconomy integration will help unlock the full potential of microalgae. Ultimately, these advancements position microalgae as a key component in developing sustainable and resilient fish larval rearing systems.

e-ISSN 2716-697X

REFERENCES

Abreu, A. P., Martins, R., & Nunes, J. (2023). Emerging applications of Chlorella sp. and Spirulina (Arthrospira) sp. *Bioengineering*, *10*(8), 955.

Ahmad, A., W. Hassan, S., & Banat, F. (2022). An overview of microalgae biomass as a sustainable aquaculture feed ingredient: food security and circular economy. *Bioengineered*, *13*(4), 9521-9547.

Anjaly, M. A., Sarasan, M., Kachiprath, B., Sukumaran, V., Singh, I. S. B., & Puthumana, J. (2025). Engineering the fish gut microbiome: Could it serve as future-proof strategy for sustainable aquaculture? Blue Biotechnology, 2, Article 6.

Annamalai, S. N., Das, P., Thaher, M. I., Abdul Quadir, M., Khan, S., Mahata, C., & Al Jabri, H. (2021). Nutrients and energy digestibility of microalgal biomass for fish feed applications. *Sustainability*, *13*(23), 13211.

Ansari, F. A., Guldhe, A., Gupta, S. K., Rawat, I., & Bux, F. (2021). Improving the feasibility of aquaculture feed by using microalgae. *Environmental Science and Pollution Research*, *28*(32), 43234-43257.

Arenas-Pardo, M. A., Gaxiola-Cortés, M. G., Barreto-Altamirano, A. F., Del Carmen Paredes-Medina, A., Palomino-Albarrán, I. G., Balam-Uc, P. M., Maldonado-Flores, J. C., & Álvarez-González, C. A. (2024). Changes in Digestive Enzyme Activities during Larval Development of Spotted Seatrout (Cynoscion nebulosus). *Aquaculture Nutrition*, *2024*, 1–12. https://doi.org/10.1155/2024/1309390

Asghari, M., Yeganeh, S., & Hafezieh, M. (2025). Effect of Nannochloropsis oculata and Isochrysis galbana on growth, water quality, biofloc, carcass fatty acids profile, and intestinal bacteria in Nile tilapia (Oreochromis niloticus) raised in zero-water exchange system. *Iranian Journal of Fisheries Sciences*, *24*(2), 305-331.

Bahi, A., Ramos-Vega, A., Angulo, C., Monreal-Escalante, E., & Guardiola, F.A. (2023). Microalgae with immunomodulatory effects on fish. *Reviews in Aquaculture*, *15*(4), 1522-1539.

Barsanti, L., & Gualtieri, P. (2022). *Algae: anatomy, biochemistry, and biotechnology*. CRC press.

Basford, A. J., Makings, N., Mos, B., White, C. A., & Dworjanyn, S. (2021). Greenwater, but not live feed enrichment, promotes development, survival, and growth of larval Portunus armatus. *Aquaculture*, *534*, 736331.

Batista, S., Pintado, M., Marques, A., Abreu, H., Silva, J. L., Jessen, F., Tulli, F., & Valente, L. M. (2020). Use of technological processing of seaweed and microalgae as strategy to improve their apparent digestibility coefficients in European seabass (Dicentrarchus labrax) juveniles. *Journal of Applied Phycology*, *32*(5), 3429–3446. https://doi.org/10.1007/s10811-020-02185-2.

Bayu, A., Noerdjito, D. R., Rahmawati, S. I., Putra, M. Y., & Karnjanakom, S. (2023). Biological and technical aspects on valorization of red microalgae genera Porphyridium. *Biomass Conversion and Biorefinery*, *13*(14), 12395-12411.

Bhattacharjya, R., Marella, T. K., Kumar, M., Kumar, V., & Tiwari, A. (2024). Diatom-assisted aquaculture: Paving the way towards sustainable economy. *Reviews in Aquaculture*, *16*(1), 491-507.

Bleakley, S., & Hayes, M. (2021). Functional and bioactive properties of protein extracts generated from Spirulina platensis and Isochrysis galbana T-Iso. *Applied Sciences*, *11*(9), 3964.

Bortolini, D. G., Maciel, G. M., Fernandes, I. D. A. A., Pedro, A. C., Rubio, F. T. V., Branco, I. G., & Haminiuk, C. W. I. (2022). Functional properties of bioactive compounds from Spirulina spp.: Current status and future trends. *Food Chemistry: Molecular Sciences*, *5*, 100134.

Boyd, C. E., & McNevin, A. A. (2022). Overview of aquaculture feeds: Global impacts of ingredient production, manufacturing, and use. In *Feed and feeding practices in aquaculture* (pp. 3-28). Woodhead Publishing.

Carrillo, M., & Anchundia, M. (2024). "Antimicrobial and antioxidant capacity of Dunaliella salina, Tetraselmis chuii and Isochrysis galbana and their potential use in food." a systematic review. *CABI Agriculture and Bioscience*, *5*(1), 108.

Chen, J. Y., & Zeng, C. (2021). The effects of live prey and greenwater on the early larval rearing fridmani. Aquaculture, of orchid dottyback Pseudochromis 543, 737008. https://doi.org/10.1016/j.aquaculture.2021.737008

Chen, J. Y., & Zeng, C. (2021). The effects of live prey and greenwater on the early larval rearing of orchid dottyback *Pseudochromis fridmani*. *Aquaculture, 543*, 737008. https://doi.org/10.1016/j.aquaculture.2021.737008.

Chuang, K. M. (2024). *Development and Evaluation of Novel Microparticulate Technologies for the Delivery of Essential Nutrients to Marine Fish Larvae*. The University of Maine.

Dammak, M., Hlima, H. B., Tounsi, L., Michaud, P., Fendri, I., & Abdelkafi, S. (2022). Effect of heavy metals mixture on the growth and physiology of Tetraselmis sp.: Applications to lipid production and bioremediation. *Bioresource Technology*, *360*, 127584.

de Moraes, L. B. S., Santos, R. F. B., Gonçalves Junior, G. F., Mota, G. C. P., Dantas, D. M. D. M., de Souza Bezerra, R., & Olivera Galvez, A. (2022). Microalgae for feeding of penaeid shrimp larvae: an overview. *Aquaculture International*, *30*(3), 1295-1313.

de Morais, E. G., Nunes, I. L., Druzian, J. I., de Morais, M. G., da Rosa, A. P. C., & Costa, J. A. V. (2022). Increase in biomass productivity and protein content of Spirulina sp. LEB 18 (Arthrospira) cultivated with crude glycerol. *Biomass Conversion and Biorefinery*, *12*(3), 597-605.

Dey, T., Hossain, M. S., Kamal, M. M., Ghosh, P. K., Uddin, M. S., Alam, M. T., Mian, S., & Islam, M. J. (2025). Impact of Vitamin C on Growth, Haemato-Immunological Characteristics and Stress Tolerance Capability of Climbing Perch, Anabas testudineus (Bloch, 1792). *Aquaculture Fish and Fisheries*, *5*(2). https://doi.org/10.1002/aff2.70048

Dikel, S., & Demirkale, I. (2024). Global aquaculture feed market: Trends and challenges. In Proceedings of the 15th International Conference on Agriculture, Animal Science & Rural Development (pp. 24). Aydın, Türkiye.

El-Sayed, H. S., Ghanem, S. F., & Barakat, K. M. (2024). Role of recent feeding protocols, rearing water systems and microbial trends in improving marine larviculture: insights into water quality and larval performance. *International Aquatic Research*, *16*(3).

El-Sayed, A. F. M., & Izquierdo, M. (2022). The importance of vitamin E for farmed fish—A review. *Reviews in Aquaculture*, *14*(2), 688-703.

Eldessouki, E. A., Elshopakey, G. E., Elbahnaswy, S., Shakweer, M. S., Abdelwarith, A. A., Younis, E. M., ... & Eissa, E. S. H. (2024). Influence of astaxanthin-enriched Haematococcus pluvialis microalgae on the growth efficacy, immune response, antioxidant capacity, proinflammatory cytokines, and tissue histomorphology of hybrid red tilapia. *Aquaculture International*, *32*(6), 7447-7468.

Fan, J., Bao, Q., Ma, K., Li, X., Jia, J., & Wu, H. (2022). Antioxidant and innate immunity of Danio rerio against Edwardsiella tarda in response to diets including three kinds of marine microalgae. *Algal Research*, *64*, 102689.

Farahin, A. W., Natrah, I., Nagao, N., Yusoff, F. M., Shariff, M., Banerjee, S., ... & Toda, T. (2021). Tolerance of Tetraselmis tetrathele to high ammonium nitrogen and its effect on growth rate, carotenoid, and fatty acids productivity. *Frontiers in Bioengineering and Biotechnology*, *9*, 568776.

Figueroa Villalobos, E., Pereira, W. A., Pérez-Atehortúa, M., Sandoval-Vargas, L., Romero, J., Oliveira, R. P., ... & Villasante, A. (2025). Influence of dietary fatty acids on fish sperm tolerance to Cryopreservation. *Reviews in Aquaculture*, *17*(1), e12968.

Food and Agriculture Organization of the United Nations. (2024). The State of World Fisheries and Aquaculture 2024. FAO.

Food and Agriculture Organization of the United Nations. (2025). Review of the State of World Marine Fishery Resources – 2025. FAO. https://www.fao.org/family-farming/detail/en/c/1742236/

Fraser, T. W., Witten, P. E., Albrektsen, S., Breck, O., Fontanillas, R., Nankervis, L., Thomsen, T. H., Koppe, W., Sambraus, F., & Fjelldal, P.
G. (2019). Phosphorus nutrition in farmed Atlantic salmon (Salmo salar): Life stage and temperature effects on bone pathologies. *Aquaculture*, *511*,734246. https://doi.org/10.1016/j.aquaculture.2019.734246

Gao, S., Chen, W., Cao, S., Sun, P., & Gao, X. (2024). Microalgae as fishmeal alternatives in aquaculture: Current status, existing problems, and possible solutions. *Environmental Science and Pollution Research*, *31*(11), 16113-16130.

Goodrich, H. R. (2025). Fish gut plasticity and its role as a potential mechanism for coping with warming and hypoxia. *Journal of Experimental Biology*, *228*(14), jeb249672.

Han, P., Lu, Q., Fan, L., & Zhou, W. (2019). A review on the use of microalgae for sustainable aquaculture. *Applied Sciences, 9*(11), 2377. https://doi.org/10.3390/app9112377.

Hossain, M. S., Small, B. C., & Hardy, R. (2023). Insect lipid in fish nutrition: Recent knowledge and future application in aquaculture. *Reviews in Aquaculture*, *15*(4), 1664-1685.

Hossain, S., Khatoon, H., Jamal, F., Islam, Z., & Kasan, N. A. (2022). Characterization of nitrogen stress-induced growth proximate and pigment contents of Nannochloropsis sp. *Journal of Aquaculture Livestock Production*, *115*(3), 2-9.

Hounslow, E., Evans, C. A., Pandhal, J., Sydney, T., Couto, N., Pham, T. K.,... & Wright, P. C. (2021). Quantitative proteomic comparison of salt stress in Chlamydomonas reinhardtii and the snow alga Chlamydomonas nivalis reveals mechanisms for salt-triggered fatty acid accumulation via reallocation of carbon resources. *Biotechnology for Biofuels*, *14*(1), 121 *International*. https://doi.org/10.1007/s10499-023-01228-y

Islam, S. I., Mahfuj, S., Baqar, Z., Asadujjaman, M., Islam, M. J., Alsiwiehri, N., Almehmadi, M., Sanjida, S., & Ahammad, F. (2024). Bacterial diseases of Asian sea bass (Lates calcarifer): A review for health management strategies and future aquaculture sustainability. *Heliyon*, *10*(9),e29793. https://doi.org/10.1016/j.heliyon.2024.e29793

Jang, B. I., Olowe, O. S., & Cho, S. H. (2022). Evaluation of the optimal protein required in granulated microdiets for rockfish (Sebastes schlegeli) larvae. *Aquaculture Nutrition*, *2022*(1), 2270384.

Joly, L. J., Loots, C., Meunier, C. L., Boersma, M., Collet, S., Lefebvre, V., ... & Giraldo, C. (2021). Maturation of the digestive system of Downs herring larvae (Clupea harengus, Linnaeus, 1758): identification of critical periods through ontogeny. *Marine Biology*, *168*(6), 82.

Jusidin, M. R., Othman, R., Shaleh, S. R. M., Ching, F. F., Senoo, S., & Oslan, S. N. H. (2022). In Vitro Antibacterial Activity of Marine Microalgae Extract against Vibrio harveyi. *Applied Sciences*, *12*(3), 1148. https://doi.org/10.3390/app12031148

Khan, N. S., & Rahman, M. S. (2025). Zooplankton in Aquaculture: A Perspective on Nutrition and Cost-Effectiveness. *Aquaculture Research*, *2025*(1), 5347147.

Kousoulaki, K., Sveen, L., Norén, F., & Espmark, Å. (2022). Atlantic salmon (Salmo salar) performance fed low trophic ingredients in a fish meal and fish oil free diet. *Frontiers in Physiology*, *13*, 884740.

Koven, W., Yanowski, E., Gardner, L., Nixon, O., & Block, B. (2024). Docosahexaenoic acid (DHA) is a driving force regulating gene expression in bluefin tuna (Thunnus thynnus) larvae development. *Scientific Reports*, *14*(1), 23191.

Lahnsteiner, F., Lahnsteiner, E., & Duenser, A. (2023). Suitability of different live feed for first feeding of freshwater fish larvae. *Aquaculture Journal*, *3*(2), 107–120. https://doi.org/10.3390/aquacj3020010

Lall, S. P., & Kaushik, S. J. (2021). Nutrition and metabolism of minerals in fish. *Animals*, *11*(9), 2711. https://doi.org/10.3390/ani11092711

Li, X., Zheng, S., & Wu, G. (2021). Nutrition and functions of amino acids in fish. In *Amino acids in nutrition and health: amino acids in the nutrition of companion, zoo and farm animals* (pp. 133-168). Cham: Springer International Publishing.

Lim, C. E., Webster, C. D., & Li, M. H. (2024). Feeding practices. In *Tilapia* (pp. 547-559). CRC Press.

Liu, T., Chen, Z., Xiao, Y., Yuan, M., Zhou, C., Liu, G., ... & Yang, B. (2022). Biochemical and morphological changes triggered by nitrogen stress in the oleaginous microalga Chlorella vulgaris. *Microorganisms*, *10*(3), 566.

López-Pacheco, I. Y., Ayala-Moreno, V. G., Mejia-Melara, C. A., Rodríguez-Rodríguez, J., Cuellar-Bermudez, S. P., González-González, R. B., ... & Parra-Saldívar, R. (2023). Growth behavior, biomass composition and fatty acid methyl esters (FAMEs) production potential of Chlamydomonas reinhardtii, and Chlorella vulgaris cultures. *Marine Drugs*, *21*(8), 450.

Ma, M., & Hu, Q. (2024). Microalgae as feed sources and feed additives for sustainable aquaculture: Prospects and challenges. *Reviews in Aquaculture*, *16*(2), 818-835.

Machado, L., Carvalho, G., & Pereira, R. N. (2022). Effects of innovative processing methods on microalgae cell wall: prospects towards digestibility of protein-rich biomass. *Biomass*, *2*(2), 80-102.

Maglie, M., Baldisserotto, C., Guerrini, A., Sabia, A., Ferroni, L., & Pancaldi, S. (2021). A co-cultivation process of Nannochloropsis oculata and Tisochrysis lutea induces morpho-physiological and biochemical variations potentially useful for biotechnological purposes. *Journal of Applied Phycology*, *33*(5), 2817-2832.

Markou, G., Economou, C. N., Petrou, C., Tzovenis, I., Doulgeraki, A., Zioga, M., Saganas, N., Kougia, E., & Arapoglou, D. (2023). Biofloc technology combined with microalgae for improved nitrogen removal at lower C/N ratios using artificial aquaculture wastewater. *Aquaculture*

Martínez-Antonio, E. M., Salgado-García, R. L., Peña-Rodríguez, A., Ruvalcaba-Márquez, J. C., Kraffe, E., Racotta, I. S., & Magallón-Barajas, F. (2024). Implications of Dietary Phosphorus Sources On Zootechnical Performance And Stress Response of The Pacific White Shrimp Litopenaeus vannamei. *Animal Feed Science and Technology*, 115889. https://doi.org/10.1016/j.anifeedsci.2024.115889

Masi, A., Leonelli, F., Scognamiglio, V., Gasperuzzo, G., Antonacci, A., & Terzidis, M. A. (2023). Chlamydomonas reinhardtii: A factory of nutraceutical and food supplements for human health. *Molecules*, *28*(3), 1185.

Mathew, R. T., Alkhamis, Y. A., Rahman, S. M., & Alsaqufi, A. S. (2021). Effects of Microalgae Chlorella vulgaris Density on the Larval Performances of Fresh Water Prawn Macrobrachium rosenbergii (De Man, 1879). *Indian Journal of Animal Research*, *55*(3).

Medagoda, N., Chotikachinda, R., Hasanthi, M., & Lee, K. J. (2023). Dietary supplementation of a mixture of nucleotides, β-glucan and vitamins c and e improved the growth and health performance of olive flounder, Paralichthys olivaceus. *Fishes*, *8*(6), 302.

Mejri, S. C., Tremblay, R., Audet, C., Wills, P. S., & Riche, M. (2021). Essential fatty acid requirements in tropical and Cold-Water marine fish larvae and juveniles. *Frontiers in Marine Science*, *8*. https://doi.org/10.3389/fmars.2021.680003

Melaku, S., Geremew, A., Getahun, A., Mengestou, S., & Belay, A. (2024). Challenges and prospects of using live feed substitutes for larval fish. *Fisheries and Aquatic Sciences*, *27*(8), 475–487. https://doi.org/10.47853/fas 2024.e45

Mendes, A. R., Spínola, M. P., Lordelo, M., & Prates, J. A. (2024). Chemical compounds, bioactivities, and applications of Chlorella vulgaris in food, feed and medicine. *Applied Sciences*, *14*(23), 10810.

Meurer, F., Novodworski, J., & Bombardelli, R. A. (2025). Protein requirements in Nile tilapia (Oreochromis niloticus) during production and reproduction phases. *Aquaculture and Fisheries*, *10*(2), 171-182.

Molinari, G. S., Wojno, M., Wick, M., & Kwasek, K. (2025). New approach to the development of tailor-made feed for fish larvae using Zebrafish Danio rerio as a model. *PLoS ONE*, *20*(6), e0326665. https://doi.org/10.1371/journal.pone.0326665

Mota, C. S., Pinto, O., Sá, T., Ferreira, M., Delerue-Matos, C., Cabrita, A. R., ... & Maia, M. R. (2023). A commercial blend of macroalgae and microalgae promotes digestibility, growth performance, and muscle nutritional value of European seabass (Dicentrarchus labrax L.) juveniles. *Frontiers in Nutrition*, *10*, 1165343.

Mourad, M. M., Shahin, S. A., El-Ratel, I. T., & El Basuini, M. F. (2022). Effect of treating eggs with coenzyme Q10 (CoQ10) on growth variables, histomorphometry, and antioxidant capacity in red tilapia (Oreochromis aureus× Oreochromis mossambicus) larvae. *Animals*, *12*(17), 2219.

Murray, C. (2023). *Minimizing the use of live feeds during the larviculture of five ornamental fish species*. University of Florida.

Næve, I., Korsvoll, S. A., Santi, N., Medina, M., & Aunsmo, A. (2022). The power of genetics: Past and future contribution of balanced genetic selection to sustainable growth and productivity of the Norwegian Atlantic salmon (Salmo salar) industry. *Aquaculture*, *553*, 738061.

Nagappan, S., Das, P., AbdulQuadir, M., Thaher, M., Khan, S., Mahata, C., ... & Kumar, G. (2021). Potential of microalgae as a sustainable feed ingredient for aquaculture. *Journal of Biotechnology*, *341*, 1-20.

Nezafatian, E., Farhadian, O., Yegdaneh, A., Safavi, M., Daneshvar, E., & Bhatnagar, A. (2023). Enhanced production of bioactive compounds from marine microalgae Tetraselmis tetrathele under salinity and light stresses: A two-stage cultivation strategy. *Bioresource Technology*, *376*, 128899.

Oslan, S. N. H., Tan, J. S., Oslan, S. N., Matanjun, P., Mokhtar, R. A. M., Shapawi, R., & Huda, N. (2021). Haematococcus pluvialis as a potential source of astaxanthin with diverse applications in industrial sectors: current research and future directions. *Molecules*, *26*(21), 6470.

Pagnini, C., Sampietro, G., Santini, G., Biondi, N., & Rodolfi, L. (2023). Tisochrysis lutea as a substrate for lactic acid fermentation: biochemical composition, digestibility, and functional properties. *Foods*, *12*(6), 1128.

Pascon, G., Messina, M., Petit, L., Valente, L. M. P., Oliveira, B., Przybyla, C., Dutto, G., & Tulli, F. (2021). Potential application and beneficial effects of a marine microalgal biomass produced in a high-rate algal pond (HRAP) in diets of European sea bass, Dicentrarchus labrax. *Environmental Science and Pollution Research*, *28*(44), 62185–62199. https://doi.org/10.1007/s11356-021-14927-x

Paterson, S., Gómez-Cortés, P., de la Fuente, M. A., & Hernández-Ledesma, B. (2023). Bioactivity and digestibility of microalgae Tetraselmis sp. and Nannochloropsis sp. as basis of their potential as novel functional foods. *Nutrients*, *15*(2), 477.

Pepin, P. (2023). Feeding by larval fish: how taxonomy, body length, mouth size, and behaviour contribute to differences among individuals and species from a coastal ecosystem. *ICES Journal of Marine Science*, *80*(1), 91-106.

Pratama, I., Susanto, R., Nopriyanto, R., & Nurhafid, M. (2024). Effectiveness of green water system as larval gourami (*Osphronemus gouramy*) cultivation technology—Efforts to increase larval productivity. *International Journal of Agriculture and Biosciences, 13*(3), 469–473.

Prates, J. a. M. (2025). The role of microalgae in providing essential minerals for sustainable swine nutrition. *Frontiers in Animal Science*, *6*. https://doi.org/10.3389/fanim.2025.1526433

Ramena, Y., Kurapati, R. B., Bosteels, T., & Ramena, G. (2025). Artemia Enrichment Strategies: A comprehensive review of nutritional enhancements with emphasis on fatty acid profiles in aquatic species. *Reviews inAquaculture*, *17*(4). https://doi.org/10.1111/raq.70080

Ramlee, A., Rasdi, N. W., Wahid, M. E. A., & Jusoh, M. (2021). Microalgae And The Factors Involved In Successful Propagation For Mass Production. *Journal of Sustainability Science and Management*, *16*(3), 21–42. https://doi.org/10.46754/jssm.2021.04.003

Ranard, K. M., & Appel, B. (2024). Creation of a novel zebrafish model with low DHA status to study the role of maternal nutrition during neurodevelopment. *Journal of Lipid Research*, 100716. https://doi.org/10.1016/j.jlr.2024.100716

Reham, A. A., Mounes, H. A., Abd El-Ghaffar, H. A., Nasr, R., & Al-Zahaby, M.A. (2025). Using Spirulina platensis as Feed Additive to Improve Color and Immunity in Goldfish (Carassius auratus). *Egyptian Academic Journal of Biological Sciences. B, Zoology*, *17*(1).

Remize, M., Brunel, Y., Silva, J. L., Berthon, J. Y., & Filaire, E. (2021). Microalgae n-3 PUFAs production and use in food and feed industries. *Marine drugs*, *19*(2), 113Ribeiro, L., Hubert, F. N., Rodrigues, V., Rojas-Garcia, C., & Dinis, M. T. (2022, March). Understanding fish larvae's feeding biology to improve aquaculture feeding protocols. In *Oceans*(Vol. 3, No. 1, pp. 94-113). MDPI.

Saadaoui, I., Cherif, M., Siddiqui, S. A., Esakkimuthu, S., AbdulQuadir, M., El Anbari, M., & Sayadi, S. (2024). Unveiling Tetraselmis subcordiformis lipidome dynamics during large-scale cultivation in open raceway pond. *Journal of Applied Phycology*, *36*(3), 1125-1134.

Safiin, N. S. Z., Mustafa, S., Ching, F. F., & Shapawi, R. (2021). Palm oil-based enriched diets for the rotifer, Brachionus plicatilis, improved the growth of Asian seabass (Lates calcarifer) larvae. Frontiers in Marine Science, 8, 613312.

Sales, R., Lopes, R. G., Derner, R. B., & Tsuzuki, M. Y. (2022). Concentrated microalgal biomass as a substitute for fresh microalgae produced on site at hatcheries. *Aquaculture Research*, *53*(17), 5771-5786.

Santin, A., Russo, M. T., Ferrante, M. I., Balzano, S., Orefice, I., & Sardo, A. (2021). Highly valuable polyunsaturated fatty acids from microalgae: strategies to improve their yields and their potential exploitation in aquaculture. Molecules, 26(24), 7697.

Sarıtaş S., Kalkan A.E., Yılmaz K., Gurdal S., Göksan T., Witkowska A.M., Lombardo M., and Karav S., 2024, Biological and nutritional applications of microalgae, Nutrients, 17(1): 93.

Sarker, P. K. (2023). Microorganisms in fish feeds, technological innovations, and key strategies for sustainable aquaculture. *Microorganisms*, *11*(2), 439.

Shochicha, A. N., Satyantini, W. H., & Md. Yassin, I. S. (2025). Microalgae-derived bioactives as immunonutrients in *Litopenaeus vannamei* aquaculture: Mechanisms, efficacy, and future prospects. *Egyptian Journal of Aquatic Biology & Fisheries, 29*(4), 2759–2774.

Siddik, M. A., Sørensen, M., Islam, S. M., Saha, N., Rahman, M. A., & Francis, D. S. (2024). Expanded utilisation of microalgae in global aquafeeds. *Reviews in Aquaculture*, *16*(1), 6-33.

Simon, C. J., Truong, H., Habilay, N., & Hines, B. (2021). Feeding behaviour and bioavailability of essential amino acids in shrimp Penaeus monodon fed fresh and leached fishmeal and fishmeal-free diets. *Animals*, *11*(3), 847.

Singh, S. K., Baidya, S., Das, P., & Biswas, P. (2021). Functional role of dietary supplements on reproductive physiology of fishes. In *Recent updates in molecular Endocrinology and Reproductive Physiology of Fish: An Imperative step in Aquaculture* (pp. 243-258). Singapore: Springer Singapore.

Smahajcsik, D., Roager, L., Strube, M. L., Zhang, S.-D., & Gram, L. (2025). Stronger together: Harnessing natural algal communities as potential probiotics for inhibition of aquaculture pathogens. *Microbiology Spectrum, 13*(7). https://doi.org/10.1128/spectrum.00421-25

Soto-Sánchez, O., Hidalgo, P., González, A., Oliveira, P. E., Arias, A. J. H., & Dantagnan, P. (2023). Microalgae as raw materials for Aquafeeds: Growth kinetics and improvement Strategies of Polyunsaturated fatty acids production. *Aquaculture Nutrition*, *2023*,119. https://doi.org/10.1155/2023/5110281

Sultana, M. S., Haque, M. M., Hossain, M. Y., Ahmed, M. K., Sumon, M. a. I., Akhi, M. S. N., & Khan, S. (2025). Improved growth and survival of Catla catla larvae using cultured microalgae and zooplankton as initial feed. *Aquaculture Reports*, *44*, 103011. https://doi.org/10.1016/j.aqrep.2025.103011

Syukri, F., Hassan, N. H., & Azaman, S. N. A. (2022). Performances of Fs Feed, Artemia Nauplii And Commercial Diet on Early Development of Clarias gariepinus LARVAE. *Journal of Sustainability Science and Management*, *17*(2),35–45. https://doi.org/10.46754/jssm.2022.02.004

Tacon, A. G., Metian, M., & McNevin, A. A. (2022). Future feeds: suggested guidelines for sustainable development. *Reviews in Fisheries Science & Aquaculture*, *30*(2), 135-142.

Tosuner, Z. V., & Urek, R. O. (2021). Effects of nutrients on lipids and biodiesel production potential of Haematococcus pluvialis. *Environmental Engineering & Management Journal (EEMJ)*, *20*(8).

Tounsi, L., Ben Hlima, H., Derbel, H., Duchez, D., Gardarin, C., Dubessay, P., ... & Abdelkafi, S. (2024). Enhanced growth and metabolite production from a novel strain of Porphyridium sp. *Bioengineered*, *15*(1), 2294160.

Wang, C. A., Onyeaka, H., Miri, T., & Soltani, F. (2024). Chlorella vulgaris as a food substitute: Applications and benefits in the food industry. Journal of food science, 89(12), 8231-8247.

Wang, Y., Tibbetts, S. M., & McGinn, P. J. (2021). Microalgae as sources of high-quality protein for human food and protein supplements. *Foods*, *10*(12), 3002.

Yaqoob, S., Riaz, M., Shabbir, A., Zia-Ul-Haq, M., Alwakeel, S. S., & Bin-Jumah, M. (2021). Commercialization and marketing potential of carotenoids. In *Carotenoids: structure and function in the human body* (pp. 799-826). Cham: Springer International Publishing.

Yu, Z. L., Yang, M. J., Song, H., Zhang, T., & Yuan, X. T. (2023). Gastropod chemoreception behaviors—Mechanisms underlying the perception and location of targets and implications for shellfish fishery development in aquatic environments. *Frontiers in Marine Science*, *9*, 1042962.

Zanella, L., & Vianello, F. (2020). Microalgae of the genus Nannochloropsis: Chemical composition and functional implications for human nutrition. *Journal of Functional Foods*, *68*, 103919. https://doi.org/10.1016/j.jff.2020.103919

Zhang, J. X., Ran, Z. S., Xie, H. X., Kong, F., Zhang, M. Q., Zhou, Y., ... & Xu, J. L. (2023). A systematic analysis and evaluation of nutritional composition of 23 strains of marine microalgae commonly used in aquaculture. *Algal Research*, *72*, 103122.

Zhang, Y., Liang, X., Zhan, W., Han, M., Liu, F., Xie, Q., Guo, D., Chen, L., & Lou, B. (2022). Effects of dietary protein levels on growth performance, muscle composition and fiber recruitment of juvenile small yellow croaker (Larimichthys polyactis). *Aquaculture Reports*, *27*, 101335. https://doi.org/10.1016/j.aqrep.2022.101335

Zhao, W., Wei, H., Wang, Z., He, X., & Niu, J. (2022). Effects of Dietary Carbohydrate Levels on Growth Performance, Body Composition, Antioxidant Capacity, Immunity, and Liver Morphology in Oncorhynchus mykiss under Cage Culture with Flowing Freshwater. *Aquaculture Nutrition*, *2022*, 1–11. https://doi.org/10.1155/2022/7820017

Zheng, L., Wang, Z., Zhang, B., Yan, L., Wang, P., Zhao, C., ... & Zhou, C. (2023). Effects of high dietary carbohydrate levels on growth performance, enzyme activities, expression of genes related to liver glucose metabolism, and the intestinal microbiota of Lateolabrax maculatus Juveniles. *Fishes*, *8*(9), 431.

Zhu, Y., Zhang, Y., Chen, H., Zhang, L., & Shen, C. (2024). Stress Responses and Ammonia Nitrogen Removal Efficiency of Oocystis lacustris in Saline Ammonium-Contaminated Wastewater Treatment. *Toxics*, *12*(5), 353. https://doi.org/10.3390/toxics12050353

Zimmermann, S., Kiessling, A., & Zhang, J. (2023). The future of intensive tilapia production and the circular bioeconomy without effluents: biofloc technology, recirculation aquaculture systems, bio-RAS, partitioned aquaculture systems and integrated multitrophic aquaculture. *Reviews in Aquaculture*, *15*, 22-31.

Zittelli, G. C., Lauceri, R., Faraloni, C., Benavides, A. M. S., & Torzillo, G. (2023). Valuable pigments from microalgae: Phycobiliproteins, primary carotenoids, and fucoxanthin. *Photochemical & Photobiological Sciences, 22*(7), 1733–1789.

Zoli, M., Rossi, L., Bibbiani, C., & Bacenetti, J. (2023). Life cycle assessment of seabass and seabream production in the Mediterranean area: a critical review. Aquaculture, 573, 739580.

Borneo International Journal of Biotechnology (BIJB)
Vol. 5 (December 2025), 112-125.

e-ISSN 2716-697X

Development of Microsatellite Markers Reveals Moderate Genetic Diversity in Sabah's Tri-Spine Horseshoe Crab, *Tachypleus tridentatus* (Leach, 1819)

Nur Syafiqah Mohamad Zul[1], Raimi Mohamed Redwan[2], Pushpalatha Palaniappan[3], Kennedy Aaron Aguol[4], Mohammad Zahirul Hoque[5], Cahyo Budiman[1] and Vijay Kumar[1]*

[1]*Biotechnology Research Institute, Universiti Malaysia Sabah, Jalan UMS, 88400 Kota Kinabalu Sabah, Malaysia*
[2]*Faculty of Agro Based Industry, Universiti Malaysia Kelantan, Jeli Campus, Locked Bag 100, 17600, Jeli, Kelantan, Malaysia*
[3]*Borneo Marine Research Institute, Universiti Malaysia Sabah, Jalan UMS, 88400 Kota Kinabalu, Sabah*
[4]*Centre of the Promotion of Knowledge and Language Learning, Universiti Malaysia Sabah, Kota Kinabalu, Sabah, Malaysia*
[5]*Faculty of Medicine and Health Sciences, Universiti Malaysia Sabah, Kota Kinabalu, Sabah, Malaysia*
*Corresponding email: vijay@ums.edu.my
Received: 15 October 2025 | Accepted: 20 December 2025 | Published: 31 December 2025

ABSTRACT

The tri-spine horseshoe crab, *Tachypleus tridentatus* (Leach,1819), is a species under conservation pressure. Anecdotal observations suggest a decline in its populations along the coasts of Sabah, northern Borneo, raising concerns over the potential loss of genetic diversity. In this study, a total of 36 individuals were collected from three localities (Sandakan, Kota Belud, and Kudat) representing both the east and west coasts of Sabah. Genomic DNA from these samples was used to develop novel microsatellite markers, enabling the assessment of population-level genetic variation. Here, we report on the characterization of 14 polymorphic microsatellite loci. All loci were observed to be polymorphic with the number of alleles ranging from 2 to 5 per locus. The overall observed heterozygosity for the 14 analyzed loci ranged from 0.03 to 0.4667 while the expected heterozygosity ranged from 0.2466 to 0.7706. The results indicate that genetic variability in the populations is moderate with signs of inbreeding and restricted gene flow. These markers have a potential application in population management where it will be used to determine if there is a loss of genetic diversity of the Asian horseshoe crab species that are present in Sabah.

Keywords: *Microsatellites, horseshoe crab, simple sequence repeat, molecular markers, Sabah*

e-ISSN 2716-697X

INTRODUCTION

Horseshoe crabs are often referred to as 'living fossils' because they have existed for more than 450 million years, retaining their distinctive three-part armor-like exoskeleton (Bennett *et al*. 2018; Størmer, 1952). Only four extant species are known today, which are, the American species *Limulus polyphemus*, and three Asian species, *Tachypleus tridentatus*, *T. gigas*, and *Carcinoscorpius rotundicauda* all of which are distributed across their respective geographical regions (Carmichael and Brush, 2012; Fu *et al*., 2019). Throughout their life cycle, horseshoe crabs occupy diverse habitats, particularly sandy beaches near the high-tide line for nesting, intertidal mudflats for juvenile development, and shallow coastal waters less than 30 meters deep as feeding grounds (Chen *et al*., 2015; Faridah *et al*., 2015; Tanacredi *et al*., 2009).

Horseshoe crabs play an essential role in both marine ecosystems and the biomedical industry, making them commercially significant. For instance, the *Limulus*/*Tachypleus* amebocyte lysate (LAL/TAL), a vital component in sterility testing that guarantees the safety of drugs and medical devices for millions of patients each year, is derived from horseshoe crab hemolymph (Krisfalusi-Gannon et al., 2018; Tinker-Kulberg et al., 2020). However, the commercial harvesting and bleeding of horseshoe crabs for hemolymph extraction have raised serious concerns about population decline and the long-term sustainability of both the species and the LAL/TAL supply chain.

Extensive studies have been conducted on the American horseshoe crab, *L. polyphemus*, covering molecular biology, population dynamics, reproductive ecology, and spawning behavior (Jackson *et al*., 2014; Nelson *et al*., 2015; Smith *et al*., 2017). In contrast, research relevant to the Asian horseshoe crabs remains limited, with ongoing studies mainly concentrated in East, South and Southeast Asian countries (Obst *et al*., 2012). The IUCN Red list of vulnerable species includes Asian horseshoe crabs under the "Data Deficient" category for *T. gigas* and *C. rotundicauda*, while *T. tridentatus* has been listed under the 'Endangered' category since 2019.

The declining status of the tri-spine horseshoe crab, *T. tridentatus*, has been reported globally specifically in China and Japan, where adult populations have become increasingly rare compared to observations from three to four decades ago (Berkson *et al*., 2009; Shin *et al*., 2009; Manca *et al*., 2017). These declines have been largely attributed to coastal development, habitat loss, overharvesting and the degradation of spawning and nursery grounds. In response, conservation efforts, including long-term monitoring of juvenile populations have been implemented in regions including Hong Kong and Taiwan, where field surveys have documented reduced recruitment and localized population fragmentation (Kwan et al., 2016). Genetic studies in these regions have further revealed significant population structuring and variable levels of genetic diversity using mitochondrial and microsatellite DNA markers (Nishida and Koike, 2009), indicating that habitat connectivity and effective population size are critical determinants of genetic resilience.

e-ISSN 2716-697X

Within the Malaysian context, research on *T. tridentatus* remains limited compared to that on *T. gigas* and *C. rotundicauda* (Robert *et al*., 2014). This is largely because *T. tridentatus* is geographically limited to northern Borneo, whereas the other two species are found in both Peninsular Malaysia and the island of Borneo. A recent genetic study in Sabah using mitochondrial and microsatellite markers reported polymorphic variation among horseshoe crab populations across multiple districts, underscoring the presence of genetic structure within the region (Kntayya, 2015). Independent studies have also provided the first population size estimates of *T. tridentatus* in Tawau and highlighted morphometric differences among Sabah populations, offering useful ecological baselines for management (Mohamad et al., 2016; Manca et al., 2017). Given the limited genetic data available, there is a need to employ molecular markers to assess the genetic diversity of *T. tridentatus* populations in Malaysia. Understanding their genetic variation is vital for developing effective conservation strategies.

This present study aims to evaluate the genetic diversity of *T. tridentatus* across three spatially distributed populations in northern Borneo i.e., Sandakan, Kota Belud and Kudat, respectively using microsatellite markers. The findings are expected to contribute valuable insights for the conservation and management of this endangered species.

MATERIALS & METHODS

Sample Collection

A total of 36 *T. tridentatus* individuals were sampled from three coastal locations in Sabah, Malaysian Borneo: Sandakan (n = 12), Kota Belud (n = 12), and Kudat (n = 12), representing populations from the east and west coasts of Sabah. The specimens were obtained opportunistically from individuals incidentally caught in fishing nets or available at wet markets or local *tamu*. Tissue samples were obtained from the walking legs of individuals and preserved immediately at 4 ^{O}C for subsequent genetic analysis. All samples used in this study were collected between 2011 and 2014, prior to the implementation of the Sabah Biodiversity Centre (SaBC) permit requirement notified by Pusat Penyelidikan Inovasi (PPI), Universiti Malaysia Sabah.

e-ISSN 2716-697X

Microsatellite Isolation and Marker Development

Genomic DNA was isolated from a single *T. tridentatus* individual and subjected to partial shotgun sequencing using the PacBio RS II long-read sequencing platform. The resulting sequence reads were then mined for simple sequence repeat to identify potential microsatellite loci suitable for marker development. The sequencing data are available at GenBank (SRA: SRR22722188, BioProject: PRJNA761241).

In this study, we focused on perfect microsatellites with a combination of di,-tri- and tetra-nucleotides motifs as these loci generally exhibit greater genetic variation than other repeat types (Merritt *et al*., 2015; Temnykh *et al*., 2001). Mononucleotide repeats were excluded due to their higher likelihood of sequencing or assembly errors, which can complicate accurate genotyping (Cai *et al*., 2013; Wattanadilokchatkun *et al*., 2022). The search criteria utilized to find the relevant microsatellite markers were restricted to a minimum of ten repeats for dinucleotides, four for trinucleotides and tetranucleotides respectively.

Search parameters for microsatellite identification were set to a minimum of ten repeat units for dinucleotides and a minimum of four repeat units for trinucleotides and tetranucleotides. Primer pairs were designed using Primer3 software (version 3) (https://primer3.ut.ee), with parameters optimized for an expected product size of 150–350 bp, primer length of 17–30 bp, and melting temperature (Tm) range of 50–65℃. From the identified microsatellite loci, sixteen markers with the longest repeat motifs were selected for downstream population genetic analyses to maximize polymorphic information content (PIC) and enhance discriminatory power among populations (Table 1).

Microsatellite Genotyping and Analysis

Total genomic DNA was isolated from the tissues using Wizard Genomic Purification Kit (Promega, USA) according to manufacturer's instruction with minor modification. The purified DNA was then used as a template for microsatellite genotyping. The PCR amplification was performed in a 10 µL reaction volume containing approximately 20 ng of genomic DNA, 0.1 U GoTaq Flexi DNA Polymerase (Promega, USA), 1x buffer, 1.0 mM $MgCl_2$, 10 pmol of each primer, 0.2 mM of dNTPs in a C1000 thermal cycler (Bio-Rad, USA). The PCR protocol was as follows: initial denaturation at 94℃ for 2 min followed by 40 cycles of denaturation at 94℃ for 25 s; annealing at 47-63℃ (depending on the primer pair) for 25 s; extension at 68℃ for 25 s; and final extension at 68℃ for 2 min. Then, the PCR products were separated using the QIAxcel Advanced capillary electrophoresis system (Qiagen, Germany). The QIAxcel ScreenGel software was used to generate the output file from the electrophoresis for allele scoring.

e-ISSN 2716-697X

Genetic diversity indices, including the number of alleles per locus, observed heterozygosity (Ho), and expected heterozygosity (He), were calculated using PopGene version 1.32 (Yeh et al., 1999). The same software was used to test for Hardy–Weinberg equilibrium (HWE) and to estimate the inbreeding coefficient (FIS) for each locus.

Table 1 Microsatellite primer sequences and amplification information for *T. tridentatus*.

Locus	Accession Number	Repeat motif	Primer Sequences (5′-3′)	Annealing temperature (℃)	Fragment size (bp)
TT02	OK396648	$(AAGT)_4$	F: CGTGTACCGTGTGCAGTATT R: ACTGCTGGGAGTCATTGTCA	55	167-188
TT03	OK396649	$(AGAT)_4$	F: AGACACTCACACACACACAGA R: GATCGGCAAGCTGTGGAAAG	62	196-216
TT04	OK396650	$(AACC)_5$	F: GGCTGCAAAATGTCGGGATA R: GACAACCAAAGCATGTATCAGGA	58	231-274
TT05	OK349170	$(AAG)_5$	F: GGGTGGAGTGCTCGAGAG R: CATCCAGGATTCAATACACAGGA	55	280-309
TT07	OK349171	$(AAC)_5$	F: GCTCAAGCGGCATGTCTG R: TGTCCTTCTTCGTACGTGGT	53	186-217
TT08	OK274271	$(AC)_{36}$	F: ACACACCCTCCACAATCCAT R: TGTAGAATGGACGGCAACTG	57	143-216
TT10	OK396651	$(AAAG)_4$	F: ACGGAGCTGGCATTCCTAAT R: GCTTCGTGACCACCTTAAAGA	55	240-263
TT12	OK349172	$(AGC)_4$	F: TGTTGGAAAGTTTGGCCACA R: CAAGACATCACAAGCCCTGG	55	182-208
TT13	OK349173	$(AAC)_6$	F: TGTGTGTCCCCTTGCAGTAT R: TCACTGCCTCGGTAACTCTC	54	204-225
TT15	OK274274	$(AG)_{11}$	F: AGGGAAAAGTGCACTGGAGA R: CCTGGACTGTACACTTGTGG	58	166-293
TT16	OK247272	$(GT)_{22}$	F: CCTAAGGACTGGGAGATAGCA R: AAGGTACACTGACGCCCTAC	59	150-204
TT17	OK349175	$(ATG)_6$	F: ACGACTTGCTAAAACTCAACAAA R: TCAGTGTCGGAGGTTCTTGA	52	201-213
TT18	OK349176	$(AAG)_5$	F: TGCCGCAGATTTGACACATG R: ACACAATTACCCATACGAACACC	55	203-225
TT20	OK396653	$(AAAC)_6$	F: CCCTTGAGTAGCTTTGCGTG R: ACCAACAAGAGAAGGAGTCCA	53	177-211

e-ISSN 2716-697X

RESULTS

A total of 16 microsatellite loci were initially identified from the *Tachypleus tridentatus* genome. Of these, 14 loci were successfully amplified and found to be polymorphic across the 36 individuals analyzed (Table 1). The repeat motifs consisted mainly of di-, tri-, and tetranucleotide repeats, with the number of repeat units ranging from four to thirty-six. The amplified fragment sizes ranged from 143 to 309 bp, and the annealing temperatures for the primers varied between 52°C and 63°C.

Across the pooled dataset of 36 individuals, the number of alleles per locus (N_A) ranged from 2 to 5, with a mean of 3.4 alleles per locus, indicating moderate polymorphism of the developed markers (Table 2). Expected heterozygosity (H_E) values ranged from 0.2003 (TT15) to 0.7524 (TT04), with an average of 0.5659, while observed heterozygosity (H_O) ranged from 0.0278 (TT02, TT03) to 0.7222 (TT16), averaging 0.3367 across all loci (Table 2). Loci TT04, TT12, and TT16, exhibited comparatively higher heterozygosity and were particularly informative for genetic analyses.

Deviations from Hardy–Weinberg equilibrium ($P_{HWE} < 0.05$) were detected at most loci when all samples were pooled, with the exception of TT07. These deviations are likely influenced by population sub-structuring and heterogeneity among sampling locations rather than reflecting locus-specific biases alone. Overall, the pooled analysis confirms that the microsatellite loci developd in this study are sufficiently polymorphic and suitable for population-level genetic analyses.

e-ISSN 2716-697X

Table 2 Polymorphism characteristics and heterozygosity estimates of 14 microsatellite loci developed for *Tachypleus tridentatus* across all sampled individuals.

Locus	Accession Number	N_A	H_E	H_O	P_{HWE}
TT02	OK396648	4	0.6960	0.0278	0.00
TT03	OK396649	2	0.5035	0.0278	0.00
TT04	OK396650	5	0.7524	0.5429	0.00
TT05	OK349170	4	0.6076	0.3056	0.00
TT07	OK349171	2	0.3416	0.3143	0.63
TT08	OK274271	4	0.4803	0.3143	0.01
TT10	OK396651	3	0.5904	0.0833	0.00
TT12	OK349172	4	0.7039	0.4571	0.00
TT13	OK349173	4	0.6553	0.3889	0.00
TT15	OK274274	2	0.2003	0.0556	0.00
TT16	OK247272	3	0.6467	0.7222	0.02
TT17	OK349175	2	0.5057	0.2941	0.01
TT18	OK349176	3	0.5622	0.6944	0.05
TT20	OK396653	4	0.6762	0.4857	0.01
	Mean		0.5659	0.3367	

Genetic diversity indices calculated separately for each of the three *T. tridentatus* populations using 14 newly isolated microsatellite markers are presented in Table 3. Mean expected heterozygosity (H_E) ranged from 0.434 in Kudat to 0.490 in Kota Belud, while the mean observed heterozygosity (H_O) ranged from 0.286 in Sandakan to 0.396 in Kota Belud. Here, all three populations show lower observed heterozygosity levels compared to the expected heterozygosity, indicating a general deficit of heterozygotes. Sandakan population was observed to have the lowest observed heterozygosity compared to the Kota Belud and Kudat populations.

Table 3 Population-specific genetic diversity indices for three *Tachypleus tridenta_tus* populations in Sabah based on 14 microsatellite loci.

Population	N	H_E	H_O	F_{IS}
Kota Belud	12	0.490	0.396	0.187
Kudat	12	0.434	0.328	0.267
Sandakan	12	0.459	0.286	0.393

The inbreeding coefficient (F_{IS}) varied among populations, with the highest value observed in Sandakan (0.393), followed by Kudat (0.267) and Kota Belud (0.187). The relatively higher F_{IS}

e-ISSN 2716-697X

values in all three populations indicate a general deficit of heterozygotes, which may reflect limited gene relatively higher F_{IS} values in all three populations indicate a general deficit of heterozygotes, which may reflect limited gene flow, small population size, or localized breeding within sampling sites. Collectively, the population-based analysis demonstrate moderate levels of genetic diversity among the *T. tridentatus* populations studied, with Kota Belud showing the highest heterozygosity and lowest inbreeding coefficient, suggesting a comparatively more genetically diverse and stable population.

DISCUSSION

This study represents one of the few molecular investigations on *Tachypleus tridentatus* populations from Malaysian waters, particularly in Sabah. Using newly developed microsatellite markers, we assessed the genetic diversity of three geographical separated populations from Kota Belud, Kudat and Sandakan, and detected moderate levels of genetic variation across loci. Although genetic variation is still present, as reflected by allelic richness and heterozygosity estimates (Tables 2 and 3), the overall pattern suggest it may be declining, likely due to limited gene flow and increasing habitat fragmentation in coastal areas.

A total of 46 alleles were identified across the three populations, with the number of alleles per locus ranging from 2 to 4 in Kota Belud and Sandakan, and from 2 to 5 in Kudat. These values indicate a modest level of genetic variation within Sabah's *T. tridentatus* populations. Our findings are consistent with a previous study on the Tuaran population, located at the west coast of Sabah (Kntayya, 2015), which reported 1 to 3 alleles per locus. In contrast, *T. tridentatus* populations in China exhibited considerably higher allelic richness, averaging 3 to 8 alleles per locus (Cai *et al*., 2015). According to Xu *et al*. (2000), higher numbers of alleles across microsatellite loci are often associated with increased mutation rates, which may in turn shape the genetic structure of populations. These comparisons suggest that *T. tridentatus* populations in China are genetically more diverse than those in Sabah, possibly due to larger effective population sizes and wider habitat connectivity. Given that the distribution of *T. tridentatus* in Malaysia is largely confined to Sabah, the lower allelic variation observed here implies a greater susceptibility to genetic drift and diversity loss.

All loci, except TT07 and TT18, deviated significantly from Hardy–Weinberg equilibrium (HWE). Such deviations may result from a combination of biological and demographic processes, including non-random mating, population sub-structuring (Wahlund effect), limited dispersal among sites, and small effective population sizes. The influence of null alleles and sampling effects associated with modest sample sizes may also contribute to these departures, as reported in other population genetic studies (Wittke-Thompson et al., 2005). Therefore, deviations from equilibrium observed in this study likely reflect both genuine population structure and methodological constraints.

e-ISSN 2716-697X

Genetic diversity among the three Sabah populations was further assessed based on heterozygosity indices. In all populations, mean observed heterozygosity (H_O) was consistently lower than mean expected heterozygosity (H_e), indicating a general deficit of heterozygotes. This pattern is commonly observed in fragmented or declining populations and may arise from restricted gene flow, localized breeding, inbreeding, or recent population bottlenecks. This pattern mirrors previous findings in Tuaran (Kntayya, 2015) but contrasts with populations from Japan and China, where higher H_O values have been reported (Li *et al*., 2009; Nishida and Koike, 2009). Despite documented population declines in those regions, their *T. tridentatus* populations appear to retain higher genetic diversity than populations in Sabah, highlighting regional differences in demographic history and habitat connectivity.

The inbreeding coefficient (F_{IS}) provides additional insight into population structure and the degree of homozygosity within populations. Positive F_{IS} values were observed in all three Sabah populations, indicating a deficit of heterozygotes, consistent with the heterozygosity results. The highest F_{IS} value was found in Sandakan, followed by Kudat and Kota Belud, implying varying degrees of inbreeding or genetic isolation. These differences likely reflect varying environmental pressures and habitat connectivity along the Sabah coastline. Similar patterns of local population differentiation have been reported in *T. tridentatus* from Hong Kong, Taiwan, and mainland China, where coastal development and declining spawning grounds have fragmented populations and reduced gene flow (Liao *et al*., 2019; Yang *et al*., 2007). Taken together, the relatively low allelic richness, reduced heterozygosity, and positive F_{IS} values observed in this study suggest limited genetic exchange among Sabah populations of *T. tridentatus*. Such patterns have been linked to habitat degradation and the loss of spawning beaches in other parts of Asia (Liao *et al*., 2019; Chen *et al*., 2015; Nishida and Koike, 2009; Yang *et al*., 2007). Continuous genetic monitoring, along with expanded sampling across Borneo and Peninsular Malaysia, will be crucial to clarify the extent of population connectivity and to inform conservation efforts for this endangered species.

Seasonal movements and environmentally driven population flux may also contribute to the genetic patterns observed in this study. Horseshoe crabs are known to exhibit seasonal migration associated with spawning activity, tidal cycles, and monsoonal changes, with adults moving between offshore feeding grounds and intertidal nesting beaches. Seasonal population flux has also been documented in Sabah for other horseshoe crab species. Robert *et al*. (2014) reported marked seasonal variation in the abundance and mating behaviour of *Carcinoscorpius rotundicauda* in the Kota Kinabalu region, with spawning activity closely linked to tidal cycles and environmental conditions. In the South China Sea region, coastal currents and monsoon-driven circulation patterns have been suggested to influence larval dispersal and juvenile distribution, potentially shaping connectivity among local populations (Yang *et al*., 2007; Liao *et al*., 2019). However, despite this potential for seasonal connectivity, the observed heterozygosity deficits and positive F_{IS} values in Sabah populations suggest that such movements may be insufficient to counteract the effects of habitat fragmentation and localized breeding.

e-ISSN 2716-697X

The microsatellite markers developed in this study included a combination of di-, tri-, and tetranucleotide repeat motifs to provide a comprehensive assessment of genetic variation. No consistent pattern of higher allele numbers was observed among tetranucleotide loci compared to other repeat types (Table 2), indicating that allelic richness was more strongly influenced by locus-specific characteristics, such as repeat length and mutation dynamics, rather than repeat motif class alone. Genetic analyses were conducted under the Infinite Alleles Model (IAM), which assumes that each mutation produces a novel allele and is appropriate for evaluating overall heterozygosity and allelic diversity across mixed microsatellite repeat types. The absence of a clear relationship between repeat motif class and allele number further supports the suitability of this model for the present dataset.

The moderate overall genetic diversity observed in this study provides a valuable foundation for future conservation genetics research on *T. tridentatus* in Sabah, Malaysian Borneo. However, the relatively small sample size and the limited availability of specimens posed significant challenges to this work. The scarcity of individuals along the Sabah coastline suggests the species' declining population and the practical difficulties of obtaining adequate samples for population-level analyses. Observations from Kota Kinabalu indicate that even relatively common horseshoe crab species such as *C. rotundicauda* exhibit strong site fidelity to spawning areas and are sensitive to coastal disturbance (Robert *et al*., 2014), emphasizing the need to protect key breeding habitats for T. tridentatus along the Sabah coastline.
Consequently, the patterns of genetic diversity reported here should be verified through broader sampling efforts, if possible.

Future studies incorporating larger sample sizes and additional molecular markers will be essential to confirm the genetic structure and connectivity of *T. tridentatus* populations in Sabah waters. Given that the species is listed as "Endangered" by the IUCN, such information is critical for guiding effective conservation and management strategies. Protecting key breeding beaches, minimizing anthropogenic disturbances, and preserving habitat connectivity among populations should remain central priorities to ensure the long-term survival of this ancient and ecologically important species.

e-ISSN 2716-697X

CONCLUSION

Overall, the microsatellite loci developed in this study proved to be informative for assessing genetic diversity in *T. tridentatus* populations from Sabah. The moderate levels of heterozygosity observed across loci and populations suggest that some degree of genetic variation is still maintained despite the species' restricted distribution in northern Borneo. However, the relatively high inbreeding coefficients, particularly in the Sandakan population, indicate potential genetic erosion due to population isolation or small effective population sizes. These findings highlight the need for continued genetic monitoring and conservation management to prevent further loss of diversity and to support the long-term viability of *T. tridentatus* populations in Sabah waters.

ACKNOWLEDGEMENTS

This research is funded by Fundamental Research Grant Scheme (FRGS), Ministry of Higher Education, Malaysia, grant number FRGS/1/2018/WAB09/UMS/02/1. from the Ministry of Higher Education, Malaysia. We also thank the financial support of the Nagao Natural Environment Foundation, Japan.

REFERENCES

Bennett, D. J., Sutton, M. D., & Turvey, S. T. (2018). Quantifying the living fossil concept. Palaeontologia Electronica, 21(1), 1–25. https://doi.org/10.26879/750.

Berkson, J., Chen, C. P., Mishra, J., Shin, P., Spear, B., & Zaldívar-Rae, J. (2009). A discussion of horseshoe crab management in five countries: Taiwan, India, China, United States, and Mexico. *Biology and conservation of horseshoe crabs*, 465-475.

Cai, G., Leadbetter, C. W., Muehlbauer, M. F., Molnar, T. J., & Hillman, B. I. (2013). Genome-Wide Microsatellite Identification in the Fungus *Anisogramma anomala* Using Illumina Sequencing and Genome Assembly. PLoS ONE 8(11), e82408. https://doi.org/10.1371/journal.pone.0082408.

Cai, L., Li, H., Zhang, J., & Rao, Y. (2015). Characterization Of Twelve New Microsatellite Markers for The Endangered Chinese Horseshoe Crab (*Tachypleus Tridentatus*) Through Next-Generation Sequencing. *Journal of Crustacean Biology* 35(4), 476–479. https://doi.org/10.1163/1937240X-00002331.

Carmichael, R. H., & Brush, E. (2012). Three decades of horseshoe crab rearing: a review of conditions for captive growth and survival. https://doi.org/10.1111/j.1753-5131.2012.01059.x.

e-ISSN 2716-697X

Chen, C. P., Yang, M. C., Fan, L. F., Qiu, G., Liao, Y. Y., & Hsieh, H. L. (2015). Co-occurrence of juvenile horseshoe crabs *Tachypleus tridentatus* and *Carcinoscorpius rotundicauda* in an estuarine bay, Southwestern China. Aquatic Biology, 24(2), 117–126. https://doi.org/10.3354/AB00641.

Faridah, M., Ismail, N., Ahmad, A. Bin, Manca, A., Rahman, M. Z. F. A., Bahri, M. F. S., Mohd Sofa, M. F. A., Ghaffar, I. H. A., Alia'm, A. A., Abdullah, N. H., & Mohd Kasturi, M. M. (2015). The Population Size and Movement of Coastal Horseshoe Crab, *Tachypleus gigas* (Müller) on the East Coast of Peninsular Malaysia. In: Carmichael, R., Botton, M., Shin, P., Cheung, S. (eds) Changing Global Perspectives on Horseshoe Crab Biology, Conservation and Management. Springer, Cham. https://doi.org/10.1007/978-3-319-19542-1_11.

Fu, Y., Huang, S., Wu, Z., Wang, C. C., Su, M., Wang, X., Xu, P., Huang, X., Wu, H., Wang, Y., Wang, J., Xiao, X., Zhou, H., Xie, X., Chen, M., Huang, S. L., Liao, Y., & Kwan, K. Y. (2019). Socio-demographic drivers and public perceptions of consumption and conservation of Asian horseshoe crabs in northern Beibu Gulf, China. Aquatic Conservation: Marine and Freshwater Ecosystems, 29(8), 1268–1277. https://doi.org/10.1002/AQC.3125.

Jackson, N. L., Nordstrom, K. F., Smith, D. R., & Saini, S. (2014). Delivery and movement of horseshoe crab eggs (Limulus polyphemus) in the breaking waves and swash uprush of an estuarine foreshore. Estuarine, Coastal and Shelf Science, 136, 191–198. https://doi.org/10.1016/J.ECSS.2013.10.025.

Kntayya, S. K. (2015). Characterization of the Genetic Diversity Within and Among Population of the Asian Horseshoe Crab in Sabah Using Cytochrome Oxidase I and Microsatellite Markers. Universiti Malaysia Sabah.

Krisfalusi-Gannon, J., Ali, W., Dellinger, K., Robertson, L., Brady, T. E., Goddard, M. K., Tinker-Kulberg, R., Kepley, C. L., & Dellinger, A. L. (2018). The Role of Horseshoe Crabs in the Biomedical Industry and Recent Trends Impacting Species Sustainability. Frontiers in Marine Science, 5, 185. https://doi.org/10.3389/fmars.2018.00185.

Kwan, B. K., Hsieh, H. L., Cheung, S. G., & Shin, P. K. (2016). Present population and habitat status of potentially threatened Asian horseshoe crabs *Tachypleus tridentatus* and *Carcinoscorpius rotundicauda* in Hong Kong: a proposal for marine protected areas. Biodiversity and Conservation, 25, 673-692. https://doi.org/10.1007/s10531-016-1084-z.

Liao, Y., Hsieh, H.L., Xu, S., *et al*. (2019). Wisdom of crowds reveals decline of Asian horseshoe crabs in Beibu Gulf, China. Oryx 53(2), 222-229. https://doi.org/10.1017/S003060531700117X.

Manca, A., Mohamad, F., Ahmad, A., Sofa, M. F. A. M., & Ismail, N. (2017). Tri-spine horseshoe crab, *Tachypleus tridentatus* (L.) in Sabah, Malaysia: the adult body sizes and population estimate. *Journal of Asia-Pacific Biodiversity*, *10*(3), 355-361. https://doi.org/10.1016/j.japb.2017.04.011.

Merritt, B. J., Culley, T. M., Avanesyan, A., Stokes, R., & Brzyski, J. (2015). An empirical review: Characteristics of plant microsatellite markers that confer higher levels of genetic variation. Applications in Plant Sciences, 3(8), 1500025. https://doi.org/10.3732/APPS.1500025.

Mohamad, F., Manca, A., Ahmad, A., Sofa, M. F. A. M., Alia'm, A. A., & Ismail, N. (2016). Width-weight and length-weight relationships of the tri-spine horseshoe crab, *Tachypleus tridentatus* (Leach 1819) from two populations in Sabah, Malaysia: Implications for population management. Journal of Sustainability Science and Management, 11(1), 1-13.

Nelson, B. R., Satyanarayana, B., Hwei Zhong, J. M., Shaharom, F., Sukumaran, M., & Chatterji, A. (2015). Episodic human activities and seasonal impacts on the *Tachypleus gigas* (Müller, 1785) population at Tanjung Selangor in Peninsular Malaysia. Estuarine, Coastal and Shelf Science, 164, 313–323. https://doi.org/10.1016/J.ECSS.2015.08.003.

Nishida, S., & Koike, H. (2009). Genetic Structure of Japanese Populations of *Tachypleus tridentatus* by mtDNA AT-Rich Region Sequence Analysis. In: Tanacredi, J., Botton, M., Smith, D. (eds) Biology and Conservation of Horseshoe Crabs. Springer, Boston, MA. https://doi.org/10.1007/978-0-387-89959-6_11.

Obst, M., Faurby, S., Bussarawit, S., & Funch, P. (2012). Molecular phylogeny of extant horseshoe crabs (Xiphosura, Limulidae) indicates Paleogene diversification of Asian species. Molecular Phylogenetics and Evolution, 62(1), 21–26. https://doi.org/10.1016/J.YMPEV.2011.08.025.

Robert, R., Muhammad Ali, S. H., & Amelia-Ng, P. F. (2014). Demographics of Horseshoe Crab Populations in Kota Kinabalu, Sabah, Malaysia with Emphasis on *Carcinoscorpius rotundicauda* and Some Aspects of its Mating Behaviour. Pertanika Tropical Agricultural Science 37 (3), 375-388.

Shin, P.K., Li, H., & Cheung, S.G. (2009). Horseshoe Crabs in Hong Kong: Current Population Status and Human Exploitation. In: Tanacredi, J., Botton, M., Smith, D. (eds) Biology and Conservation of Horseshoe Crabs. Springer, Boston, MA. https://doi.org/10.1007/978-0-387-89959-6_22.

Smith, D. R., Brockmann, H. J., Beekey, M. A., King, T. L., Millard, M. J., & Zaldívar-Rae, J. (2017). Conservation status of the American horseshoe crab, (*Limulus polyphemus*): a regional assessment. Reviews in Fish Biology and Fisheries, 27(1), 135–175. https://doi.org/10.1007/s11160-016-9461-y.

Størmer, L. (1952). Phylogeny and Taxonomy of Fossil Horseshoe Crabs. Journal of Paleontology, 26(4), 630–640.

Tanacredi, J. T., Botton, M. L., & Smith, D. R. (2009). Biology and conservation of horseshoe crabs. Springer New York, NY. p 662. . https://doi.org/10.1007/978-0-387-89959-6.

Temnykh, S., DeClerck, G., Lukashova, A., Lipovich, L., Cartinhour, S., & McCouch, S. (2001). Computational and Experimental Analysis of Microsatellites in Rice (*Oryza sativa* L.): Frequency, Length Variation, Transposon Associations, and Genetic Marker Potential. Genome Research, 11(8), 1441–1452. https://doi.org/10.1101/GR.184001.

Tinker-Kulberg, R., Dellinger, K., Brady, T. E., Robertson, L., Levy, J. H., Abood, S. K., LaDuca, F. M., Kepley, C. L., & Dellinger, A. L. (2020). Horseshoe Crab Aquaculture as a Sustainable Endotoxin Testing Source. Frontiers in Marine Science, 7, 153. https://doi.org/10.3389/fmars.2020.00153.

Wattanadilokchatkun, P., Panthum, T., Jaisamut, K., Ahmad, S. F., Dokkaew, S., Muangmai, N., Duengkae, P., Singchat, W., & Srikulnath, K. (2022). Characterization of Microsatellite Distribution in Siamese Fighting Fish Genome to Promote Conservation and Genetic Diversity. Fishes, 7(5), 251. https://doi.org/10.3390/FISHES7050251/S1.

Wittke-Thompson, J. K., Pluzhnikov, A., & Cox, N. J. (2005). Rational Inferences about Departures from Hardy-Weinberg Equilibrium. American Journal of Human Genetics, 76(6), 967. https://doi.org/10.1086/430507.

Xu, X., Peng, M., Fang, Z., & Xu, X. (2000). The direction of microsatellite mutations is dependent upon allele length. Nature Genetics, 24(4), 396–399. https://doi.org/10.1038/74238.

Yang, M.C., Chen, C.A., Hsieh, H.L. & Chen, C.P. (2007). Population subdivision of the tri-spine horseshoe crab, *Tachypleus tridentatus*, in Taiwan Strait. Zoological Science 24(3), 219-24. https://doi.org/10.2108/zsj.24.219.

Yeh, F. C., Yang, R. C., & Boyle, T. (1999). POPGENE version 1.32: Microsoft Window-based freeware for population genetics analysis. Edmonton, Canada: University of Alberta.

Borneo International Journal of Biotechnology (BIJB) Vol. 5 (December 2025), 126-142.

e-ISSN 2716-697X

Antibiofilm Activity of *Pseudomonas Sp.* (Mb273n) Cell-Free Supernatant Against Pathogenic Bacteria

Izzah Mardhiyyah Nurrohmah[1], Anto Budiharjo[2*], Zarina Amin[3*]

[1]Department of Biology, Faculty of Science and Mathematics, Diponegoro University, Jl. Prof. Soedarto, SH, Tembalang, 50275 Semarang, Central Java, Indonesia.
[2]Biotechnology Study Program, Faculty of Science and Mathematics, Diponegoro University, Jl. Prof. Soedarto, SH, Tembalang, 50275 Semarang, Central Java, Indonesia.
[3]Biotechnology Research Institute, University Malaysia Sabah, Jalan UMS, 88450, Kota Kinabalu, Sabah, Malaysia.
*Corresponding author's e-mail: zamin@ums.edu.my
Received: 15 October 2025 | Accepted: 20 December 2025 | Published: 31 December 2025

ABSTRACT

Bacterial biofilms pose a significant global health challenge due to their resistance to antibiotics and the host immune system, leading to persistent infections. Developing effective strategies to control biofilm formation is therefore crucial for preventing persistent infections. This study investigated the antibiofilm potential of the cell-free supernatant (CFS) from *Pseudomonas* sp. (MB273N) against biofilms of *Escherichia coli*, *Pseudomonas aeruginosa*, *Staphylococcus aureus*, and *Chromobacterium violaceum*. Additionally, the study examined biofilm structural changes following CFS treatment. The CFS was obtained by centrifuging bacterial cultures three times at 11,000 rpm for 15 minutes. A biofilm inhibition assay was conducted to assess the antibiofilm activity of CFS at a sub-lethal concentration, and biofilm morphology was examined using scanning electron microscopy (SEM). Statistical analysis was performed using SPSS version 26. The CFS significantly ($p<0.05$) inhibited biofilm formation, with inhibition rates of 14.15% for *E. coli*, 32.46% for *P. aeruginosa*, 30.83% for *S. aureus*, and 37.5% for *C. violaceum*. SEM analysis revealed that untreated biofilms formed dense, multilayered structures, while CFS-treated biofilms appeared less dense, more dispersed, and exhibited altered cell morphology. The CFS of *Pseudomonas* sp. (MB273N) demonstrates potential as an antibiofilm agent against *E. coli*, *P. aeruginosa*, *S. aureus*, and *C. violaceum*, highlighting its possible application in biofilm control strategies.

e-ISSN 2716-697

INTRODUCTION

Biofilms have become a major concern in public health because biofilm-associated microorganisms are less susceptible to antimicrobial treatments (Arampatzi *et al.*, 2011). Biofilms are responsible for various infections. It has been reported that around 50% of hospital-acquired infections in immunodeficient patients are linked to biofilms, and as much as 80% of chronic infections globally are also associated with biofilms (Asma *et al.*, 2022; Meroni *et al.*, 2021). Therefore, effective control of biofilm is necessary to overcome various health problems.

This study investigated four model organisms, namely *Escherichia coli*, *Pseudomonas aeruginosa*, *Staphylococcus aureus*, and *Chromobacterium violaceum* to investigate biofilm inhibition. Urinary tract infections (UTIs) associated with biofilms are often caused by *E. coli*, and Uropathogenic *Escherichia coli* (UPEC) is the primary etiological agent of UTIs (Alshammari *et al.*, 2023; Zagaglia *et al.*, 2024). *P. aeruginosa* is known for its ability to form biofilms, which play a crucial role in establishing persistent lung infection (Davis and Brown, 2016). *S. aureus* biofilm infections are very common in orthopedic infections, and it has been demonstrated *in vitro* that *S. aureus* biofilms may cause bone loss during chronic osteomyelitis (Sanchez *et al.*, 2013; Yu *et al.*, 2020). Moreover, *C. violaceum* can become a pathogen and possesses the ability to form biofilm, which may increase its resistance to antibiotics and promote the initiation of infections in the host (Alisjahbana *et al.*, 2021; Dimitrova *et al.*, 2024). These four model organisms are recognized as the causative agents of many infections.

Cell-free supernatant (CFS), a microbiological culture medium containing metabolites that exclude bacterial cells (Liu *et al.*, 2023), may serve as an alternative to antimicrobial agents against biofilms. Prior studies have found that CFS from certain bacteria contain compounds with antibiofilm properties that inhibit biofilm development of bacterial pathogens (Al-Barhawee and Al-Rubyee, 2024; Ray *et al.*, 2023). Therefore, cell-free supernatant may become an effective solution for controlling biofilms.

A previous study identified *Pseudomonas* sp. (MB273N), a novel bacterial species isolated from the Maliau Basin Conservation Area (data not published). The antibiofilm activity of *Pseudomonas* sp. (MB273N) cell-free supernatant against biofilms formed by *E. coli*, *P. aeruginosa*, *S. aureus*, and *C. violaceum* has not been evaluated. This study aimed to investigate whether there is a potency of *Pseudomonas* sp. (MB273N) cell-free supernatant as an antibiofilm agent against these bacteria, and to observe the characteristics of these four bacterial biofilms both before and after treatment with CFS.

e-ISSN 2716-697X

MATERIALS AND METHODS

Bacterial Cultivation

The bacterial strains used in this study (*Escherichia coli, Pseudomonas aeruginosa, Staphylococcus aureus, Chromobacterium violaceum,* and *Pseudomonas* sp. (MB273N)) were obtained from the frozen stocks of the Biotechnology Research Institute, Universiti Malaysia Sabah. Glycerol stocks of these strains were stored at -80°C. Prior to use, the stocks were thawed at room temperature until liquid cultures were observed. A loopful of each bacterial strain was streaked onto nutrient agar (Oxoid) and incubated at 28°C overnight. Single colonies were then sub-cultured in nutrient broth (Merck KGaA) and incubated at 28°C for 14 hours in a shaking incubator (Innova) at 180 rpm.

Preparation of Cell-Free Supernatant (CFS)

The culture of *Pseudomonas* sp. (MB273N) was transferred into Falcon tubes and centrifuged at 11,000 rpm for 15 minutes at 4°C. The supernatant was separated from the pellet and centrifugation was repeated three times. The final supernatant was filter-sterilized using a 0.22 µm syringe filter. The bacterial pellet was used for colony-forming unit (CFU) enumeration by resuspending in 100 mL of NaCl solution, followed by a 1:10 serial dilution. The cultures were then plated onto nutrient agar using the spread plate method and incubated overnight at 28°C. The bacterial concentration was determined to be 1.1×10^{11} CFU/mL, representing the neat concentration of *Pseudomonas* sp. (MB273N) CFS.

Preparation of 2,3,5-Triphenyltetrazolium Chloride (TTC) Solution

TTC solution was prepared following Mukti (2019) with modifications. Briefly, 75 mg of TTC was dissolved in 15 mL of sterile distilled water at room temperature, filtered through a 0.22 µm syringe filter, and stored at 4°C until use.

Minimum Inhibitory Concentration (MIC) Assay

The MIC assay was adapted from Mukti (2019) with modifications. A 96-well microtiter plate was prepared with 100 µL of nutrient broth (NB) per well. CFS was serially diluted two-fold in NB, and 50 µL of bacterial suspension (OD600 = 0.5, adjusted using a Bio-Rad SmartSpec Plus spectrophotometer) was added to each well.

Controls included:

a) **Positive control:** 100 µL NB + 50 µL bacterial suspension
b) **Negative control:** 100 µL NB + 100 µL CFS

e-ISSN 2716-697X

The plate was incubated at 37°C overnight. After incubation, 40 µL of TTC was added to each well and further incubated for 3 hours at room temperature. Bacterial growth was indicated by red spot formation at the well bottom. The MIC was determined as the lowest CFS concentration that inhibited visible bacterial growth (absence of red spot formation). The assay was performed in technical triplicates. The sub-lethal concentrations of CFS were then determined and used for the biofilm inhibition assay.

Biofilm Inhibition Assay

The biofilm inhibition assay followed Mukti (2019) with modifications. A 96-well microtiter plate was prepared by adding 100 µL of NB per well. CFS was added and serially diluted two-fold. Then, 50 µL of bacterial suspension (OD600 = 0.5) of *P. aeruginosa, E. coli, S. aureus,* and *C. violaceum* was introduced into each well.

Controls included:

a) **Positive control:** 100 µL NB + 50 µL bacterial suspension (untreated sample)

b) **Negative control:** 100 µL NB + 100 µL CFS

The plate was incubated at 37°C overnight. After incubation, culture media were aspirated, and the wells were rinsed three times with sterile distilled water to remove planktonic bacteria. Wells were then stained with 200 µL of 0.1% (w/v) crystal violet solution for 30 minutes at room temperature. After washing and air-drying, bound crystal violet was solubilized with 95% ethanol. The absorbance (OD570) of solubilized dye was measured using a microplate reader (Tecan Sunrise). The percentage of biofilm inhibition was calculated as follows:

$$\text{Biofilm inhibition} = \left(1 - \frac{\text{Mean OD treated}}{\text{Mean OD untreated}}\right) \times 100$$

Scanning Electron Microscopy (SEM) Analysis

SEM was used to visualize the effects of *Pseudomonas* sp. (MB273N) CFS on biofilms of *E. coli, P. aeruginosa, S. aureus,* and *C. violaceum*, following Mukti (2019) with modifications. Test bacteria were cultured in the presence and absence of CFS and incubated at 37°C for 24 hours without shaking. The optical density of the cultures was adjusted to OD600 = 0.5 before biofilm samples were fixed in fixative solution and incubated at 4°C for a minimum of 4 hours.

The samples were dehydrated through a graded ethanol series (35%, 50%, 75%, 95%, and 100%) and dried overnight using silica gel, following the method of Raab and Bachelet (2017), where silica gel reduces moisture by gradually absorbing water vapor. Dried samples were sputter-coated with gold and examined under a Scanning Electron Microscope (Hitachi S-3400N).

e-ISSN 2716-697X

Data Analysis

Statistical analyses were conducted using SPSS version 26. Data normality was assessed using the Shapiro-Wilk test. Paired t-tests and Wilcoxon signed-rank tests were used to compare mean values before and after CFS treatment, with statistical significance set at $p < 0.05$.

RESULTS AND DISCUSSION

MIC and Sub-lethal Concentration of CFS for Pathogenic Bacteria

MIC assay results of *Pseudomonas* sp. (MB273N) CFS are shown in figures 1 and 2. The MIC value of CFS against *E. coli* was observed at a concentration of 1.4×10^{10} CFU/mL, whereas the CFS demonstrated the same MIC value against *P. aeruginosa*, *S. aureus*, and *C. violaceum* bacteria, with a concentration of 1.1×10^{11} CFU/mL. The MIC results showed that *Pseudomonas* sp. (MB273N) CFS inhibited bacterial growth. The solution in the well remained clear or turned pale pink after adding TTC and being incubated, indicating growth inhibition (Panphut *et al.*, 2020). In accordance with our study, Chythanya *et al.* (2002) revealed that the chloroform extract of *Pseudomonas* CFS exhibited inhibitory effects on the growth of a bacterial pathogen, as determined by the MIC assay. MIC is the lowest antimicrobial concentration that will inhibit a microorganism's visible growth after overnight incubation (Wahi *et al.*, 2011). Referring to Table 1, the higher MIC value of 1.1×10^{11} CFU/mL for *P. aeruginosa*, *S. aureus*, and *C. violaceum* indicates greater resistance compared to *E. coli*. According to Mombeshora and Mukanganyama (2017), a high MIC value demonstrates that a high concentration of the antimicrobial agent is needed to inhibit microbial growth, hence, the test isolate is resistant to the specific antimicrobial.

e-ISSN 2716-697X

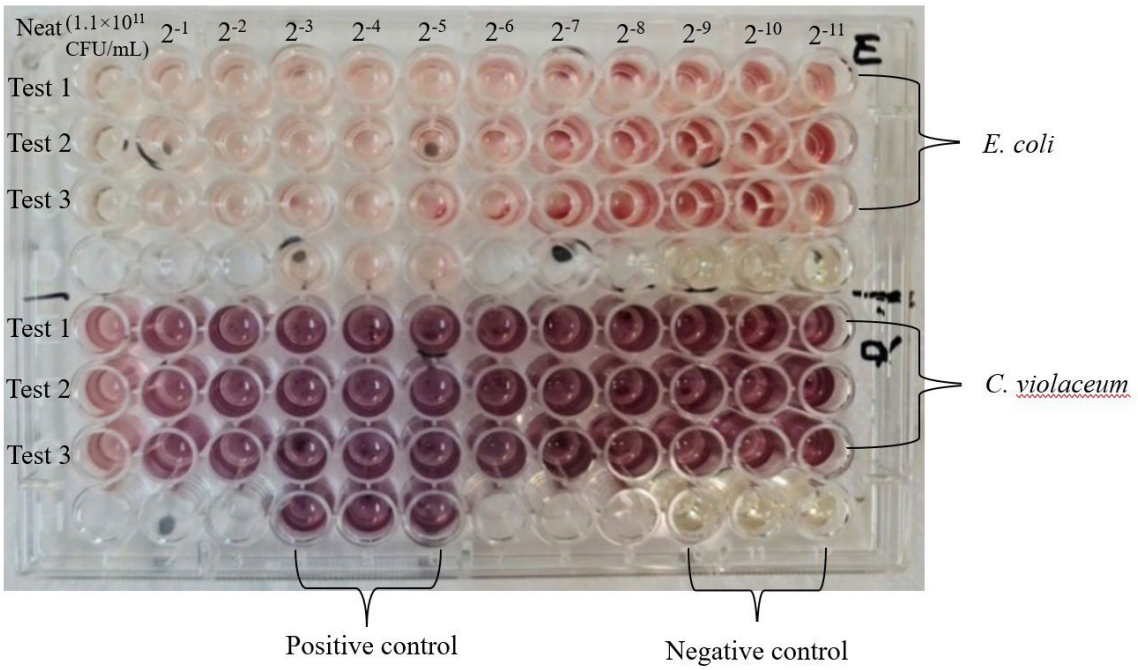

Figure 1 Minimum inhibitory concentration of (MB272N) CFS against *E. coli* and *C. violaceum*.

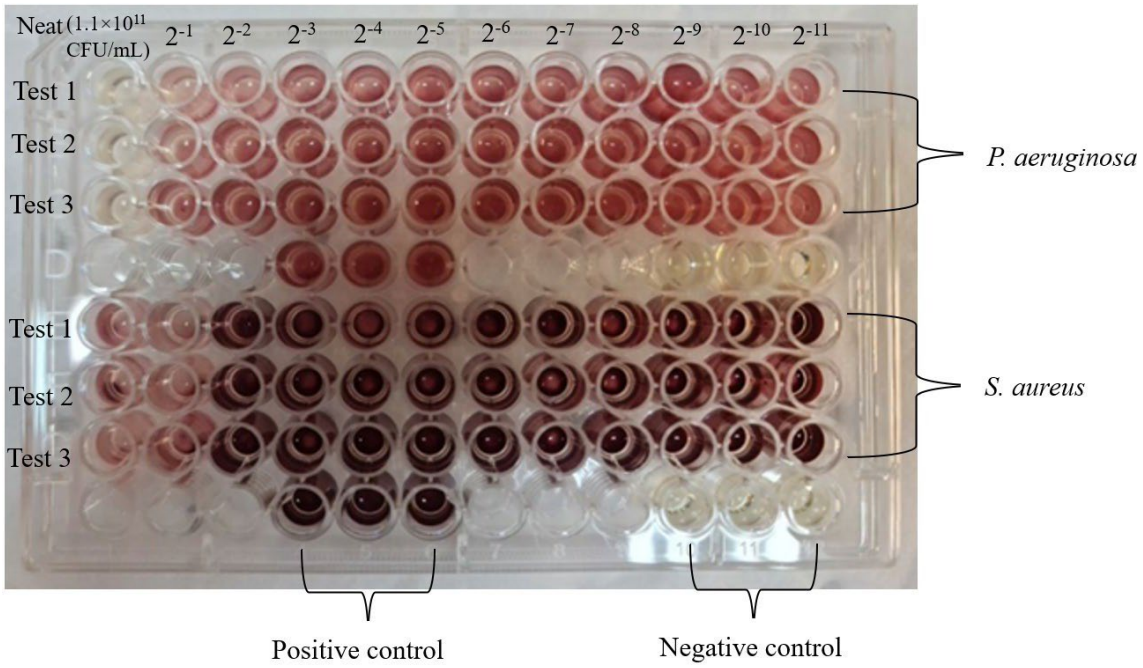

Figure 2 Minimum inhibitory concentration of (MB272N) CFS against *P. aeruginosa* and *S. aureus*.

e-ISSN 2716-697X

The sub-lethal concentration of CFS against *E. coli* and *P. aeruginosa* was 0.07×10^{11} and 0.55×10^{11} respectively. CFS exhibited the same sub-lethal concentration value against *S. aureus* and *C. violaceum*, measuring 1.1×10^{11} CFU/mL. Sub-lethal concentration is the concentration of antimicrobial agent in the well immediately before the MIC concentration. The concentration of *Pseudomonas* sp. (MB273N) CFS for the biofilm inhibition assay was below the MIC to ensure that the concentration used to inhibit biofilm formation was not lethal to the test bacteria. The selection of sub-lethal concentration for the CFS was based on the premise that alternative anti-infective treatments should not directly cause bacterial death, as antimicrobial resistance to various antibiotics arises from gene mutations in pathogenic bacteria, which serves as a defense mechanism against cell death (Mukti *et al.*, 2019).

Table 1 MIC and sub-lethal concentration of *Pseudomonas* sp. (MB272N) CFS against tested bacteria.

Microorganisms	*Pseudomonas sp.* (MB273N) CFS	
	MIC (CFU/mL)	Sub-lethal (CFU/mL)
Pseudomonas aeruginosa	1.1×10^{11}	0.55×10^{11}
Escherichia coli	0.14×10^{11}	0.07×10^{11}
Staphylococcus aureus	1.1×10^{11}	1.1×10^{11}
Chromobacterium violaceum	1.1×10^{11}	1.1×10^{11}

Biofilm Inhibition of Pseudomonas sp. (MB273N) CFS

A biofilm inhibition assay was conducted to evaluate the ability of *Pseudomonas* sp. (MB273N) CFS in inhibiting bacterial biofilm formation. In figure 3, it can be seen that the OD values of tested microorganisms after exposure to a sub-lethal concentration of CFS were lower than the OD values before CFS treatment, indicated a reduction in biomass. According to Liu *et al.* (2021), a reduction in the biomass may indicates a decrease in the biofilm matrix content. These results suggested that CFS *Pseudomonas* sp. (MB273N) exhibited biofilm inhibitory activity against *P. aeruginosa*, *E. coli*, *S. aureus*, and *C. violaceum*.

e-ISSN 2716-697X

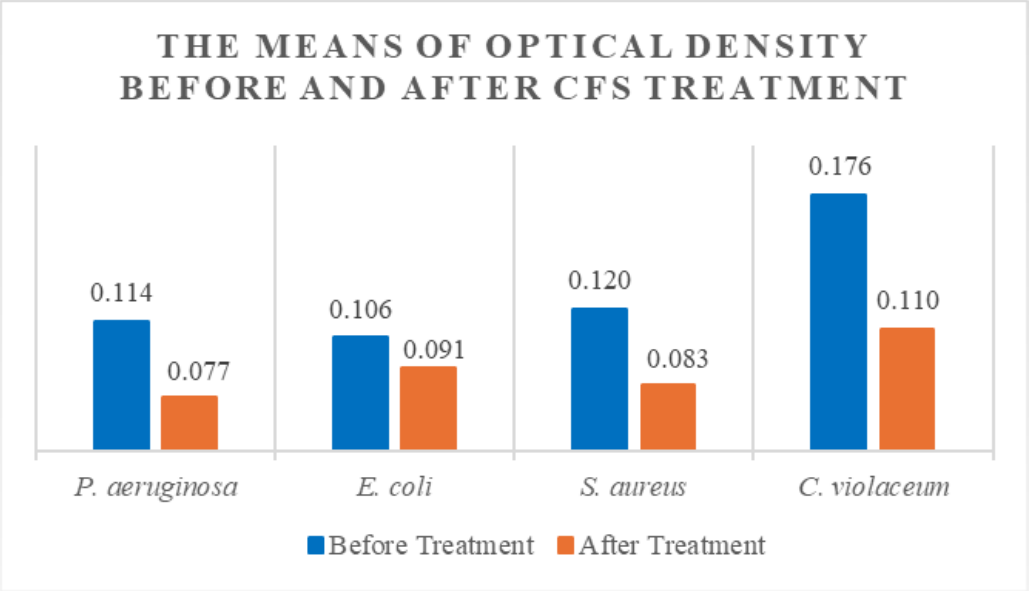

Figure 3 The means of optical density before and after CFS treatment

Biofilm inhibition percentage of tested bacteria is shown in Figure 4. Biofilm formation of *P. aeruginosa*, *S. aureus*, and *C. violaceum* was significantly inhibited by *Pseudomonas* sp. (MB273N) CFS ($p < 0.05$). The biofilm inhibition percentages of CFS-treated *S. aureus*, *P. aeruginosa*, and *C. violaceum* were 30.83%, 32.46%, and 37.5%, respectively. No significant difference was observed between before and after CFS treatment biofilm inhibition of *E. coli* ($p > 0.05$). Biofilm inhibition of 14.15% was noted when *E. coli* was exposed to CFS. According to Famuyide et al. (2019), antibiofilm activity is considered good when the percentage inhibition is above 50%, whereas percentages between 0% and 49% indicate poor antibiofilm activity. Thus, it can be concluded that the CFS from *Pseudomonas* sp. (MB273N) at sub-lethal concentration exhibited low biofilm inhibition against *E. coli*, *P. aeruginosa*, *S. aureus*, and *C. violaceum*, as the inhibition percentages were below 50%. However, the observed low inhibition does not indicate an absence of antibiofilm effect, as the CFS may still contain bioactive compounds that exert partial or concentration-dependent antibiofilm activity, which may become more pronounced under different experimental conditions or at higher concentrations.

e-ISSN 2716-697X

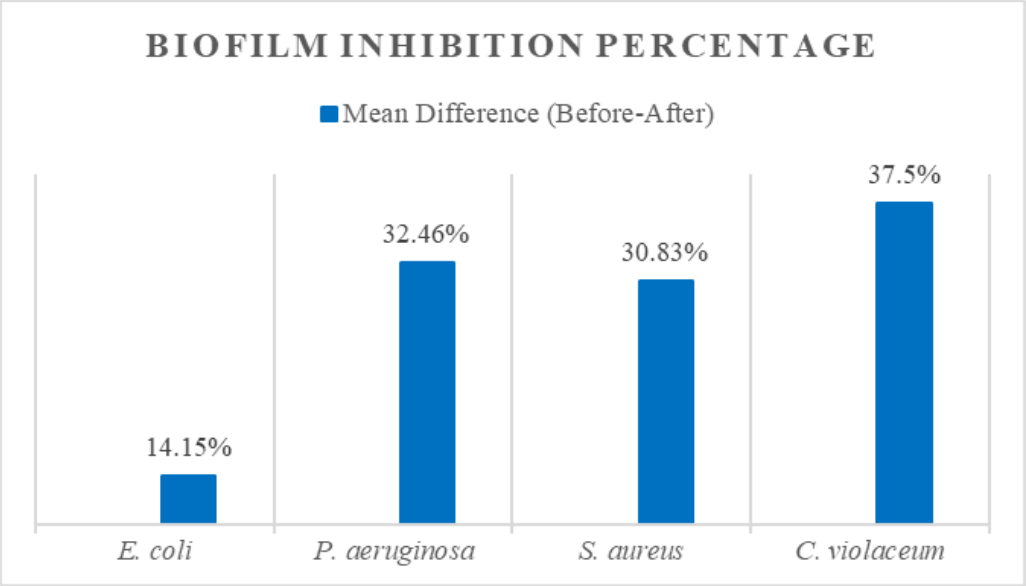

Figure 4 Biofilm inhibition percentage

The inhibition of biofilm formation was assessed using crystal violet solution. Aiyer and Vijaykumar (2019) noted that crystal violet stains living biomass and the extracellular matrix of the biofilm. Additionally, crystal violet is suitable for qualitative and quantitative measurements of biofilms adhered to various surfaces (Haney *et al.*, 2018). Gene expression of biofilm is regulated by quorum sensing, and the activity of biofilm inhibition may occur due to the disruption of quorum sensing (Theodora *et al.*, 2019). Besides, interfering quorum sensing system may hinder the assembly of biofilm matrix and the further establishment of infection in host cells (Venkatramanan *et al.*, 2020). The biofilm inhibition may occur because the bacterial cells produce compounds that can disrupt quorum sensing. These compounds, known as quorum quenching compounds, can work in several ways, by interfering synthesis of autoinducer, degrading the autoinducer, or preventing the binding of a signal molecule to the receptor (Mulya and Waturangi, 2021).

Biofilms With and Without CFS Treatment under Scanning Electron Microscope

To verify that *Pseudomonas* sp. (MB273N) CFS exhibited biofilm inhibitory activity of *P. aeruginosa*, *E. coli*, *S. aureus*, and *C. violaceum*, the bacterial biofilm was observed using Scanning Electron Microscope (SEM). In untreated *E. coli* group, biofilms displayed dense cellular aggregates, typical rod-shaped cells with normal size, and the presence of extracellular polysaccharide (EPS) matrix (Figure 5a). Meanwhile, morphological or ultrastructural changes were observed in the microbial cells treated with CFS. Some cells became shorter, appeared wrinkled, and had altered shape, invaginations and looser cell aggregation after CFS treatment. Furthermore, an obvious reduction of the EPS matrix was also detected (Figure 5b).

e-ISSN 2716-697X

Our results were similar to those reported in previous studies. Chaichana *et al.* (2023) found that *E. coli* strain exhibited looser cell aggregation and less extracellular matrix production when treated with *Staphylococcus warneri* CFS. Famuyide *et al.* (2020) reported that the exposure of *E. coli* to *Syzygium legatii* acetone leaf extracts caused invagination of some cells, wrinkled surface, and alteration in bacterial cell shape. These characteristics, which are like our findings, demonstrated that *E. coli* biofilm treated with *Pseudomonas* sp. (MB273N) CFS was disrupted compared to the untreated group.

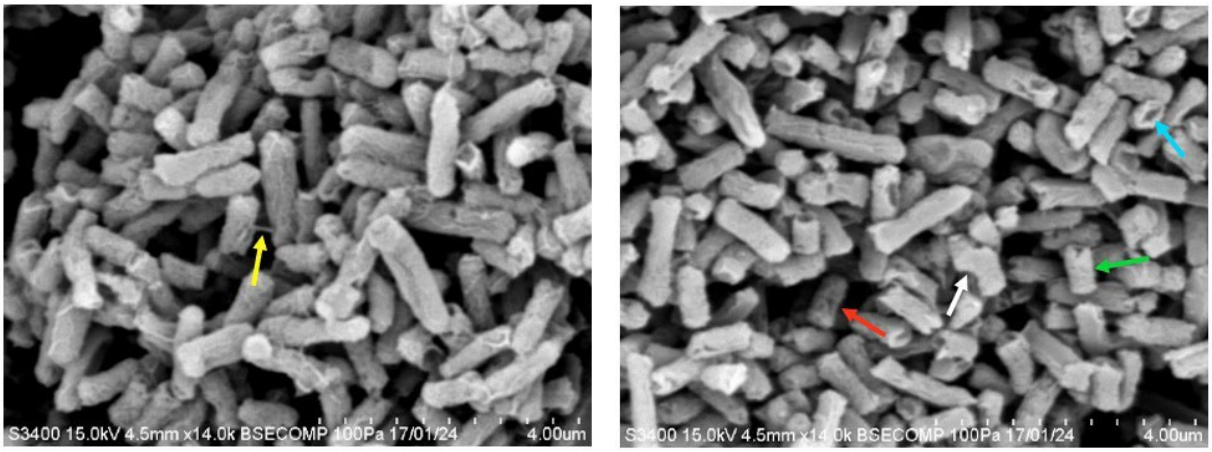

(a) (b)

Figure 5 *E. coli* untreated [(a) (15.0 kV; magnification: 14000 ×)] and treated [(b) (15.0 kV; magnification: 14000 ×)] with *Pseudomonas* sp. (MB273N) CFS. In Figure 5.a, the yellow arrow indicates the EPS matrix, while Figure 5.b shows several changes: shorter cells (green arrow), a wrinkled cell surface (red arrow), cell shape alteration (white arrow), and invagination (blue arrow).

Untreated *P. aeruginosa* cells exhibited tight cellular aggregates (Figure 6a), whereas more dispersed cells and alteration in bacterial cell shape were observed after CFS treatment (Figure 6b). These findings were consistent to those reported by Drumond *et al.* (2023), who revealed that the treatment of *P. aeruginosa* with the cell-free spent medium (CFSM) of lactic acid bacteria caused a reduction in the cell's compaction. Moreover, Liu *et al.* (2020) showed that bacterial cells were bent after treated with linalool. As confirmed by these results, it can be concluded that CFS of *Pseudomonas* sp. (MB273N) was effective in altering the structure of biofilm.

Pseudomonas sp. is known to produce antimicrobials that can inhibit closely related species. A previous study done by Snopková *et al.* (2022) reported that selected *Pseudomonas* sp. strains isolated from Antarctica were able to inhibit one other *Pseudomonas* strain. These strains produced antimicrobials, and no strain was sensitive to its own antimicrobial agent.

e-ISSN 2716-697X

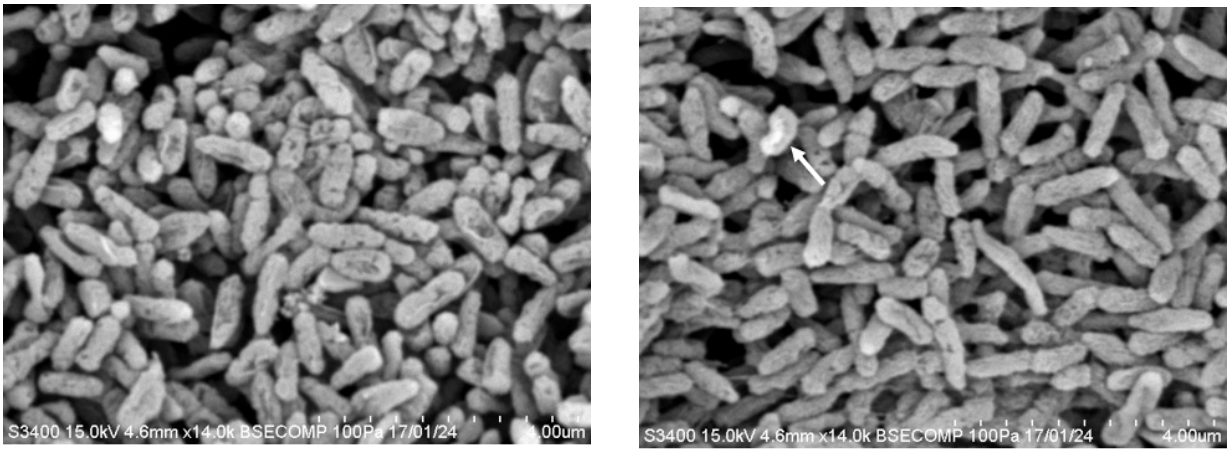

Figure 6 *P. aeruginosa* untreated [(a) (15.0 kV; magnification: 14000 ×)] and treated [(b) (15.0 kV; magnification: 14000 ×)] with *Pseudomonas* sp. (MB273N) CFS. The white arrow indicates an altered cell shape.

S. aureus groups without CFS treatment portrayed dense and clumped biofilm structures with multiple layers were formed. Many cells showed spherical shape intact cell morphology, and the formation of a septum and cell splitting was also observed (Figure 7a). On the other hand, CFS-treated biofilms exhibited altered morphology, more dispersed cells, and wrinkles on the cell surface. The treated cells appeared elongated, and septum formation was reduced compared with the untreated group (Figure 7b).

Similar findings were also observed in previous studies on *S. aureus* cells treated with various antimicrobial agents. Kim *et al.* (2020) reported that *S. aureus* treated with *S. cerevisiae* CFS exhibited decreased cell attachment and aggregation. Furthermore, *S. aureus* treated with *Perilla frutescens var. acuta* leaf extract presented wrinkled abnormalities on the morphology of the cells (Kim *et al.*, 2011). Moreover, Matijašević *et al.* (2016) revealed that untreated *S. aureus* cells were spherical and exhibited a septum formation, whereas those treated with *Coriolus versicolor* extracts appeared elongated and deformed. Interestingly, the septum formation in the treated sample was not detected. The formation of a septum indicated active proliferation, and the authors assumed that the treatment of *S. aureus* with methanol extract of *C. versicolor* disables cell division because the septum formation in the treated sample was not observed. From the previous study, we could conclude that *Pseudomonas* sp. (MB273N) CFS had an inhibitory effect on cell division, as evidenced by the reduction in the formation of septa, and similar changes obtained from previous works also proved that the CFS of *Pseudomonas* sp. (MB273N) caused damage to the cell shape of *S. aureus*.

e-ISSN 2716-697X

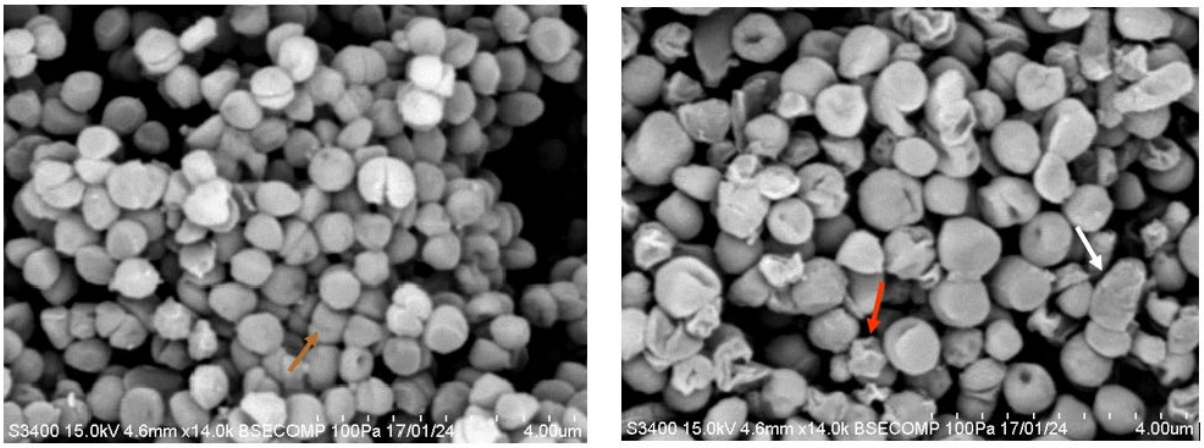

Figure 7: *S. aureus* untreated [(a) (15.0 kV; magnification: 14000 ×)] and treated [(b) (15.0 kV; magnification: 14000 ×)] with *Pseudomonas* sp. (MB273N) CFS. The brown arrow shows septum formation. The red arrow indicates a wrinkled cell, and the white arrow shows a shape alteration.

C. violaceum biofilm without CFS formed a cohesive aggregate with rod-shaped cells closely adhered to each other. Moreover, the bacterial cells can also be seen enclosed in a polymeric matrix (EPS) forming a clump of cells (Figure 8a). In contrast, CFS-treated samples exhibited reduced EPS matrix, dispersed cells, and surface invagination. Additionally, an elongation of cell size with abnormally shaped bacterial cells was observed, likely resulting from incomplete cell division (Figure 8b). This observation is consistent with findings reported by Dimitrova *et al.* (2024) utilizing lactone-enriched fraction from *I. Britannica*, where the cell elongation was observed in *C. violaceum*. Their study also highlighted incomplete cell division as the likely cause of the abnormal bacterial cell shape.

Similar observations have also been reported by previous studies on *C. violaceum* treated with various antibiofilm agents. The SEM results of *C. violaceum* treated with silver nanoparticles made from *Moringa oleifera* revealed biofilm inhibition with scattered cells compared with untreated cells (Haris and Ahmad, 2024). Furthermore, Dimitrova *et al.* (2024) reported that invagination on the cell surface and alterations in bacterial cell shape were found in *C. violaceum* treated with plant extracts of the genus *Inula*. These findings supported the present study, indicating that *C. violaceum* treated with *Pseudomonas* sp. (MB273N) CFS exhibited morphological deformations.

e-ISSN 2716-697X

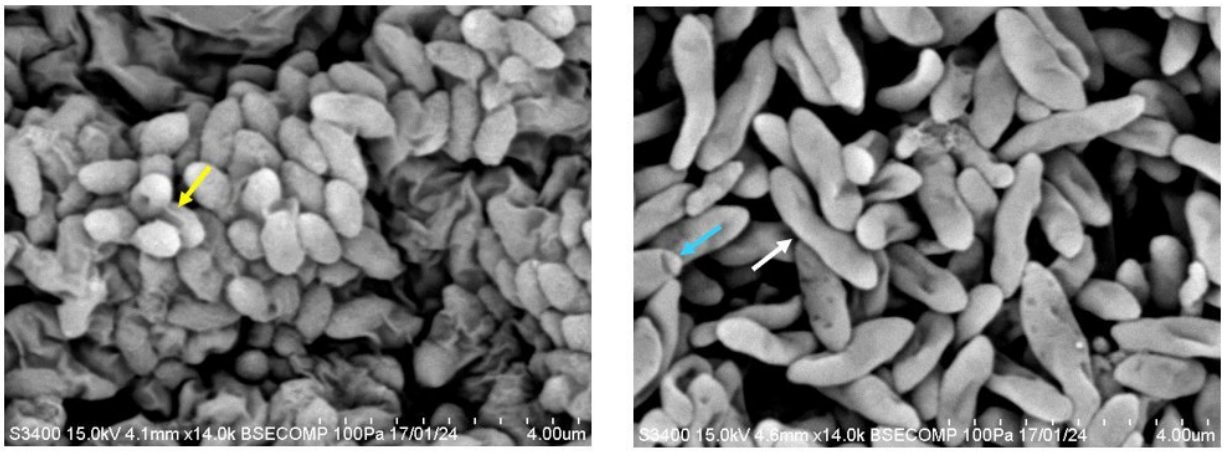

(a) (b)

Figure 8 : *C. violaceum* untreated [(a) (15.0 kV; magnification: 14000 ×)] and treated [(b) (15.0 kV; magnification: 14000 ×)] with *Pseudomonas* sp. (MB273N) CFS. The yellow arrow indicates EPS matrix. The blue arrow shows invagination of the cell. The white arrow indicates elongated cell.

The present study found that four bacterial biofilms treated with CFS exhibited reduced cell attachment and aggregation. This demonstrates that the treatment with the CFS resulted in a reduction in the ability of cells to adhere to each other, which led to less dense and more dispersed biofilm structures. The EPS matrix plays a crucial role in microbial adhesion to a surface, aggregation in multilayered biofilms, and protection against antimicrobial compounds, as well as antibiotics (Mishra *et al.*, 2020). According to Saptami *et al.* (2022), a reduction in EPS may lower the surface adhesion resulting in the loosening and dispersion of the cells. EPS contains exopolysaccharides, which play a major role in the integrity of the biofilm matrix. Biofilm maturation requires the secretion of EPS to bind cells together and maintains cohesive biofilm architecture. Therefore, a reduction in EPS production will cause the biofilm structure weak and susceptible (Husain *et al.,* 2015).

The CFS treatment also altered bacterial morphology. When bacteria change shape from a rod-like shape to shortened rods, they may decrease their surface area in contact with the surface and adjacent cells, resulting in impaired attachment to the surface and other cells (van Teeseling *et al.*, 2017). According to Baquero *et al.* (2024), environmental stress, either natural or anthropogenic, affects the shape of bacterial cells. Antimicrobial agents alter bacterial functions and cellular structures, causing cellular stress and alterations to bacterial forms.

Several changes observed within the biofilms treated with *Pseudomonas* sp. (MB273N) CFS are assumed to be the results of the activity of compounds present in the CFS, which possess antimicrobial or antibiofilm properties. A previous study reported that CFS from *Pseudomonas*, isolated from a hot spring, produced a bacteriocin-like substance and exhibited a large antibacterial activity against *E. coli* and *Pseudomonas* sp. (Ghrairi *et al.*, 2014). Bacteriocins can interfere in the early stages of biofilm formation by inhibiting the attachment of bacterial cells to other cells or their surface, or by killing the cells before they can integrate into biofilm structure (Duraisamy *et al.*, 2020). Additionally, pyocyanin from *Pseudomonas* has demonstrated

antibiofilm activity against Methicillin-resistant *Staphylococcus aureus* (MRSA) by reducing bacterial viability and EPS matrix (Kamer *et al.*, 2023). Based on these findings, it can be assumed that *Pseudomonas* sp. (MB273N) CFS may contain these compounds. However, further studies are needed to verify whether these compounds contribute to its antibiofilm activity.

The results of our study demonstrated that the cell-free supernatant of *Pseudomonas* sp. (MB273N) affected the structure and morphological characteristics of bacterial biofilms, thereby disrupting biofilm formation process in *E. coli*, *P. aeruginosa*, *S. aureus*, and *C. violaceum*. Based on the data obtained from the Scanning Electron Microscopy (SEM) observation, the interference of biofilm formation was indicated by reduced cell aggregation and morphological alterations in bacterial cells.

CONCLUSION

Cell-free supernatant of *Pseudomonas* sp. (MB273N) exhibited antibiofilm activity against *E. coli*, *P. aeruginosa*, *S. aureus*, and *C. violaceum*, with inhibition percentages below 50%. These findings were further supported by scanning electron microscopy observations, which showed that before CFS treatment, the four bacterial biofilms displayed dense cellular aggregates and multilayered structures, whereas after CFS treatment, the biofilms became less dense, more dispersed, and exhibited alterations in cell morphology.

REFERENCES

Aiyer, K. S. and Vijayakumar, B. S. (2019). An improvised microtiter dish biofilm assay for non-invasive biofilm detection on microbial fuel cell anodes and studying biofilm growth conditions. *Brazilian Journal of Microbiology* 50(3), 769-775.

Al-Barhawee, N. I. K. and Al-Rubyee S. S. (2024). Inhibition of Biofilm Formation in *Agrobacterium tumefaciens* by Cell-Free Supernatants of *Pseudomonas aeruginosa* Analyzed by GC-MS. *Baghdad Science Journal* 21(7), 2222-2236.

Alisjahbana, B., Debora, J., Susandi, E. and Darmawan, G. (2021). *Chromobacterium violaceum*: a review of an unexpected scourge. *International journal of general medicine* 14, 3259-3270.

Alshammari, M., Ahmad, A. AlKhulaifi, M., Al Farraj, D., Alsudir, S., Alarawi, M., Takashi, G. and Alyamani, E. (2023). Reduction of biofilm formation of *Escherichia coli* by targeting quorum sensing and adhesion genes using the CRISPR/Cas9-HDR approach, and its clinical application on urinary catheter. *Journal of Infection and Public Health* 16(8), 1174-1183.

Arampatzi, S. I., Giannoglou, G. and Diza, E. (2011). Biofilm formation: A complicated microbiological process. *Aristotle University Medical Journal* 38(2), 21-29.

Asma, S.T., Imre, K., Morar, A., Herman, V., Acaroz, U., Mukhtar, H., Arslan-Acaroz, D., Shah, S. R. A. and Gerlach, R. (2022). An Overview of Biofilm Formation–Combating Strategies and Mechanisms of Action of Antibiofilm Agents. *Life* 2022 12(8), 1110.

Baquero, F., Moreno-Blanco, A. and del-Campo, R. (2024). Environmental Stress, Bacterial Cell Differentiation, and Antimicrobial Resistance.

Chaichana, N., Muneerungsee, N., Sukpondma, Y. and Sermwittayawong, N. (2023). *Escherichia coli* virulence inhibition by cell-free supernatants from mangrove forest bacteria producing quorum sensing inhibitor. *LWT* 185, 115182.

Chythanya, R., Karunasagar I. and Karunasagar. I (2002). Inhibition of shrimp pathogenic vibrios by a marine *Pseudomonas* I-2 strain. *Aquaculture* 208(1-2), 1-10.

Davis, R. and Brown, P. D. (2016). Multiple antibiotic resistance index, fitness and virulence potential in respiratory *Pseudomonas aeruginosa* from Jamaica. *Journal of medical microbiology* 65(4), 261-271.

Dimitrova, P. D., Ivanova, V., Trendafilova, A. and Paunova-Krasteva, T. (2024). Anti-Biofilm and Anti-Quorum-Sensing Activity of Inula Extracts: A Strategy for Modulating Chromobacterium violaceum Virulence Factors. *Pharmaceuticals* 17(5), 573.

Drumond M. M., Tapia-Costa, A. P., Neumann, E., Nunes, Á. C., Barbosa, J. W., Kassuha, D.E. and Mancha-Agresti, P. (2023). Cell-free supernatant of probiotic bacteria exerted antibiofilm and antibacterial activities against *Pseudomonas aeruginosa*: A novel biotic therapy. *Front. Pharmacol* 14, 1152588.

Duraisamy, S., Balakrishnan, S., Ranjith, S., Husain, F., Sathyan, A., Peter, A. S., Prahalathan, C. and Kumarasamy, A. (2020). Bacteriocin—a potential antimicrobial peptide towards disrupting and preventing biofilm formation in the clinical and environmental locales. *Environmental Science and Pollution Research* 27: 44922-44936.

Famuyide, I. M., Aro, A. O., Fasina, F. O., Eloff, J. N. and McGaw, L. J. (2019). Antibacterial and antibiofilm activity of acetone leaf extracts of nine under-investigated south African Eugenia and Syzygium (Myrtaceae) species and their selectivity indices. *BMC complementary and alternative medicine* 19, 1-13.

Famuyide, I. M., Fasina, F. O., Eloff, J. N and McGaw, L. J. (2020). The ultrastructural damage caused by Eugenia zeyheri and Syzygium legatii acetone leaf extracts on pathogenic Escherichia coli. *BMC veterinary research* 16(1), 326.

Ghrairi, T., Braiek, O. B. and Hani, K. (2014). Detection and characterization of a bacteriocin, putadicin T01, produced by *Pseudomonas putida* isolated from hot spring water. *Apmis* 123(3), 260-268.

Haney, E. F., M. J. Trimble, J. T. Cheng, Q. Vallé and R. E. W. Hancock. (2018). Critical assessment of methods to quantify biofilm growth and evaluate antibiofilm activity of host defence peptides. *Biomolecules* 8(2), 29.

Haris, Z. and Ahmad, I. (2024). Green synthesis of silver nanoparticles using Moringa oleifera and its efficacy against gram-negative bacteria targeting quorum sensing and biofilms. *Journal of Umm Al-Qura University for Applied Sciences* 10(1), 156-167.

Husain F. M., Ahmad, I. Khan, M. S., Ahmad, E., Tahseen, Q., Khan, M. S. and Alshabib, N. A. (2015). Sub-MICs of Mentha piperita essential oil and menthol inhibits AHL mediated quorum sensing and biofilm of Gram-negative bacteria. *Frontiers in microbiology* 6, 420.

Kamer, A. M. A., Abdelaziz, A. A. Al-Monofy, K. B. and Al-Madboly, L. A. (2023). Antibacterial, antibiofilm, and anti-quorum sensing activities of pyocyanin against methicillin-resistant Staphylococcus aureus: in vitro and in vivo study. *BMC microbiology* 23(1), 116.

Kim, D. H., Kim Y. C. and Choi, U. K. (2011). Optimization of antibacterial activity of *Perilla frutescens var. acuta* leaf against *Staphylococcus aureus* using evolutionary operation factorial design technique. *International journal of molecular sciences* 12(4), 2395-2407.

Kim, Y. J., Yu, H. H., Park, Y. J., Lee, N. K. and Paik, H. D. (2020). Anti-biofilm activity of cell-free supernatant of *Saccharomyces cerevisiae* against *Staphylococcus aureus*. *Journal of Microbiology and Biotechnology* 30(12), 1854.

Liu, H., Zhang, R., Zhang, Q., Tian, M., Ren, X., Wang, L. and Wang, X. (2023). Antifungal Activity of Cell-Free Supernatants from *Lactobacillus pentosus* 86 against *Alternaria gaisen*. *Horticulturae* 9(8), 911.

Liu, J., Madec, J. Y., Bousquet-Mélou, A., Haenni, M. and Ferran, A. A. (2021). Destruction of *Staphylococcus aureus* biofilms by combining an antibiotic with subtilisin A or calcium gluconate. *Scientific reports* 11(1), 6225.

Liu, X., Cai, J., Chen, H., Zhong, Q., Hou, Y., Chen, W. and Chen, W. (2020). Antibacterial activity and mechanism of linalool against *Pseudomonas aeruginosa*. *Microbial Pathogenesis* 141, 103980.

Matijašević, D., Pantić, M., Rašković, B., Pavlović, V., Duvnjak, D., Sknepnek, A. and Nikšić, M. (2016). The antibacterial activity of *Coriolus versicolor* methanol extract and its effect on ultrastructural changes of *Staphylococcus aureus* and *Salmonella Enteritidis*. *Frontiers in Microbiology* 7, 1226.

Meroni, G., Panelli, S., Zuccotti, G., Bandi, C., Drago, L. and Pistone, D. (2021). Probiotics as Therapeutic Tools against Pathogenic Biofilms: Have We Found the Perfect Weapon?. *Microbiology Research* 12(4), 916–937.

Mishra, R., Panda, A. K., De Mandal, S., Shakeel, M., Bisht, S. S. and Khan, J. (2020). Natural Anti-biofilm Agents: Strategies to Control Biofilm-Forming Pathogens. *Frontiers in microbiology* 11, 566325.

Mombeshora, M. and Mukanganyama, S. (2017). Development of an accumulation assay and evaluation of the effects of efflux pump inhibitors on the retention of chlorhexidine digluconate in *Pseudomonas aeruginosa* and *Staphylococcus aureus*. *BMC research notes* 10, 1-9.

Mulya, E. and Waturangi, D. E. (2021). Screening and quantification of anti-quorum sensing and antibiofilm activity of Actinomycetes isolates against food spoilage biofilm-forming bacteria. *BMC microbiology* 21, 1-8.

Mukti, K. (2019). Biofilm Inhibition of Pathogenic Bacteria by Mangrove Plant Extracts. Dissertation. Biotechnology Research Institute, University Malaysia Sabah, Malaysia.

Panphut, W., Budsabun, T. and Sangsuriya, P. (2020). In vitro antimicrobial activity of *Piper retrofractum* fruit extracts against microbial pathogens causing infections in human and animals. *International Journal of Microbiology* 2020(1), 5638961.

Raab, N. and Bachelet, I. (2017). Resolving biofilm topography by native scanning electron microscopy. *Journal of Biological Methods* 4(2), 1-5.

Ray, S., Jin, J. O., Choi, I. and Kim, M. (2023). Cell-Free Supernatant of *Bacillus thuringiensis* Displays Anti-Biofilm Activity against *Staphylococcus aureus*. *Applied Biochemistry and Biotechnology* 195(9), 5379-5393.

Sanchez, C. J., Ward, C. L., Romano, D. R., Hurtgen, B. J., Hardy, S. K., Woodbury, R. L., Trevino, A. V., Rathbone, C. R. and Wenke, J. C. (2013). *Staphylococcus aureus* biofilms decrease osteoblast viability, inhibits osteogenic differentiation, and increases bone resorption in vitro. *BMC musculoskeletal disorders* 14, 1-11.

Saptami, K., Arokia Balaya Rex, D., Chandrasekaran, J. and Rekha, P. D. (2022). Competitive interaction of thymol with cviR inhibits quorum sensing and associated biofilm formation in *Chromobacterium violaceum*. *International Microbiology* 25(3), 629-638.

Snopková, K., Dufková, K., Chamrád, I., Lenobel, R., Čejková, D., Kosina, M., Hrala, M., Holá, V., Sedláček, I. and Šmajs, D. (2022). Pyocin-mediated antagonistic interactions in Pseudomonas spp. isolated in James Ross Island, Antarctica. *Environmental Microbiology* 24(3), 1294-1307.

Theodora, N. A., Dominika, V. and Waturangi, D. E. (2019). Screening and quantification of anti-quorum sensing and antibiofilm activities of phyllosphere bacteria against biofilm forming bacteria. *BMC research notes* 12, 1-5.

van Teeseling, M. C., de Pedro, M. A. and Cava, F. (2017). Determinants of Bacterial Morphology: From Fundamentals to Possibilities for Antimicrobial Targeting. *Frontiers in microbiology* 8, 1264.

Venkatramanan, M., Ganesh, P. S., Senthil, R., Akshay, J., Ravi, A. V., Langeswaran, K., Vadivelu, J., Nagarajan, S., Rajendran, K. and Shankar, E. M. (2020). Inhibition of quorum sensing and biofilm formation in *Chromobacterium violaceum* by fruit extracts of *Passiflora edulis*. *ACS omega* 5(40), 25605-25616.

Wahi, A. K., Singh, A. and Singh, A. K. (2011). Determination of minimum inhibitory concentration (MIC) of some novel triazole derivative. *International Journal of Research in Pharmacy and Chemistry* 1(4), 1108-1114.

Yu, S., Jiang, B., Jia, C., Wu, H., Shen, J., Hu, X. and Xie, Z. (2020). Investigation of biofilm production and its association with genetic and phenotypic characteristics of OM (osteomyelitis) and non-OM orthopedic *Staphylococcus aureus*. *Annals of clinical microbiology and antimicrobials* 19, 1-9.

Zagaglia, C., Ammendolia, M. G., Maurizi, L., Nicoletti, M. and Longhi, C. (2022). Urinary tract infections caused by uropathogenic *Escherichia coli* strains—new strategies for an old pathogen. *Microorganisms* 10(7), 1425.

Borneo International Journal of Biotechnology
(BIJB) Vol. 5 (December 2025), 143-156.

e-ISSN 2716-697X

Development of an *In Vitro* Culture Protocol for *Gigantochloa levis* Using Nodal Segments

Mohammad Rahmat Derise[1], Anis Adilah Mustafa[1], Kenneth Francis Rodrigues[1], Chee Wei Yew[1], Wilson Thau Lym Yong[1]*

[1]Biotechnology Research Institute, Universiti Malaysia Sabah, Jalan UMS, 88400 Kota Kinabalu, Sabah, Malaysia.
*Corresponding author's email: wilsonyg@ums.edu.my

Received: 4 December 2025 | Accepted: 20 December 2025 | Published: 31 December 2025

ABSTRACT

Bamboo is a giant perennial arborescent grass in the Poaceae family and a fast-growing, economically important plant. However, conventional propagation is constrained by limited planting material, genetic variation, and the risk of disease and pest transmission. *In vitro* propagation using nodal segments has become an effective method for the large-scale multiplication of bamboo species. This study aimed to establish an *in vitro* culture system for the tropical bamboo *Gigantochloa levis*. Nodal segments containing axillary buds were selected as explants and surface-sterilized using an optimized protocol. Sterilized explants were cultured on full-strength semi-solid Murashige and Skoog (MS) medium for shoot initiation. MS medium supplemented with 6-benzylaminopurine (BAP) at 2, 3 and 4 mg/L was evaluated for shoot induction and multiplication. Medium containing 3 mg/L BAP produced the highest number of shoots (6.80 ± 0.49) after six weeks of culture. Rooting was optimized using liquid half-strength MS medium supplemented with 0.5 mg/L indole-3-butyric acid (IBA). The results provide a baseline protocol for efficient *in vitro* propagation of *G. levis*, supporting future efforts in bamboo multiplication and conservation.

Keywords: *Gigantochloa levis*, tropical bamboo, *in vitro* propagation, nodal segments, 6-benzylaminopurine (BAP), indole-3-butyric acid (IBA)

e-ISSN 2716-697X

INTRODUCTION

Tissue culture, also known as *in vitro* propagation or micropropagation, is a widely used biotechnological approach in plant science. It involves cultivating plant cells, tissues, or organs on sterile synthetic media under controlled temperature, light, and humidity (Sudheer et al., 2022; Bansal et al., 2024). Beyond its role in plant propagation, tissue culture supports a broad range of basic and applied research applications, including studies on plant developmental processes, functional gene analysis, production of transgenic plants with desirable traits, and crop improvement through plant breeding. It is also employed for germplasm conservation, long-term preservation of vegetatively propagated crops, and the rescue of rare, threatened, or endangered species (Espinosa-Leal et al., 2018; Loyola-Vargas & Ochoa-Alejo, 2018). Furthermore, tissue culture enables mass multiplication of elite plants, production of disease-free planting material, and propagation of species that are difficult to multiply using seeds or cuttings (Espinosa-Leal et al., 2018; Bansal et al., 2024; Bao et al., 2024; Eliwa et al., 2024). It also promotes the rapid generation of genetically uniform plants, supporting vigorous growth in subsequent developmental stages (Permadi et al., 2023).

Seed-based bamboo propagation is constrained by sporadic flowering, long flowering cycles, seed recalcitrance, and vulnerability to predation. Vegetative propagation techniques such as culm cuttings and air layering are widely practiced but are limited to small-scale applications because they damage mother plants, require bulky planting material, and depend on specific seasons (Sandhu et al., 2018). *In vitro* propagation has therefore emerged as a practical alternative, enabling large-scale clonal multiplication, providing planting material for breeding programmes, and supporting germplasm conservation. Across forestry, agriculture, and horticulture, *in vitro* culture plays a crucial role not only in propagation but also in genetic improvement and conservation strategies (Ahmed, 2022; Liu et al., 2024)

In recent years, substantial progress has been made in developing *in vitro* culture systems for many bamboo species, offering an effective alternative to conventional propagation. Successful micropropagation protocols have been reported for *Dendrocalamus asper* (Gunasena et al., 2024), *Bambusa vulgaris* (Gonçalves et al., 2023; Sarker et al., 2024), *Bambusa tulda* and *Dendrocalamus stocksii* (Choudhary et al., 2022), *Bambusa tuldoides* (Sharothi et al., 2022), *Bambusa balcooa* (Rajput et al., 2020), *Melocanna baccifera* (Waikhom & Louis, 2014), and *Gigantochloa atroviolaceae* (Bisht et al., 2010). However, despite these advances, studies on *Gigantochloa levis* remain scarce. This species is highly valued for its strong culms, extensive use in construction and handicrafts, and its emerging potential in the development of sustainable biomaterials.

e-ISSN 2716-697X

Increasing demand has placed pressure on natural stands, yet large-scale cultivation is limited by inadequate availability of high-quality planting material. Therefore, establishing a reliable *in vitro* propagation protocol for *G. levis* is essential to support commercial-scale cultivation, ensure genetic uniformity, and promote conservation and sustainable utilization of this economically important tropical bamboo.

MATERIALS AND METHODS

Sample Collection

Culms of *Gigantochloa levis* were collected from the Institute for Tropical Biology and Conservation (ITBC), Universiti Malaysia Sabah (UMS). Species identity was confirmed by an authorized plant taxonomist. Culms and branches containing internodes were selected and transported to the climate-controlled greenhouse at the Biotechnology Research Institute (BRI), UMS. The culms were established in polybags for acclimatization prior to explant preparation (Figure 1).

Figure 1 (a) *Gigantochloa levis* at the Institute for Tropical Biology and Conservation (ITBC), Universiti Malaysia Sabah (UMS); **(b)** culms of *G. levis* established in polybags for acclimatization in the greenhouse

e-ISSN 2716-697X

Explants Surface Sterilization

Nodal segments of *G. levis* containing axillary buds were used as explants. Explants were trimmed to 4-5 cm using a sterilized blade, and the outer layers were gently scrubbed to remove dust and wax. The explants were first washed three times with sterile distilled water for 3 minutes each, followed by washing in 0.5% commercial detergent for 3 minutes and rinsing 4-5 times with sterile distilled water. Explants were then soaked in 1.5% Antracol 70 WP (fungicide) for 30 minutes on a rotary shaker and rinsed three times with sterile distilled water. This was followed by washing in 2.5% commercial detergent for 5 minutes and rinsing 5-6 times with sterile distilled water. Surface disinfection was carried out using 70% ethanol for 1 minute, followed by three rinses with sterile distilled water. Explants were then sterilized in 0.1% (v/v) mercuric chloride ($HgCl_2$) for 5 minutes and washed four times, with each wash lasting 5 minutes. Sterilized explants were air-dried in a laminar airflow workstation. The sterilization protocol was adapted and optimized based on Kaladhar et al. (2017).

Media and Culture Conditions

Murashige and Skoog (MS) medium was prepared in glass jar and used as the basal medium. The medium contained 3% (w/v) sucrose and was supplemented with varying concentrations of 6-benzylaminopurine (BAP). The pH was adjusted to 5.8 ± 0.1 before adding 3% sucrose, 1.0 g/L gelrite, and autoclaving at 121°C for 15 minutes. Cultures were maintained under a 16/8-hour (light/dark) photoperiod at 26 ± 2°C and 70% relative humidity in a SANYO Versatile Environmental Test Chamber (SANYO Electric Co., Ltd., Japan) (Mustafa et al., 2023).

Shoot Initiation (Bud Break)

A total of 36 nodal explants containing axillary buds were used for shoot initiation, with 12 explants allocated to each BAP concentration (2.0, 3.0, and 4.0 mg/L). Sterilized explants were inoculated onto MS medium supplemented with 3% sucrose, 1.0 g/L gelrite, and the respective BAP concentrations (Figure 2). All procedures were carried out under aseptic conditions in an ESCO laminar flow cabinet (ESCO Micro Pte. Ltd., Singapore). The percentage of shoot initiation (bud break) was recorded after four weeks (Mustafa et al., 2023).

e-ISSN 2716-697X

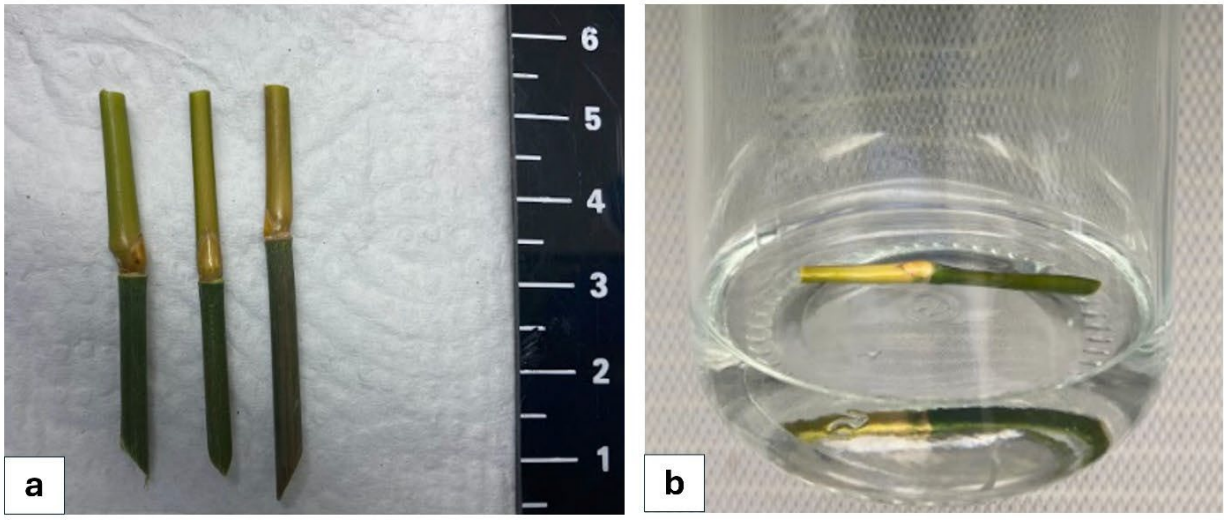

Figure 2 (a) Nodal segments of *Gigantochloa levis* containing axillary buds; **(b)** inoculation of explant onto Murashige and Skoog (MS) medium.

Shoot Multiplication

Proliferated axillary shoots were transferred to MS medium containing 2.0, 3.0, or 4.0 mg/L BAP supplemented with 3% sucrose and 1.0 g/L gelrite. Subculturing was carried out every seven days under sterile conditions to minimize browning and maintain healthy cultures. Shoot multiplication performance (n=5) was evaluated after six weeks by recording the number of shoots per explant (Choudhary et al., 2022). The percentage of microbial contamination and browning was also assessed.

Rooting and Acclimatization

After six weeks of culture, axillary shoots were excised and transferred to liquid half-strength MS medium supplemented with indole-3-butyric acid (IBA) at concentrations of 0.5, 1.0, 2.0, 3.0, 4.0, and 5.0 mg/L. Rooting response was evaluated after eight weeks by recording the rooting percentage, average number of roots, and mean root length. Rooted plantlets were acclimatized in peat moss (Kekkilä, Finland) for four weeks and maintained at 25 ± 2°C in the greenhouse (Mustafa et al., 2023).

e-ISSN 2716-697X

RESULTS AND DISCUSSION

Establishment of *In Vitro* Shoots of *Gigantochloa levis*

Shoot Initiation (Bud Break)

Nodal segments containing axillary buds successfully initiated shoot development across all BAP concentrations tested. Shoot bud initiation was observed between 4 and 7 days after inoculation. After 14 days, visible bud sprouting was recorded at 2.0, 3.0, and 4.0 mg/L BAP (Figure 3). After four weeks, 3.0 mg/L BAP produced the highest shoot initiation percentage (100%), followed by 2.0 mg/L BAP, while the lowest initiation (75%) occurred at 4.0 mg/L BAP (Figure 4). No buds initiated after the fourth week, suggesting a limited response window.

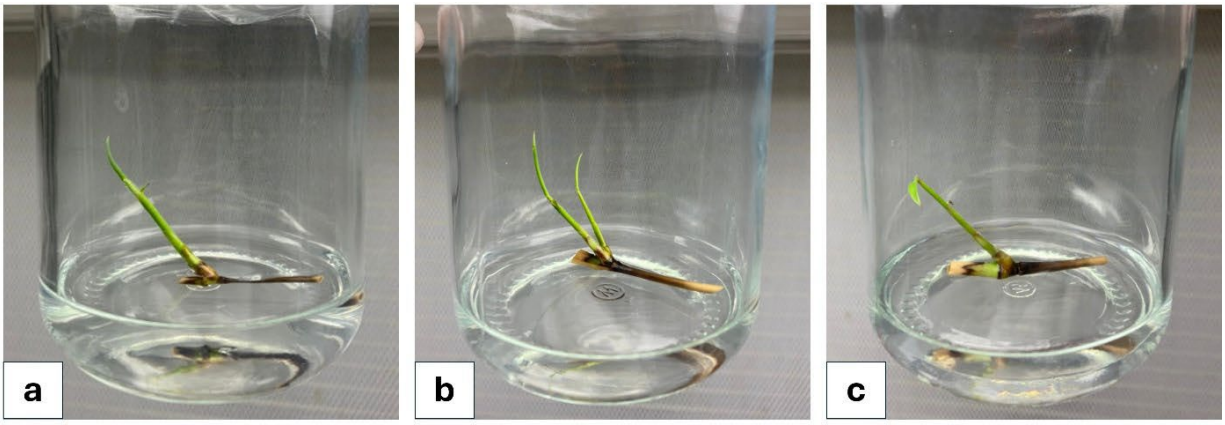

Figure 3 Bud sprouting of *Gigantochloa levis* at 14 days: (a) 2.0 mg/L BAP; (b) 3.0 mg/L BAP; (c) 4.0 mg/L BAP.

e-ISSN 2716-697X

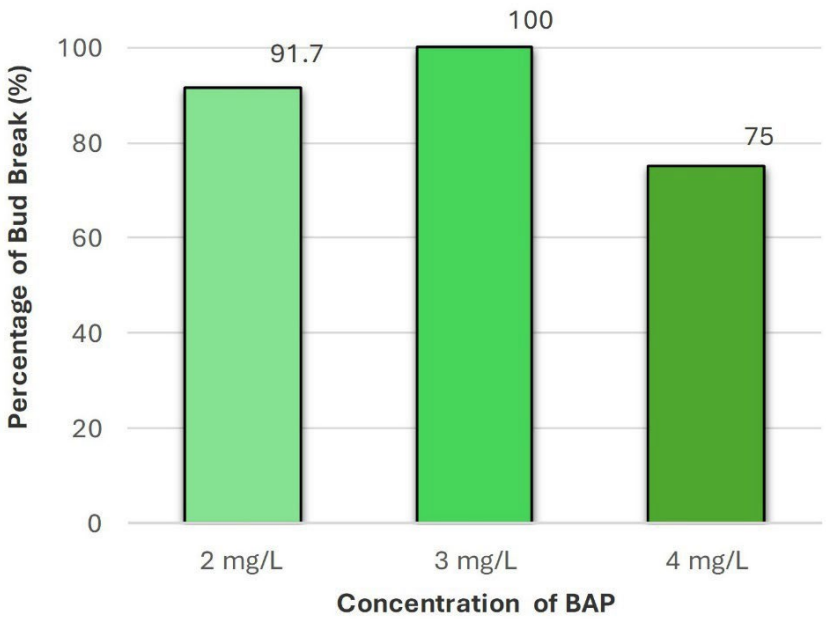

Figure 4 Percentage of shoot bud initiation after four weeks.

The successful and rapid bud break (4-7 days) demonstrates the strong responsiveness of *G. levis* nodal explants to BAP, consistent with established findings for bamboo tissue culture. Nodal segments perform well because they contain organized meristems with high regenerative capacity (Waikhom & Louis, 2014), which also exhibit greater genetic stability than disorganized tissues (Nowakowska et al., 2020; Duta-Cornescu et al., 2023). BAP is widely reported as the most effective cytokinin for bud break in bamboo, including *Bambusa nutans*, *B. tulda*, *Dendrocalamus strictus*, and *D. asper* (Ray & Ali, 2017). The optimal concentration of 3.0 mg/L BAP identified in this study aligns with reports for *Guadua angustifolia* (Jiménez et al., 2006) and several other bamboo species. Higher BAP concentrations reduced bud initiation, likely due to cytokinin-induced stress or hormonal imbalance (Mahardhini et al., 2023).

Shoot Multiplication

Shoot multiplication varied significantly among BAP concentrations (Figure 5). The highest shoot number (6.80 ± 0.49) was obtained with 3.0 mg/L BAP, while the lowest (5.40 ± 0.51) occurred at 4.0 mg/L BAP (Figure 6). BAP concentrations above 3.0 mg/L reduced shoot proliferation. MS medium containing 3.0 mg/L BAP produced vigorous shoots with minimal browning and no contamination, making it the most suitable treatment.

e-ISSN 2716-697X

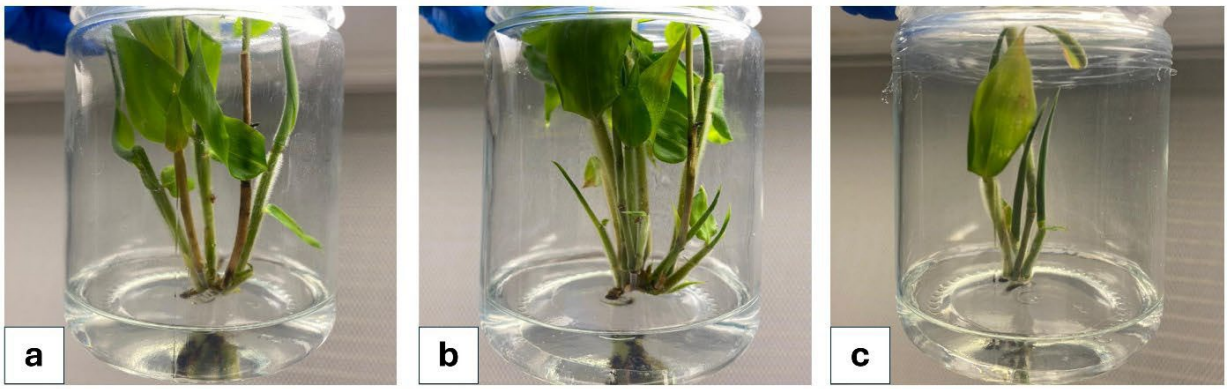

Figure 5 Shoot multiplication after six weeks at **(a)** 2.0 mg/L BAP; **(b)** 3.0 mg/L BAP; **(c)** 4.0 mg/L BAP.

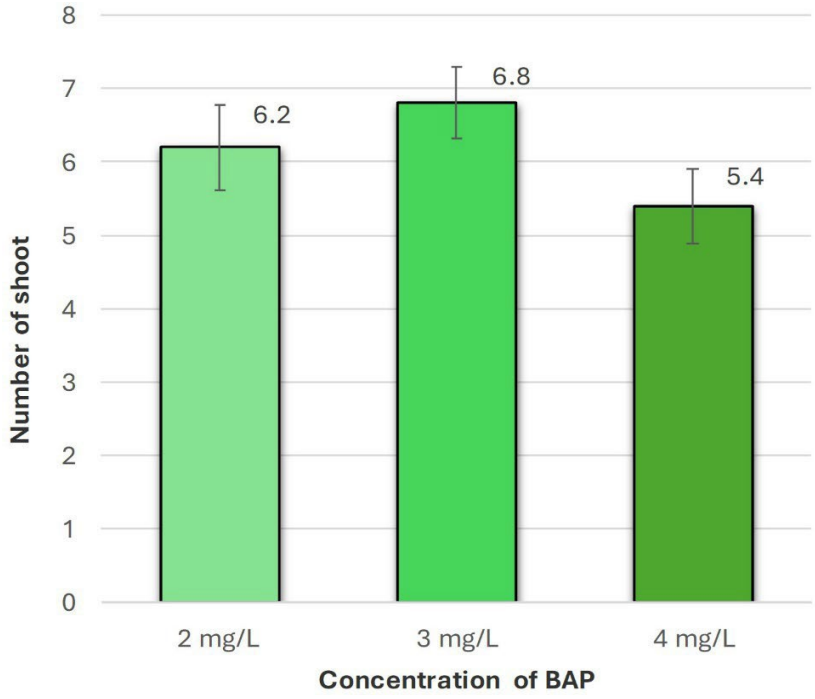

Figure 6 Number of shoots formed at different BAP concentrations.

The superior performance of 3.0 mg/L BAP is consistent with findings in *B. tulda*, *M. baccifera* (Waikhom & Louis, 2014), and *Bambusa bambos* (Muthukumaran et al., 2018), reinforcing the suitability of this concentration for bamboo shoot proliferation. Higher BAP levels typically reduce shoot multiplication, as reported in *D. strictus* and other bamboo species (Pandey & Singh, 2012). Excess cytokinin may inhibit bud development by disrupting hormonal balance (Wu et al., 2021). The results suggest that3.0 mg/L BAP provides a favourable hormonal environment for *G. levis*, supporting both bud break and shoot multiplication.

e-ISSN 2716-697

Contamination and Browning of *In Vitro* Cultures

Application of the optimized surface sterilization protocol significantly improved culture establishment. After six weeks, only 11.11% of *G. levis* explants showed microbial contamination, whereas the original method described by Kaladhar et al. (2017), when applied without modification, resulted in 94.44% contamination. Browning was observed in 19.44% of cultures during both the initiation and multiplication stages. Regular subculturing at seven-day intervals reduced browning symptoms and supported healthier explant growth.

Bamboo explants are highly susceptible to microbial contamination due to the presence of both epiphytic and endophytic microorganisms that inhabit their woody culm and nodal tissues (Ray & Ali, 2017; Pasqualini et al., 2019). The optimized sterilization protocol effectively addressed these challenges through several key improvements. Replacing tap water with sterile distilled water during explant washing eliminated a major source of contamination. The two-step detergent wash enhanced the removal of debris and microbial residues, while extended fungicide exposure combined with rotary shaking improved contact between the explant surface and sterilizing agents. Furthermore, thorough rinsing following the 0.1% $HgCl_2$ treatment helped prevent phytotoxic damage to the tissues (Kodape et al., 2024). These refinements contributed to the substantial reduction in contamination rates and improved the overall success of culture establishment.

Browning, a common physiological disorder in bamboo tissue culture, results from the oxidation of phenolic compounds released during explant wounding (Permadi et al., 2023). The trimming of explants to 4-5 cm likely increased phenolic exudation, contributing to the browning observed in this study. Regular subculturing to fresh medium was effective in mitigating browning by diluting oxidized phenolics and maintaining a more favorable environment for growth (Amente & Chimdessa, 2021). This approach is widely recommended in bamboo micropropagation to prevent phenolic accumulation and maintain culture viability.

Rooting and Acclimatization

Rooting of *G. levis* shoots occurred only on half-strength MS medium supplemented with 0.5 mg/L IBA. At this concentration, 80% of the shoots produced roots, with an average of 7.60 ± 1.96 roots per shoot and a mean root length of 8.96 ± 2.39 cm (**Figure 7**). No rooting was observed at higher IBA concentrations ranging from 1.0 to 5.0 mg/L. The rooted plantlets were successfully acclimatized in peat moss under greenhouse conditions, producing healthy and vigorous young bamboo plants (**Figure 8**).

e-ISSN 2716-697X

Figure 7 Root induction on half-strength MS medium supplemented with 0.5 mg/L IBA.

Figure 8 Hardened *G. levis* plantlets acclimatized in the greenhouse.

The finding that rooting occurred only at the lowest IBA concentration demonstrates the high auxin sensitivity of *G. levis*. A similar response has been reported in *D. asper*, where elevated auxin concentrations inhibit root formation rather than promote it (Mustafa et al., 2023). Excessive auxin can disrupt root initiation by causing hormonal imbalances or inducing tissue stress, leading to suppression of root primordia development.

The effectiveness of half-strength MS medium supplemented with 0.5 mg/L IBA is consistent with reports from other bamboo species, confirming its suitability for promoting root induction in *G. levis*. The high rooting percentage, coupled with the robust and well-developed root system, indicates that this protocol provides favorable physiological conditions for root formation. Successful acclimatization of rooted plantlets further supports the reliability of this rooting method, suggesting its potential for efficient nursery production and subsequent field establishment of *G. levis*.

CONCLUSION

This study established an efficient and reliable *in vitro* propagation protocol for *G. levis*, providing a practical solution to the limitations of its conventional propagation. The optimized sterilization method, together with the identified culture conditions for shoot induction, multiplication, and rooting, enabled consistent production of healthy plantletsthat acclimatized successfully under greenhouse conditions. The protocol offers a feasible approach for large-scale propagation, supporting the conservation, commercial cultivation, and sustainable utilization of this economically important bamboo species. Future work may focus on confirming genetic fidelity and refining acclimatization techniques to enhance field performance .

ACKNOWLEDGEMENTS

This research was supported by the Malaysian Ministry of Higher Education through the Fundamental Research Grant Scheme (Grant No. FRGS/1/2020/STG01/UMS/02/4).

REFERENCES

Ahmed, M.E.A.E. (2022). *In vitro* propagation for conservation and genetic fidelity of the near threatened *Dimocarpus longan* plant. Journal of Genetic Engineering and Biotechnology 20(1), 130. https://doi.org/10.1186/s43141-022-00406-4

Amente, G. and Chimdessa, E. (2021). Control of browning in plant tissue culture: a review. Journal of Scientific Agriculture 5, 67-71.

Bansal, S., Sharma, M.K., Joshi, P., Malhotra, E.V., Latha, M. and Malik, S.K. (2024). An efficient direct organogenesis protocol for *in vitro* clonal propagation of *Rubia cordifolia* L. Industrial Crops and Products 208, 117856. https://doi.org/10.1016/j.indcrop.2023.117856

Bao, J., O'Donohue, B., Sommerville, K.D., Mitter, N., O'Brien, C. and Hayward, A. (2024). Tissue culture innovations for propagation and conservation of Myrteae — a globally important Myrtaceae tribe. Plants 13(16), 2244. https://doi.org/10.3390/plants13162244

Bisht, P., Pant, M. and Kant, A. (2010). *In vitro* propagation of *Gigantochloa atroviolaceae* Widjaja through nodal explants. Journal of American Science 6(10), 1019-1025. https://doi.org/10.25081/jsa.2021.v5.7266

Choudhary, A.K., Kumari, P. and Kumari, S. (2022). *In vitro* propagation of two commercially important bamboo species (*Bambusa tulda* Roxb. and *Dendrocalamus stocksii* Munro.). African Journal of Biotechnology 21(2), 83-94. https://doi.org/10.5897/AJB2021.17437

Pasqualini, A.P.A., Schneider, G.X., Fraga, H.P.F., Biasi, L.A. and Quoirin, M. (2019). *In vitro* establishment of *Bambusa oldhamii* Munro from field-grown matrices and molecular identification of endophytic bacteria. Pesquisa Agropecuária Tropical 49, e53673. https://doi.org/10.1590/1983-40632019v4953673

Duta-Cornescu, G., Constantin, N., Pojoga, D.M., Nicuta, D. and Simon-Gruita, A. (2023). Somaclonal variation — advantage or disadvantage in micropropagation of the medicinal plants. International Journal of Molecular Sciences 24(1), 838. https://doi.org/10.3390/ijms24010838

Eliwa, G.I., El-Dengawy, E.F., Gawish, M.S. and Yamany, M.M. (2024). Comprehensive study on *in vitro* propagation of some imported peach rootstocks: *in vitro* explant surface sterilization and bud proliferation. Scientific Reports 14, 5586. https://doi.org/10.1038/s41598-024-55685-3

Espinosa-Leal, C.A., Puente-Garza, C.A. and García-Lara, S. (2018). *In vitro* plant tissue culture: means for production of biological active compounds. Planta 248, 1-18. https://doi.org/10.1007/s00425-018-2910-1

Gonçalves, D.S., Souza, D.M.S.C., de Carvalho, D., de Oliveira, L.S., Teixeira, G.L. and Brondani, G.E. (2023). *In vitro* cloning of *Bambusa vulgaris* Schrad. ex J. C. Wendl.: effect of culture systems, sucrose and activated charcoal supplementation. Advances in Bamboo Science 3, 100024. https://doi.org/10.1016/j.bamboo.2023.100024

Gunasena, M.D.K.M., Chandrasena, P.H. and Senarath, W.T.P.S.K. (2024). *In vitro* mass propagation of *Dendrocalamus asper* (Giant bamboo) through direct organogenesis. Advances in Bamboo Science 8, 100090. https://doi.org/10.1016/j.bamboo.2024.100090

Jiménez, V.M., Castillo, J., Tavares, E., Guevara, E. and Montiel, M. (2006). *In vitro* propagation of the neotropical giant bamboo, *Guadua angustifolia* Kunth, through axillary shoot proliferation. Plant Cell, Tissue and Organ Culture 86, 389-395. https://doi.org/10.1007/s11240-006-9120-4

Kaladhar, D.S.V.G.K., Tiwari, P. and Duppala, S.K. (2017). A rapid *in vitro* micro propagation of *Bambusa vulgaris* using inter- node explant. International Journal of Life-Sciences Scientific Research 3(3), 1052-1054. https://doi.org/10.21276/ijlssr.2017.3.3.14

Kodape, S.V, Baviskar, S.B., Shende, P.V., Patil, S.R., Patil, S.A., Tinpayale, A.D. and Khandare, K.G. (2024). Comprehensive study on explant surface sterilisation of *in vitro* culture of bamboo species (*Bambusa balcooa*). International Journal of Advanced Biochemistry Research 8(S9), 1208-1210. https://doi.org/10.33545/26174693.2024.v8.i9So.2337

Liu, C., Fan, H., Zhang, J., Wu, J., Zhou, M., Cao, F., Tao, G. and Zhou, X. (2024). Combating browning: mechanisms and management strategies in *in vitro* culture of economic woody plants. Forestry Research 4, e032. https://doi.org/10.48130/forres-0024-0026

Loyola-Vargas, V.M. and Ochoa-Alejo, N. (2018). An introduction to plant tissue culture: advances and perspectives. In: Plant Cell Culture Protocols. Methods in Molecular Biology, vol 1815 (V.M. Loyola-Vargas and N. Ochoa-Alejo, eds.), pp 3-13. Humana Press, New York, NY. https://doi.org/10.1007/978-1-4939-8594-4_1

Mahardhini, A.D., Anwar, S. and Karno (2023) BAP and kinetin application for *in vitro* bud induction of vanilla (*Vanilla planifolia* Andrews.) from stem node explants in the initiation stage. IOP Conference Series: Earth and Environmental Science 1246, 012030. https://doi.org/10.1088/1755-1315/1246/1/012030

Mustafa, A.A., Yong, W.T.L., Kulip, J. and Rodrigues, K.F. (2023). Establishment of an *in vitro* mass propagation system for *Dendrocalamus asper*. Journal of Tropical Biology and Conservation 20, 193-202. https://doi.org/10.51200/jtbc.v20i.4644

Muthukumaran, P., Saraswathy, N., Abarna, S., Kanthimathi, R., Monisha, V., Devi, N.N. and Nivetha, M.R. (2018). Protocol for induction of multiple shoot through nodal explants culture of *Bambusa bambos* for biomass production. International Journal of Life-Sciences Scientific Research 4(2), 1634-1638. https://doi.org/10.21276/ijlssr.2018.4.2.2

Nowakowska, M., Pavlović, Ž., Nowicki, M., Boggess, S.L. and Trigiano, R.N. (2020). *In vitro* propagation of an endangered *Helianthus verticillatus* by axillary bud proliferation. Plants 9(6), 712. https://doi.org/10.3390/plants9060712

Pandey, B.N. and Singh, N.B. (2012). Micropropagation of *Dendrocalamus strictus* nees from mature nodal explants. Journal of Applied and Natural Science 4(1), 5-9. https://doi.org/10.31018/jans.v4i1.213

Permadi, N., Nurzaman, M., Alhasnawi, A.N., Doni, F. and Julaeha, E. (2023). Managing lethal browning and microbial contamination in *Musa* spp. tissue culture: synthesis and perspectives. Horticulturae 9(4), 453. https://doi.org/10.3390/horticulturae9040453

Rajput, B.S., Jani, M., Ramesh, K., Manokari, M., Jogam, P., Allini, V.R., Kher, M.M. and Shekhawat, M.S. (2020). Large-scale clonal propagation of *Bambusa balcooa* Roxb.: an industrially important bamboo species. Industrial Crops and Products 157, 112905. https://doi.org/10.1016/j.indcrop.2020.112905

Ray, S.S. and Ali, M.N. (2017). Factors affecting macropropagation of bamboo with special reference to culm cuttings: a review update. New Zealand Journal of Forestry Science 47, 17. https://doi.org/10.1186/s40490-017-0097-z

Sandhu, M., Wani, S.H. and Jiménez, V.M. (2018). *In vitro* propagation of bamboo species through axillary shoot proliferation: a review. Plant Cell, Tissue and Organ Culture 132, 27-53. https://doi.org/10.1007/s11240-017-1325-1

Sarker, S., Rahman, K.T., Raju, M.R.I. and Hossain, M.T. (2024). *In vitro* regeneration of *Bambusa vulgaris* var. *striata* using nodal explants. Bangladesh Journal of Botany 53(4), 939-947. https://doi.org/10.3329/bjb.v53i4.78094

Sharothi, P., Raju, R.I. and Hossain, M.T. (2022). *In vitro* propagation of an ornamental bamboo (*Bambusa tuldoides* Munro). Plant Tissue Culture and Biotechnology 32(157-166. https://doi.org/10.3329/ptcb.v32i2.63550

Sudheer, W.N., Praveen, N., Al-Khayri, J.M. and Jain, S.M. (2022). Role of plant tissue culture medium components. In: Advances in Plant Tissue Culture: Current Developments and Future Trends (A.C. Rai, A. Kumar, A. Modi and
M. Singh, eds.), pp 51-83. Academic Press. https://doi.org/10.1016/B978-0-323-90795-8.00012-6

Waikhom, S.D. and Louis, B. (2014). An effective protocol for micropropagation of edible bamboo species (*Bambusa tulda* and *Melocanna baccifera*) through nodal culture. The Scientific World Journal 2014(1), 345794. https://doi.org/10.1155/2014/345794

Wu, W., Du, K., Kang, X. and Wei, H. (2021). The diverse roles of cytokinins in regulating leaf development. Horticulture Research 8, 118. https://doi.org/10.1038/s41438-021-00558-3